Inaugural Dissertation
for
obtaining the doctoral degree
of the
Combined Faculty of Mathematics, Engineering and Natural Sciences
of the
Ruprecht - Karls - University
Heidelberg

Presented by
M.Sc (Biotechnology) Gayatri Ajit Kavishwar
born in Pune, India
Oral Examination on 16th October 2023

Boosting the Immune System:
A Drug Combination Augments H-1 Parvovirus Mediated Oncolysis and Immunogenicity in Prostate Cancer

Referees:
Prof. Dr. Martin Müller
Prof. Dr. Dirk Grimm

The presented research was carried out under the supervision of Dr. Antonio Marchini and Dr. Dirk Nettelbeck in the Laboratory of Oncolytic virus Immunotherapeutics (LOVIT) and the Clinical Co-operation Unit (CCU)-Virotherapy at the German Cancer Research Center (DKFZ), Heidelberg, Germany, between June 2019 and June 2023.

Figure 1: *AI Generated image with the prompt of the thesis title*

"अनेकसंशयोच्छेदि, परोक्षार्थस्य दर्शकम् । सर्वस्य लोचनं शास्त्रं, यस्य नास्त्यन्ध एव सः ॥" [1]

anekasaṃśayocchedi, parokṣārthasya darśakam. sarvasya locanaṃ śāstraṃ, yasya nāstyandha eva saḥ.

The power of science is unparalleled in dispelling doubts and revealing the ultimate truth,
It imparts clarity to the mind, Else even with eyes, one is but blind.

Contents

List of Figures

Acknowledgements

A lot gets said about finding or choosing a good PhD supervisor, but perhaps not enough gets said about what good supervisors bring to a PhD. I have had the privilege of working with two supervisors throughout my PhD who have provided me with support and insight. There are no proper words to convey my deep gratitude and respect for my thesis and research advisor, **Dr. Antonio Marchini**. He has inspired me to become an independent researcher and helped me realise the power of critical reasoning. He has also hugely helped me write this thesis. I would also like to deeply thank my supervisor **PD. Dr. Dirk Nettelbeck**. He has been the most kind, supportive and helpful supervisor for the past two years.

I would like to sincerely thank my thesis advisory committee and my examination committee, apl. **Prof. Dr. Martin Müller**, **Prof. Dr. Dirk Grimm**, **Prof. Dr. Ralf Bartenschlager** and **Dr. Richard Harbottle**. They generously gave their time to offer me valuable comments toward improving my work and finishing my PhD. I am most grateful to our collaborator, **Priv.-Doz. Dr. med. Johannes Linxweiler** at UKS Homburg, without whom I would not have had the opportunity to work with patient derived cells.

I am very thankful to the Helmholtz International Graduate School for Cancer Research for supporting me through my PhD research at the DKFZ. I would like to thank **Dr. Lindsay Murrells**, **Dr. Barbara Janssens**, and their teams for helping me flourish as a graduate student, outside the lab as well.

There is no way to express how much it meant to me to have been a member of two wonderful labs. For all the members of LOVIT and CCU Virotherapy, thank you for being supportive and providing me with a very healthy work environment. Thank you Annabel and Steffi, for helping me out with all lab organisation and lab orders. Without your efficient work, I wouldn't have been able to finish my experiments on time.

I cannot have an acknowledgement without thanking my dear friends who made Heidelberg, a home away from home. I am thankful to **Tiago** for being my first friend in Heidelberg, I am keeping you forever now. **Aga**, I don't think words can express how grateful I am for you. Thank you for being the most thoughtful friend with the biggest heart, I will cherish you forever.

I think **Aleks** and **Alice** are more family than friends at this point. I have no words to express my love and gratitude to both of you. You have been monumental through my journey in Heidelberg, from the beginning to the end. Alice,

I think I have to thank the PhD for bringing you into my life because I don't think I can have a meaningful life without a non-negotiable friend like you. We started this chapter together and are ending it together as well and I couldn't have asked for a better companion looking over the horizon with me.

I would like to thank **Namrata**. She motivated me personally and professionally since I met her. She started out as my mentor but now is one of my closest friends that I am proud and happy to have in my life. I am thankful for **Siddie** and **Rishabh**. Rishabh and I started our PhDs together and are now passing on the baton to Siddie! I am thankful to **Kunal**, for being with me since university times. Thank you for always being the most understanding, sweet and fun.

I am immensely grateful for **Komal**, my best friend since kindergarten. Thank you for being there for me, through think and thin. If anyone has supported my ambitions and dreams for the longest, it has been her. She has been an immense support through everything and I am forever indebted for having such a pillar of a friend in my life.

I don't have enough words to express gratitude to the love of my life, **Pascal**. I consider myself extraordinarily fortunate to have crossed paths with you and to be able to share my life with you. You have been a beacon of support for me, cheer-leading from the sidelines and constantly motivating me to be a better version of myself. I hope to be the same for you.

Lastly, I wouldn't have been motivated and inspired to even attempt an ounce of my life's work without my family. I had read somewhere, "The first generation braves the storm, the second generation respects the efforts and the third generation reaps the benefits". I am grateful for **my grandparents** and **Taii** for being that first generation and to have built a strong foundation for the rest of us to lean on.

I express my gratitude to **Priya Maushi** and **Ashutosh Kaka**, who have played the role of my second parents, acted as true friends, set exemplary ideals by blending tradition and modernity, and showered me with love and unwavering support in every aspect of my life.

Last but not the least, I am especially thankful to my parents, **Aai** and **Pappa**, for always believing in me, for being the biggest pillars of support, for motivating me to take on my ambitions and most importantly for loving me unconditionally. I dedicate my thesis to the both of you.

Abbreviations

Ad Adeno

APAR Autonomous Parvovirus-Associated Replication

APC Antigen Presenting Cell

ATF (Activating transcription factors

BH3 Bcl-2 homology 3

BSA Bovine serum albumin

CD Cluster of differentiation

cGAS cyclic GMP-AMP Synthase

CREB cAMP response element binding protein

CRT Calreticulin

CXCL-10 C-X-C motif chemokine ligand 10

DAMP Danger Associated Molecular Pattern

DAPI 4,6-diamidino-2-phenylindole

DC Dendritic Cell

DMEM Dulbecco's modified Eagle medium

DMSO Dimethyl sulfoxide

DNA Deoxyribonucleic acid

DNAM-1 DNAX accessory molecule-1

ds Double Stranded

EDTA Ethylenediamine tetraacetic acid

EGFP Enhanced green fluorescent protein

EGFR Epidermal growth factor receptor

FACS Fluorescence-activated cell sorting

FBS Fetal bovine serum

FIC Fractional Inhibitory Concentration

GAL Galectin

GAPDH Glyceraldehyde 3-phosphate dehydrogenase

GFP Green Fluorescent Protein

GM-CSF Granulocyte-macrophage colony-stimulating factor

HDAC Histone deacetylases

H-1PV H-1 parvovirus

HLA Human Leukocyte Antigen

HMGB-1 High-Mobility-Group-Protein B1

hpi hours post infection

HSC Hematopoetic Stem Cell

HSV Herpes Simplex Virus

HSP Heat Shock Protein

IFN Interferon

IL Inter Leukin

ICD Immunogenic Cell Death

JAM-1 Junction Adhesion Molecule 1

LRP LDL-receptor related protein

MCP Monocyte Chemoattractant Protein

MEM Minimum Essential Medium

MHC Major Histocompatibility Complex

MIP Macrophage inflammatory protein

MOI Multiplicity of infection

MTT 3-(4,5-dimethylthiazol-2-yl)-2,5-diphenyl tetrazolium bromide

NDV New Castle's Disease Virus

NK Natural Killer

NKG2D natural killer group 2D

ns Not significant

NS Non-structural protein

NY-ESO1 New York esophageal squamous cell carcinoma-1

OD Optical Density

OV Oncolytic Virus

PBS Phosphate-buffered saline

PAMP Pathogen Associated Molecular Pattern

PCNA Proliferating cell nuclear antigen

PDAC Pancreatic Ductal Adenocarcinoma

pfu Plaque-forming unit

pH Potential hydrogen

PLA_2 Phospholipase A2

PLK1 Polo-like kinase 1

PKR Protein Kinase R

PRR Pattern Recognition Receptor

PS Phosphatidylserine

qPCR Quantitative polymerase chain reaction

RANTES regulated on activation, normal T cell expressed and secreted

RIG Retinoic acid-inducible gene

RNA Ribonucleic acid

RGD Arginylglycylaspartic acid

ROS Reactive oxygen species

RPA Replication Protein A

RPMI Roswell Park Memorial Institute Medium

RTCA Real Time Cell Analysis

SAT Spermidine/spermine N(1)-acetyltransferase

SD Standard deviation

ss Single-stranded

STING Stimulator of Interferon Genes

TAA Tumor Associated Antigen

TCR T-Cell Receptor

TF Transcription Factor

TGF Transforming Growth Factor

TLR Toll Like Receptor

TRAIL TNF-related apoptosis-inducing ligand

TNF Tumor Necrosis Factor

VPA Valproic Acid

VSV Vesicular Stomatitis Virus

VP Viral structural protein

VV Vaccinia Virus

Abstract

Over the past decade, cancer therapy has witnessed significant advancements, particularly in the field of oncolytic virotherapy. Oncolytic viruses specifically target cancer cells and trigger an immune response through immunogenic cell death. H-1 Parvovirus (H-1PV) is an oncolytic virus which has shown extensive potential in various cancer models. Phase I and IIa clinical evaluation of H-1PV in pancreatic cancer and glioblastoma has demonstrated a safe and non-toxic profile of the virus. The virus treatment showed initial signs of effectiveness, such as a shift in the tumour microenvironment towards improved immune response, effective distribution of the virus within the tumour bed, and overall better patient survival. However, it was also observed that monotherapy alone is insufficient for complete tumour eradication.

Thus, there is a need for improving H-1PV virotherapy. A promising approach involves the utilization of H-1PV in combination with other drugs. H-1PV has already shown promising results when combined with different drugs, especially HDAC inhibitor VPA and pro-apoptotic drug ABT-737. In this regard, this study aims to investigate the effects of combining clinically tested oncolytic H-1PV with two different classes of therapeutics- HDAC inhibitors and BH3 mimetics- in prostate cancer.

In order to identify an effective combination treatment, I adapted an assay to test the efficacy of the combination using a cell viability assay. My findings reveal that the combination of H-1PV with BH3 mimetic, pro-apoptotic drug ABT-737 is synergistic in killing PC3 prostate cancer cells.

The combination of H-1PV and ABT-737 was able to induce upregulation of activated caspase 3/7 and mitochondrial outer membrane permeabilization (MoMP) in PC3 cells, which are both markers of apoptosis. After rescuing the cells by using an apoptosis inhibitor, Z-VAD-FMK, I was able to confirm that H-1PV/ABT-737 combination was inducing an apoptotic cell death in PC3 cells. The dying cells were also expressing cell surface calreticulin, Hsp70 and Hsp90, which are all Danger associated molecular patterns (DAMPs) associated with an immunogenic cell death.

Moreover, I was able to show that the immunogenic cell death of PC3 cells triggered by the H-1PV/ABT-737 co-treatment was able to induce the maturation and activation of dendritic cells (DCs). These DCs were further capable of phagocytosis and T-cell priming, thus indicating that H-1PV/ABT-737 combination treatment

triggers the DC/T-cell axis in engaging the adaptive immune system for tumour clearance.

I could show that H-1PV and ABT-737 co-treated PC3 cells displayed an up-regulated cell surface expression of pro-cytotoxicity natural killer cell associated ligands, MICA/MICB, CD155 and ULBP 2/5/6. Furthermore, this was capable of inducing NK cell activation, engaging the respective cell cytotoxicity receptors, NKG2D and DNAM-1 on NK cells. Thus, accelerating NK cell mediated clearance of PC3 cells.

This impact was notably higher in the combination treated cells as compared to the individual therapies alone. This emphasizes the potential of the combination in enhancing immune cell-mediated clearance of the tumour.

Furthermore, the combination of H-1PV and ABT-737 was able to synergize in killing patient derived LuCaP 136 and LuCaP 147 cells, further cementing the potential of this combination across multiple cell types.

Overall, this study highlights the potential benefits of combining H-1PV with BH3 mimetic ABT-737 in improving the immune response against prostate cancer, thereby suggesting its potential as a valuable treatment strategy.

Zusammenfassung

Im zurückliegenden Jahrzehnt konnten in der Behandlung von Krebserkrankungen signifikante Erfolge erzielt werden, vor allem im Bereich der onkolytischen Virotherapie. Onkolytische Viren greifen gezielt Tumorzellen an und lösen immunogenen Zelltod aus. Das Parvovirus H-1 (H-1PV) hat in verschiedenen Modellen solche erfolgversprechenden onkolytischen Eigenschaften gezeigt. Klinische Tests (Phase I und IIa) mit Bauchspeicheldrüsenkrebs und Glioblastom bestätigten ein sicheres, nicht-toxisches Profil für H-1PV. Behandlung mit dem Virus zeigte erste Anzeichen von Effektivität, wie eine Veränderung der Mikroumwelt des Tumors im Sinne einer verbesserten Immunantwort, effektiver Ausbreitung des Virus im Tumorbett, und erhöhter Überlebensrate der Patienten. Allerdings zeigte sich, dass eine monofaktorielle Therapie für eine vollständige Entfernung des Tumors nicht ausreichend ist.

Ein möglicher Ansatz für eine nötige Verbesserung der H-1PV-Virotherapie ist daher die Kombination mit anderen Medikamenten. H-1PV hat bereits bewiesen, dass seine Effektivität in solchen kombinierten Behandlungen vielversprechende Steigerungen erfährt, vor allem mit dem HDAC-Inhibitor VPA und dem pro-apoptotischen Wirkstoff ABT-737. Meine Arbeit hatte zum Ziel, die Effekte zu studieren, die bei der Kombination von klinisch getesteten onkolytischen H-1PV mit zwei unterschiedlichen Therapeutika – HDAC-Inhibitoren und BH3-Mimetika – in der Behandlung von Prostatakrebs auftreten.

Um eine wirkungsvolle Therapiekombination zu identifizieren, wurde ein Versuchsaufbau angepasst, um die Effektivität verschiedener Kombinationen mittels Monitoring der Zellengesundheit zu messen. Die Befunde zeigen, dass die Verbindung von H-1PV mit dem pro-apoptotischen BH3-Mimetikum ABT-737 zu Synergieeffekten im Abtöten von PC3-Prostatakrebszellen führt.

Die Kombination von H-1PV mit ABT-737 führte zu einem Anstieg von aktivierten Caspasen 3/7 und mitochondrialer Membranpermeabilisierung (MoMP) in den PC3-Zellen, beides Anzeichen von Apoptose. Nach Konservierung der Zellen durch Nutzung eine Apoptose-Inhibitors (Z-VAD-FMK) konnte nachgewiesen werden, dass die H-1PV/ABT-737-Kombination den apoptotischen Zelltod der PC3-Zellen auslöste. Die absterbenden Zellen wiesen außerdem Calreticulin, Hsp70 und Hsp90 an der Zelloberfläche auf, die als Danger Associated Molecular Patterns (DAMPs) mit immunogenem Zelltod in Verbindung stehen.

Darüber hinaus konnte nachgewiesen werden, dass dieser von der Kombinationstherapie induzierte immunogene Zelltod auch das Wachstum und die Aktivierung dendritischer Zellen (DCs) begünstigt. Diese DCs sind zur Phagozytose und T-Zell-Priming in der Lage und legen nahe, dass die Kombinationstherapie mit H-1PV und ABT-737 die DC/T-Zellen-Achse aktiviert, die das adaptive Immunsystem zur Tumorentfernung anregt. Ich konnte zeigen, dass die so behandelten PC3-Zellen eine erhöhte Expression von Liganden an der Oberfläche aufwiesen, die mit pro-zytotoxischen natürlichen Killerzellen in Verbindung stehen (MICA/MICB, CD155 und ULBP 2/5/6). Darüber hinaus war es möglich, zu zeigen, dass die Behandlung in der Lage, ist natürliche Killerzellen zu aktivieren, indem die jeweiligen Zytotoxizitätsrezeptoren NKG2D und DNAM-1 auf den Killerzellen selbst angesprochen wurden – folglich beschleunigt dies die Entfernung von PC3-Zellen durch die natürlichen Killerzellen.

Dieser Effekt war merklich höher in jenen Zellen, die mit der Kombination behandelt wurden, als in den jeweiligen monofaktorierellen Therapien. Dies verdeutlicht das Potential der Kombinationstherapie, die natürliche immunogene Tumorbekämpfung zu verbessern.

Zusätzlich konnte das kombinierte Agens aus H-1PV und ABT-737 Erfolge in der Bekämpfung von Patientenzellen (LuCaP 136 und LuCaP 147) erzielen, was das Potential des Ansatzes noch stärker betont.

Insgesamt zeigte meine Studie das Potential auf, das in den positiven Effekten der Kombination von H-1PV und dem BH3-Mimetikum ABT-737 auf die Immunantwort gegen Prostatakrebszellen liegt, womit ein Weg zu einer möglichen verbesserten Therapie eröffnet ist.

Chapter 1

Introduction

1.1 Cancer and The Evolution of Cancer Therapeutics

Cancer is a global health conundrum. It was estimated that in 2020, it caused about 10 million deaths worldwide [2]. Cancer can be defined as a malignancy caused by uncontrolled division of cells, which leads to a formation of a mass of cells or a 'tumor'. Cancer cells, although homologous to non-cancerous cells, have very distinct metabolic pathways, owing to the accumulation of mutations that occur during tumor development, that have been attuned for an uninterrupted cell division. These altered pathways also ensure that cancer cells evade the immune system, through the silencing of innate immune or adaptive immune function, making tumor microenvironment dysfunctional for efficient immune clearance [3].

Surgical excision of a growing tumor remains one of the most important and efficient ways of treating most solid tumors. However, this is not effective in cases with non-localized tumors or metastasized tumors that report the re-occurrence of the tumor post-surgery [4]. At the turn of the 20^{th} century, treatment of cancer with radiation therapy emerged as an alternative or complementary anti-cancer strategy. Relying on the ability of ionizing radiation to obliterate genetic material of cells, thus halting cell division, radiation therapy was used in fractionated doses to treat tumors [5]. As the aberrant cell metabolism of cancer cells was understood in a better way in the next few decades, chemical intervention to eradicate these aberrant cells came to the forefront as a treatment option, a term later coined as chemotherapy. Most early chemotherapeutic interventions focused on killing cancer cells, and stopping the cell division [6, 7]. Surgical excision and a regimen of chemo and radiotherapy thus became a standard for conventional cancer therapy that was seen to be effective over a variety of cancer types, however not for all sub-types such as Non-Hodgkin Lymphomas [8]. Although this is effective in killing the cancer cells in some cancer models, it is also seen to have a multitude of challenges, primary being that of non-specific killing. Since cancer cells are homologous to the other cells in the body, any effort directed to the killing of cancer cells was toxic to the normal cells in the body, thus compromising

bodily functions and severe loss in quality of life of the patients. Thus restricting to doses such that they are non-toxic to normal cells. However this also may end up being ineffective for cancer eradication, causing failure in many cases. [6, 7].

Targeted approaches were thus required in tackling the management of cancer, while leaving the quality of life of patients relatively untouched, while improving efficacy higher therapeutic doses. Towards the second half of the 20^{th} century, cancer research saw an upsurge in newer and more targeted approaches to treat cancer. Cell and gene therapy [9], oncolytic virotherapy [10], immunotherapy [11] have since evolved as some of the next generation cancer therapeutics showing improved survival and quality of life for patients afflicted with a variety of malignancies. However, some cancer forms still remain incurable and their prognosis is very dismal [7].
Many of the newly evolved therapeutic approaches were based on biological observations about cancer, which were then looked-at with newer perspectives, over the next few decades, owing to advances in technological platforms such as genomics, DNA sequencing, metabolomics, etc. For instance, the use of viruses for treatment of cancer was a concept, which had seen its origins over 100 years before it emerged as a treatment option, as discussed in the following section.

1.2 Oncolytic Viruses (OVs)

1.2.1 A Brief History and State of the Art

In the late 1800s, it was observed that some cancer patients who contracted infectious diseases would suddenly go in remission for a short period of time [12]. In 1904, it was reported that in a case of Leukemia, infection with “flu-like” symptoms caused beneficial effects in the treatment. The “flu-like” symptoms would later be identified as an influenza virus infection. In 1912, parallel research in Italy showed that rabies vaccine infection caused a remission in cervical cancer [13]. These observations, although rudimentary, made the scientific community curious to explore this aspect of pathogenic infections on cancer.

Multiple clinical trials were conducted using human pathogenic viruses in the 1940s and 1950s. In 1949, 22 patients suffering from Non-Hodgkin’s lymphoma were administered extracts containing Hepatitis B virus. 7 out of these 22, showed improved clinical prognosis and 4 showed direct tumor regression [12, 14]. However, pathogenic nature of these agents in humans was a disadvantage that was detrimental to the prospect of using these viruses in clinics. Thus, animal viruses were then considered as options for developing viruses to treat cancer. For instance, avian paramyxovirus Newcastle Disease Virus (NDV), pathogenic in chicken, showed anti-tumour effects in an Ehrlich ascites carcinoma mouse model. A virus strain isolated from this batch of NDV, was found to be anti-neoplastic in humans and was purified, isolated and characterized thoroughly through the 1950s and 1960s to emerge as an anti-cancer virus [15]. Sim-

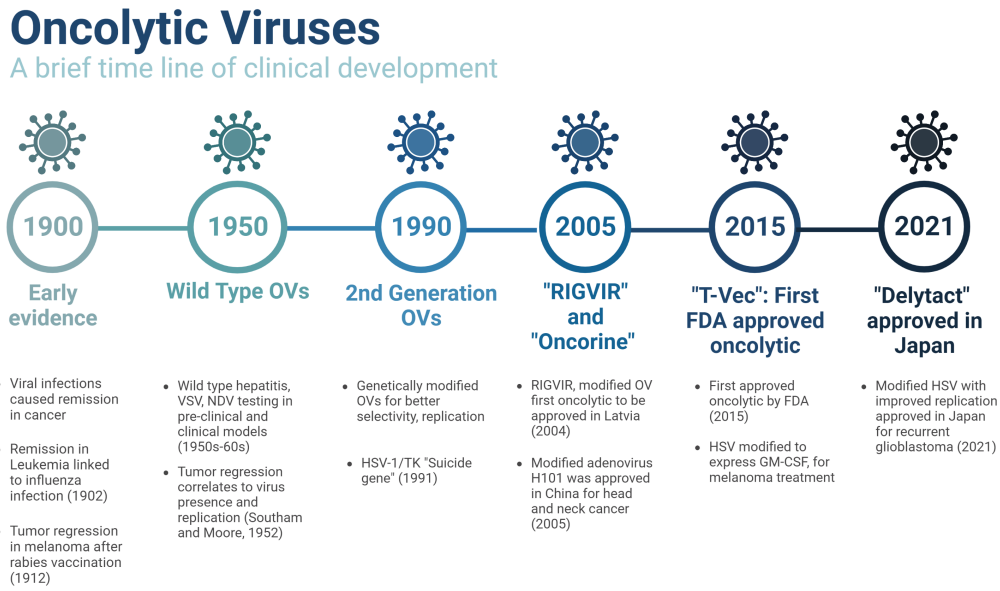

Figure 1.1: *Timeline for Oncolytic Virotherapy. Anti-cancer activity of viruses was observed in the early 1900s. After a thorough development of non-pathogenic (in humans) and more onco-selective viruses, four different oncolytic viruses, RIGVIR, Oncorine, T-Vec and now Delytact have received approval for cancer therapy. Illustration was created with BioRender.com.*

ilarly a variety of animal pathogenic viruses, were adapted as human viruses to treat cancer, such as Vesicular Stomatitis Virus (VSV) [16], Vaccinia Virus (VV) [17] and H-1 Parvovirus (H-1PV) [18] among others.

With the advent of DNA technology in the 1980s, more specific and less toxic oncolytic viruses were now also engineered to improve specificity, minimize toxic side effects on normal cells and to enhance the 'oncolytic' properties. Many of these viruses were non-pathogenic in humans, showed no pre-existing immunity and were more specific to cancer cells. A thymidine kinase-negative mutant of Herpes Simplex Virus -1 (HSV-1) was one of the first recombinant viruses to emerge as an effective virus therapeutic. It showed tumor regression in mouse models of glioma, with reduced neurotoxicity [19]. Through the 1990s, there were various species of viruses such as adenoviruses [20], paramyxoviruses [21], herpes viruses [22] and poxviruses [23] which were genetically engineered for cancer therapeutic purposes [12]. Through the early 2000s, a special sub-class of viruses thus emerged, termed as "oncolytic viruses", as a distinct class of novel therapeutics, which specifically targeted and killed cancer cells, while sparing the normal cells.

In 2004, Latvia approved the first oncolytic virus "RIGVIR", an Enetrovirus of the ECHO group type 7, which was naturally selected and adapted for the treatment of melanoma, although the approval was withdrawn in 2019 [24]. Closely following that, a modified adenovirus, with an E1B gene deletion, marketed as

"Oncorine" was approved in China in 2005 for head and neck cancer [25]. A successful Phase III clinical trial in Melanoma encouraged Talimogene laherparepvec (T-Vec) to be the first FDA approved oncolytic virus for melanoma therapy. It is a modified HSV-1, engineered to selectively replicate in cancer cells and harboring two copies of the gene encoding the cytokine GM-CSF with confer to the virus enhanced immunostimulatory properties [26]. Recently in 2021, a modified HSV-1 G47Δ (Delytact), with deletions for multiple genes for virulence and a better selectivity for cancer cells, was approved by Japan for the treatment of malignant glioma [27]. Currently, there are more than 400 ongoing clinical trials with 31 different kind of Oncolytic Viruses (OVs) [11]. Although most of them account for phase I/II, it is still a promising prospect for the future of oncolytic virotherapy.

1.2.2 Classification

There are different ways of classifying oncolytic viruses owing to their differences in genetic material, or their natural versus engineered propensity towards cancer cells. With respect to their genetic material, there can be two different kinds of viruses, DNA and RNA viruses. DNA and RNA viruses further can be classified as enveloped viruses and non-enveloped viruses [28] (Figure 1.2). In the realm of oncolytic viruses, enveloped DNA viruses include poxviruses and herpes viruses where as non-enveloped DNA viruses group adenoviruses and parvoviruses. All currently approved and available oncolytics in the market are DNA viruses, two being modified HSV-1s and the other being a modified adenovirus.

Oncolytic RNA viruses are slightly more diverse than DNA viruses. Enveloped RNA viruses include four different classes: paramyxoviridae, rhabdoviridae, togaviridae and orthomyxiviridae. Non-enveloped RNA viruses that are oncolytic in nature comprise of two classes, reoviridae and poxviridae. NDV, VSV, Reovirus, Measles virus are among the widely studied RNA viruses for their oncolytic properties.

DNA and RNA viruses differ in their mode of replication as well as their stability, oncolytic activity and capacity to induce immune responses. DNA viruses are more stable than RNA viruses, as RNA is more volatile molecule by virtue. RNA viruses are generally more immunogenic than DNA viruses as the presence of viral RNA in cytoplasm triggers a more potent anti-viral immune response, making them easily detectable. Since RNA viruses do not require integration into the host genome, as opposed to some DNA viruses, they are more preferred "gene expression" vessels than DNA viruses [29]. Irrespective of the genetic material of the virus, the propensity of the virus towards the host cancer cell is a very dynamic process and it varies from virus to virus. The unique property of oncolytic viruses is however the selective ability of the virus to infect and lyse a cancer cell, while sparing the normal cells.

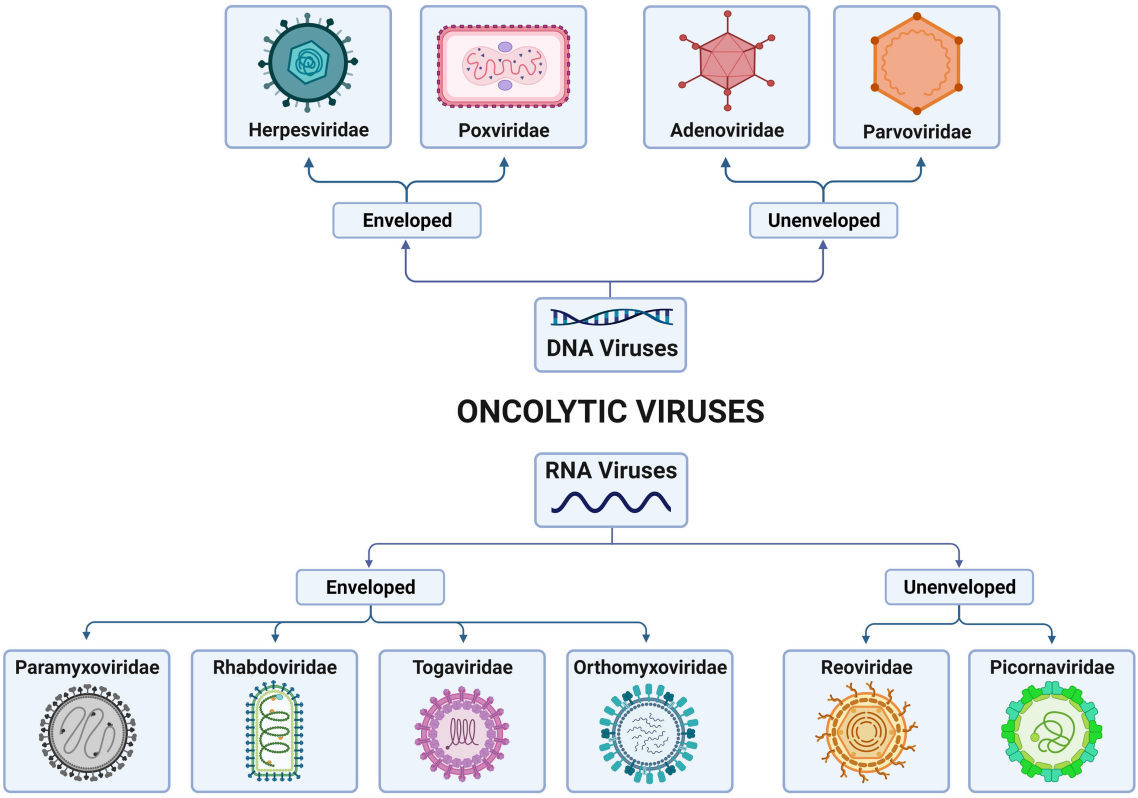

Figure 1.2: *Classification of Oncolytic viruses based on their genetic material. Figure adapted from [28]*

1.2.3 Oncotropism

"Oncotropism" is the capability of oncolytic viruses to selectively target cancer cells (Figure 1.3). This virtue is present inherently in some viruses such as the measles virus [30] and parvovirus [31]. Oncotropism can also be a direct result of virus adaption, as seen in NDV or Reovirus. Oncotropism can also be induced by genetically modifying the virus in its ability to either enter or replicate in cancer cells, as seen in T-Vec [26] or H-1PV expressing RGD4C peptide [32] Either way, this property of the viruses directly correlates to their ability to utilize the aberrant molecular and cellular properties of cancer cells.

One of the common ways through which oncolytic viruses are able to infect and kill cancer cells is exploiting the impaired innate immune pathways in cancer cells. For instance, NDV exploits the defective type I interferon signaling to infect and lyse cancer cells. In normal cells, the double stranded RNA molecule of NDV triggers the type I interferon signaling, through accumulation of Protein Kinase R (PKR). This shuts down the virus infection and calls for immune clearance. However, since cancer cells have a defective signaling, there is an increased sensitivity for NDV infection in cancer cells [33] (Figure 1.3). The immune evasion of NDV also comes from the fact that NDV does not have preexisting immunity in humans, since it is an avian virus.

Certain oncolytic viruses rely on aberrant cell signaling of cancer cells as a means for infection. Oncolytic reovirus relies on the Ras signaling in cancer cells

for a successful infection. Epidermal Growth Factor Receptor (EGFR) activates Ras signaling which is crucial for countering a double stranded RNA dependent kinase, in turn promoting viral replication. EGFR is one of the most common oncogenic protein in humans, thus facilitating the oncolytic infection of these cells by reovirus [34].

Certain OVs such as rodent parvoviruses require transcription factors and cell metabolites, usually present in highly proliferating cells, to facilitate viral replication [35]. Some of these cellular factors, such as Protein Kinase C eta H/Protein Kinase Cη (PRKCH/PKCη) are also required for carrying out post-translational modifications of viral proteins. PRKCH/PKCη are overexpressed in many cancer types, thus making these cancer cells susceptible to oncolytic parvovirus infections. [35].

Apart from being selective towards cancer cells, Oncolytic viruses also possess the unique ability to induce immune cell responses against cancer, as a bystander effect of the incurred oncolysis.

1.2.4 Oncolytic Viruses and Immunotherapy

Immunogenic Cell Death (ICD)

Oncolytic viruses are capable of infecting cancer cells, replicate using the host machinery and eventually cause cell lysis to release viral progeny. Furthermore, this cell lysis has a very crucial bystander effect, especially in immunotherapy. As the cell lysis occurs, it releases some cellular material into the tumor microenvironment. This cellular material contains the viral progeny particles along with viral DNA/RNA and remnant proteins.These are also known as “Pathogen Associated Molecular Patterns (PAMPs). However, along with viral cargo, a lot of host cell material is also released into the extracellular space. This contains certain characteristic proteins and molecules, which are termed as “Danger Associated Molecular Patterns (DAMPs)”. These molecular signals (DAMPs/PAMPs) attract and engage with immune cells, triggering a cascade of immune activation and clearance at the tumor site. Such a cell death event is defined as an “Immunogenic Cell Death (ICD)” [36] (Figure 1.3). The DAMPs can be different forms of molecular signals imparted by dying cells such as,

- Translocation of intracellular proteins to the cell membrane, such as calreticulin [37], Hsp70/90 [38]
- Secretion of otherwise intrinsic proteins, such as HMGB-1 or Annexin I [39]
- Release of metabolites, such as extracellular ATP [40]
- Secretion of cytokines, such as type I IFN or CXCL-10 [41]

Different triggers and inducers of cell death will dictate the expression of different types of DAMPs for each cell type.

Cancer cells are known to have multiple mutations in their DNA, which leads to yet unique metabolic and proteomic signature of the cancer cells as compared to the normal cells. This property helps in the marking the cancer cells as “non-self” and in advent of an immune surveillance and can be exploited to identify and clear tumor cells. These mutated proteins are also known as ”Tumor Neo-antigens” [42]. There are also certain proteins which are over-expressed or aberrantly expressed in cancer as compared to normal cells. Such aberrant proteins are known as ”Tumor Associated Antigens” (TAAs) [43]. Through the general cell lysis triggered by oncolytic viruses, these tumor neo-antigens and TAAs are also exposed to the extracellular space, which then can be picked up by Antigen Presenting Cells (APCs), to trigger a T-cell immune cell response against the tumor [42].

Cell lysis induced release of DAMPs/PAMPs, TAAs and tumor neo-antigens causes the infiltration of immune cells to the site of cell death. These proteins, expressed on the surface of the lysing cell or released in the extracellular space are known to trigger “Pattern recognition receptors (PRRs)” on infiltrating immune cells [44]. Dendritic cells (DC) express a high repertoire of Pattern recognition receptors (PRRs) on their surface, which then engage with these DAMPs.

Many oncolytic viruses have been reported to trigger ICD in different cell types [44]. For instance, measles virus was shown to upregulate the expression of a range of pro-inflammatory cytokines associated with type I IFN signaling including IFNα/β, RANTES and IL-28, in melanoma cells. It also triggered the release of HMGB-1 in these cells, characterizing the cell death to be an ICD event. This further triggered the activation of DCs, T-cells and NK cells on the advent of virus infection [45]. H-1PV, an oncolytic parvovirus, was able to induce ICD in pancreatic cancer cells by substantial secretion of HMGB-1 and IL-1β, although no effect was seen on the expression of CRT or ATP release [46]. This goes on to show that a few, not all factors are necessary to characterize a cell death as ICD and this ICD is sufficient in inducing activation of a functional immune response downstream. (Figure 1.3)

Dendritic Cells and T-cell axis in Oncolytic Virus Therapy

Dendritic cells (DCs) are a heterogeneous population of antigen presentation cells (APCs). CD34+ Hematopoietic Stem Cells (HSCs) in the bone marrow form myeloid as well as lymphoid precursors. Myeloid precursors differentiate into monocytes, macrophages and a pre-DC precursor, which are capable of differentiating into functional dendritic cells of different kinds. These DCs have a phenotypical and functional profile of immature DCs and these then mature on encountering pathogens or pro-inflammatory signals [48, 49]. Mature DCs cells take up, process and present antigens to trigger and maintain an innate and adaptive immune response. T-cell mediated cytotoxicity is dependent on antigen presentation by DCs. The chemokine and cytokine release through DC activation such as IL-12p40, MIP

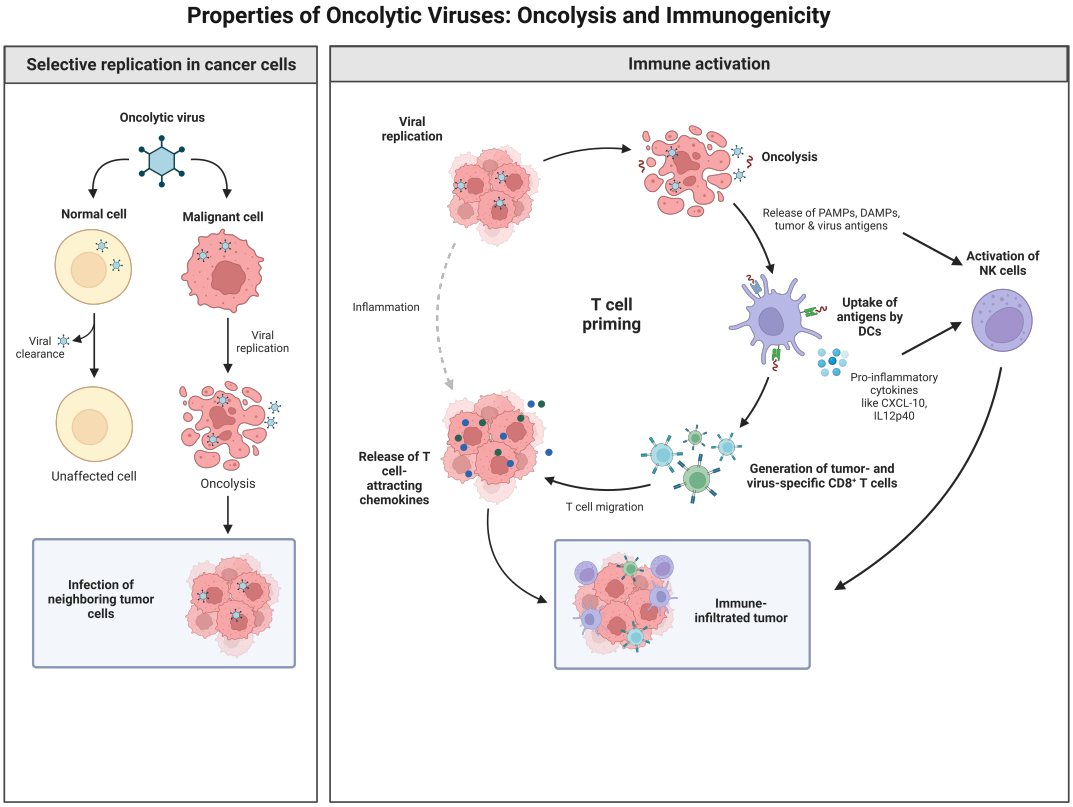

Figure 1.3: *Oncolytic viruses: Mechanism and OV induced immune activation of tumor microenvironment. Left panel- Oncolytic viruses specifically target cancer cells, while sparing normal cells. Right Panel-Oncolytic virus infection induces an immunogenic cell death associated with the release of certain Danger or Pathogen Associated Molecular Patterns (DAMPs/PAMPs). These DAMPs, PAMPs and TAAs then engage with the Pattern Recognition Receptors (PRRs) on antigen presenting cells such as DCs and eventually trigger T-cell activation to induce tumor cell clearance. Virus infected cells also induce NK cell activation through associated cytotoxic ligands expressed on the cancer cells. This results in NK cell mediated clearing of these infected cancer cells. Illustration was created with BioRender.com. Template adapted from [47].*

and MCP are also responsible for activating Natural Killer (NK), NKT cells and neutrophils. Thus making DCs crucial for anti-tumor immunity, with not just antigen presentation but also through the release of various pro-inflammatory cytokines and chemokines in the tumor microenvironment [49, 50].

However, the immunosuppressive nature of the tumor microenvironment impairs the DC function thus hindering a step in anti-tumor immunity. Oncolytic virus induced cell death however is one of the mechanisms by the virtue of which DC function can be restored. [51]

Viral progeny, proteins and genetic material released through oncolysis (PAMPs) are recognized by DCs and triggers the Toll Like Receptors (TLRs) signaling, inducing the secretion of type I IFN. DCs can also engage via TLR independent signaling pathways such as Protein Kinase R (PKR) or retinoic acid-inducible gene 1 (RIG-I) which are also capable of detecting viral dsRNA molecules. These pathways too trigger the release of type I IFN and an anti-viral immune response [52]. Virus induced cell death also accounts for DAMPs which are essentially cellular factors which if expressed on the surface of cells or released by dying cells are recognized by DCs as “find me” and “eat me” signals.

For instance, ATP is released by dying cells in an ICD event. Extracellular ATP then acts a classical a “find me” signal, binding to the purinergic receptor P2Y2 (P2RY2, a metabotropic receptor) on DCs, ultimately facilitating the recruitment of DCs and macrophages into the tumor microenvironment [29, 53]. Another important DAMP, calreticulin when expressed on the surface of cells during an ICD event, acts as an “eat me” signal. It binds to LDL-receptor related protein 1 (LRP1 or CD91) on DCs which triggers phagocytosis the dying cells for antigen processing [37]. Similarly different DAMPs engage with the PRRs on DCs triggering the activation of co-stimulatory molecules, CD80 and CD86 [54]. OVs such as reovirus [55], measles virus [45], HSV [56] and vaccinia virus [17] have been reported for also inducing the secretion of cytokines in these activated DCs. Although OVs can naturally trigger the DCs, there are engineered OVs that have been constructed specifically for DC activation. Oncolytic adenovirus has been engineered to express growth factors such as GM-CSF or cytokines such as RANTES aid in enhancing the effect of DC activation [57].

Activated dendritic cells also secrete IL-12/p40, which is an important cytokine for Natural Killer (NK) cell activation as well. DCs promote NK cell activation, proliferation and NK cell mediated cytotoxicity through the release of cytokines as well as direct cell-cell interactions ([58]. Thus, DC activation is an important event not only for adaptive, T-cell responses but also for engaging other immune cells. Thus, an otherwise immunosuppressive tumor microenvironment that is non-conducive to DC function can be made pro-inflammatory through OV infection and OV induced ICD. (Figure 1.3)

Activated dendritic cells then can act as antigen presentation cells to trigger the cytotoxic effect of T-cells, which is one of the primary functions of DCs. These

activated DCs subsequently migrate to lymph nodes for priming of T-cells [59]. The priming of T-cells occurs in the lymphoid tissue. T-cell activation requires three important steps,

- Major Histocompatibility Complex (MHC) mediated antigen presentation by APCs,
- Co-stimulation through CD80/CD86 on the APCs and CD28 on T-cells
- Cytokines produced by APCs. For instance, IL-12 and IFNα/β can act as a stimulatory factor for CD8+ T-cell activation

Some of the cell surface markers present on primed DCs such as CD80, CD86 and CD40 act as co-stimulatory molecules for T-cell activation [59]. DCs which are then able to phagocytose antigens are eventually are able to induce T-cell activation and T-cell mediated cytotoxicity, in an MHC-I dependent manner. These antigens presented on the MHC complexes on APCs are then recognized by T-cell receptor (TCR) complexes present on the surface of CD8 T-cells. TCR complexes are a combination of TCRα/β chains as well as CD3 subunits present on the surface of the cells. VDJ recombination process enables the generation of unique and specific TCRα/β chains, which are majorly responsible for binding to antigen and MHC complexes. Thus, TCR complexes are antigen specific and each unique TCR will generate a specific population of T-cells engaging to a specific antigen-MHC complex. TCR engagement is an important step and triggers downstream signaling cascades to induce T-cell differentiation, activation, proliferation and survival [59, 60]. Thus, through an intricate interaction with the APCs, T-cell priming and activation occurs. These T-cells then migrate to the tumor site to engage with the respective infected cancer cells. Thus, through an intricate interaction with the APCs, T-cell priming and activation occurs through a cascade of cell signaling occurring in T-cells. These activated T-cells then migrate to the tumor site to engage with respective infected cancer cells.

Activated dendritic cells also secrete IL-12/p40, which is an important cytokine for Natural Killer (NK) cell activation as well. DCs promote NK cell activation, proliferation and NK cell mediated cytotoxicity through the release of cytokines as well as direct cell-cell interactions [58]. Thus, DC activation is an important event not only for adaptive, T-cell responses but also for engaging other immune cells.

OV infection mediated activation of DCs, thus is able to convert a cold tumor immune microenvironment to a hot tumor immune microenvironment (Figure 1.3).

Natural Killer Cells in Oncolytic Virus Therapy

Innate immunity forms a major part of immune response against pathogens. Natural Killer cells in particular, form a large sub-type of lymphocytes, which are involved in the immune response against pathogens, and pathogen infected cells.

Similar to T-cells, NK cells have the ability to exact a cytotoxic effect on infected cells, albeit without the pre-requisition of antigen presentation. This effect of NK cells is not limited to pathogen infected cells, but also extends to tumor cells [61]. Absence of NK cells has been previously linked to spontaneous tumor formation in mouse models, highlighting the importance of functional NK cells in the context of anti-tumor immunity [62].

Although NK cell mediated cytotoxicity is independent of antigen presentation, it is regulated via a repertoire of regulatory receptors present on NK cells as well as on the surface of the target cells (cancerous or infected cells). The target cells upon infection or altered cell metabolism in case of cancer, activate various signaling pathways such as the IFN-I, RIG-I, C/GAS-STING signaling. This causes the upregulation of pro-cytotoxicity markers on the target cells, such as CD155 or CD112. This is also associated with release of pro-inflammatory cytokines such as IFNα/β. These receptors then trigger the activation of cytotoxicity receptors present on NK cells, such as NKG2D or DNAM-1. This in combination with the cytokines triggers cytotoxic signaling pathways [61]. NK cells will then kill the target cells either through

- the release of perforin and granzyme granules, puncturing the cell membrane of the target cells eventually lysing them,

- engagement of the death receptor mediated apoptosis through CD95/Fas and TRAIL signaling

NK cells, like other immune cells in the tumor microenvironment, are usually present in an immunosuppressed state. However, through OV infection and lysis, NK cells are able to engage and trigger an anti-viral immune response against the infected cancer cells.
NK cells have also been reported to aid in OV mediated cell clearance for multiple types of OVs. Oncolytic HSV, for instance, has been shown to improve NK and T-cell recruitment, release of pro-inflammatory cytokines as well as a mild decrease in regulatory T-cells, in a melanoma model [63]. Oncolytic Reovirus has also been reported to increase the infiltration of NK and T-cells to the tumor site in a clinical prostate cancer model. These cells were also shown to be functional in clearing infected tumor cells [64]. Oncolytic H-1PV was shown to improve NK cell mediated killing in pancreatic cancer cells, with the production of pro-inflammatory cytokines [65].

All of this evidence points to the fact that OV infections aid NK cell activation, which plays a crucial role in immune based clearance of cancer cells. (Figure 1.3).

1.3 Oncolytic H-1PV

1.3.1 Introduction

H-1 is a non-enveloped, single strand DNA virus, belonging to the family *Parvoviridae* and genus *Protoparvovirus*. The natural host of this virus is a rat in which it causes neonatal and fetal lethality in infected females.

H-1PV is one of the smallest parvoviruses, 25nm in diameter. The virus has a concise 5kb genome, which includes two gene units encoding for non-structural (NS) and viral capsid proteins (VP). Two different promoters transcriptionally regulate these gene units. P4 early promoter regulates the NS gene unit encoding for the non-structural proteins, NS1 and NS2 that are involved in cellular toxicity and virus replication whereas the P38 late promoter regulates the expression of the VP gene encoding the VP1 and VP2, structural proteins and SAT1 nonstructural protein. The gene structures and promoter units are flanked by unique palindromic sequences, at the right (250nt) and left (120nt) terminus. These palindromic sequences have been shown to be crucial for viral replication [18] (Figure 1.4).

The NS1 protein of H-1PV is very crucial for regulatory functions of the virus life cycle. The 83kDa protein is mainly located in the nucleus, with a DNA binding domain and a transcriptionally activating domain for regulating the P4 and P38 promoters. NS1 plays a major role in virus DNA replication and transcription, and its activities are modulated by post-translational modifications that are important to ensure the DNA binding capacity of the protein and the regulation of virus transcription. The NS1 protein also is the main trigger of H-1PV-incuced oncotoxicity. Its expression is associated with oxidative stress, ER stress and DNA damage, which contribute to lyse the cell, and releasing the viral progeny into the tumor microenvironment.

VP1 and VP2 are structurally similar proteins, which are the components of the viral capsid. The major difference between the two proteins is that VP1 includes a unique phospholipase A (PLA2) region at its N-terminus. It has been shown in parvoviruses that this domain is important for cytosolic transfer of the viral genome from the late endosomes to the nucleus creating the right conditions for the viral replication. These sequences are highly conserved within the genus [66].

1.3.2 Cell-entry, Viral Replication and Egress

H-1PV cell-entry is mediated by Galectin-1 and Laminin $\gamma 1$ on the cell surface. The sialic acid residues presented by laminins play a key role in the virus binding and entry process [67, 68]. The virus then enters into the cell through clathrin-mediated endocytosis, an event that requires dynamin and an acidic pH as well as excision of the vesicle into the cytosol. The PLA2 region of the capsid proteins

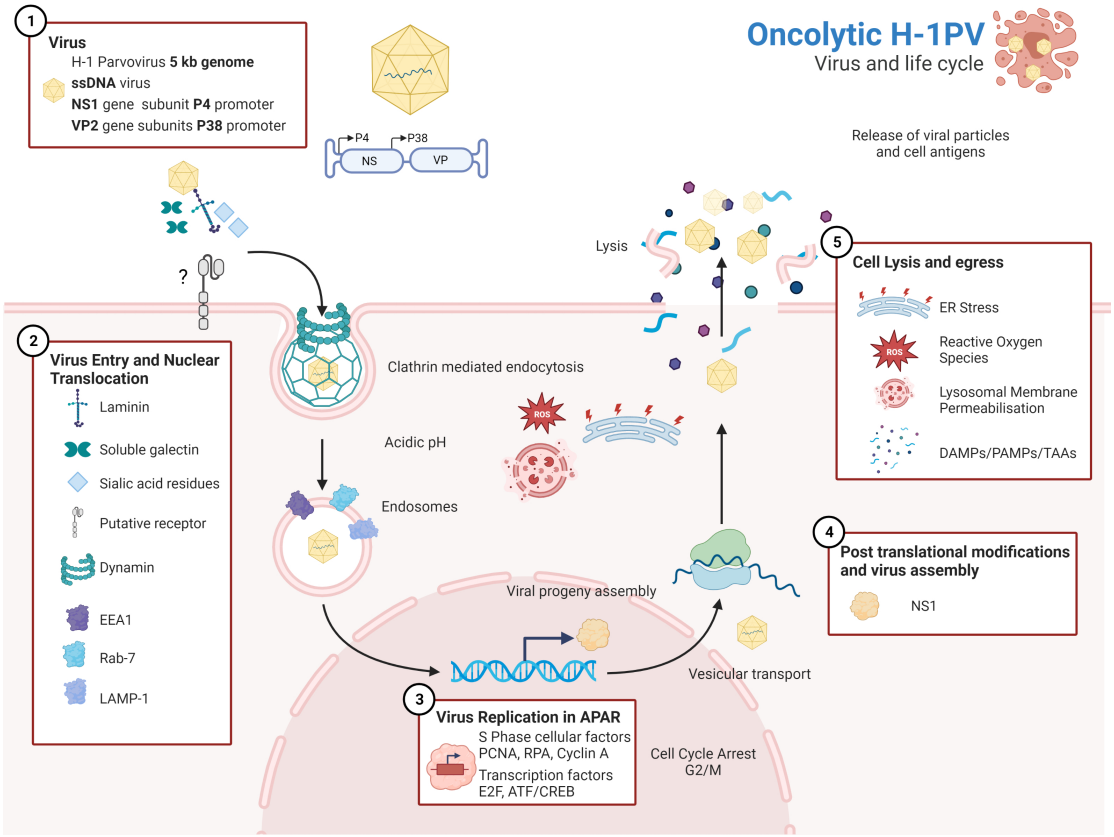

Figure 1.4: *Oncolytic H-1PV: Lytic life cycle, cell entry to cell lysis and egress. H-1 is an oncolytic parvovirus, with a modest 5kb genome encoding NS1 and VP2 gene subunits. H-1PV has been shown to mediate cell entry through interactions between laminin, soluble galectin. The virus then enters the cell through clathrin mediated endocytosis. H-1PV trafficking occurs through endosomes, with a requirement for an acidic pH. After nuclear translocation, NS1 mediated virus replication occurs in "Autonomous Parvovirus-Associated Replication (APAR)" space in the nucleus. Host cellular factors are recruited for this replication and vesicular transport aids in egress of the virions in the cytosolic space, along with host cell lysis. Virions along with Danger/Pathogen Associated Molecular Patterns (DAMPs/PAMPs) and Tumor associated antigens (TAAs) are then released in the extracellular space thus completing the virus life cycle. Illustration was created with BioRender.com.*

then facilitates the cytosolic release of the viral particles, through degradation of the endosomal membrane. Since the capsid size is very small, it has been suggested that they transport directly through the nuclear pore complex (NPC) [69].

Virus replication is a dynamic process, which occurs in the host cell nuclear space called "Autonomous Parvovirus-Associated Replication" (APAR). Replication is heavily dependent on the S-phase cellular factors such as Proliferative Cell Nucleus factor (PCNA), Replication protein A (RPA), DNA polymerases and cyclin A [70]. These factors are recruited for the viral replication in the APAR bodies. Thus, virus DNA synthesis and virus gene transcription requires the host cells to be in a proliferative S-phase state for successful infection. The single stranded viral DNA is first converted to a double stranded, which is then used as a template for viral mRNA synthesis. Double stranded DNA molecules as well as viral genomes are then produced inside the nucleus. NS1 and NS2 expression is triggered by transcription factors such as E2F, ATF/CREB among others, which are also usually present only in highly proliferative cells. Once the NS1 is expressed, it triggers the P38 promoter, initiating the expression of the capsid proteins. NS1 is also then responsible to carry out the capsid formation and virus assembly through engagement with RPA and transcription factors such as TFIIA [35]. Once the capsids are formed, the virions are then egressed into the cytosolic space through vesicular transport involving the endoplasmic reticulum and Golgi complex [69, 71].

In order to facilitate viral DNA replication, the host cell undergoes cell cycle arrest to shut down cellular replication. The viral replication also induces a general genotoxic and ER stress on the cell, which when coupled with the cell cycle arrest induce cell lysis and release of virus particles. However, each cancer cell type is different, with a different metabolic fingerprint. Thus, naturally the susceptibility of each cell to a virus will vary according to the genetic and molecular signatures of the cell. Depending on the type of cells, H-1PV is known to induce different kinds of cell death pathways. In pancreatic cells, it has been shown to be apoptosis [72] where as in glioma cells it has been shown to induce an alternative cell death pathway involving cathepsins [73].

1.3.3 An Immune Perspective to H-1PV Based Therapy

Although H-1PV selectively target and kills cancer cells, it is still able to infect different populations of non-cancerous cells, e.g. Immune cells such as DCs, T-cells, NK cells and Macrophages. However, these infections are always abortive and do not result in virus production or cell lysis [74]. H-1PV infection is still able to activate immune cells and trigger cytokine production. PBMCs from healthy human donors when infected with H-1PV were able to show an upregulation of maturation and activation markers as well as induce the release of pro-inflammatory cytokines such as IFNγ and TNFα. H-1PV infection was also able to induce CD4+ T-cells activation and IL-2, IL-4 and IFNγ release [74]. This property of the virus

makes it a viable option to trigger activation of immune cells in the tumor microenvironment, which are otherwise dormant because of tumor immune evasion mechanisms.

H-1PV has been shown to be effective in infecting many kinds of neoplastic cells [46, 72, 75–79]. As a direct consequence of H-1PV mediated oncolysis, immune cells are engaged to further enhance the anti-cancer activity of the virus. Although H-1PV does not trigger the production of type I IFN, it is able to induce markers for ICD in different cancer cells, thus engaging the ICD-induced bystander immune response against the cancer. H-1PV infection in melanoma cells induced a release of Hsp72, which is one of the important markers for ICD [80, 81]. It has been shown to induce DC and NK cell activation. It was further shown that H-1PV infection of these melanoma cells was also able to induce the upregulation of CD80 and CD86, co-stimulatory markers in DCs required for T-cell activation [81]. This upregulation was also associated with cytokine release by DCs. These activated DCs also showed an upregulation in TLR3 and NFκB signaling, which is classically associated with a pro-inflammatory response. H-1PV induced cancer cell lysis was associated with the activation of DCs, which were further shown to be functional in their ability to present antigens to T-cells [81].

H-1PV infection of colon carcinoma cells and pancreatic cells was also able to induce enhanced NK cell activation and engagement. H-1PV infection resulted in the upregulation of NK cell activating ligands that led to the increased NK cell activation and NK cell mediated cytotoxicity of these cancer cells. These activated NK cells were able to release pro-inflammatory cytokines such as IFNγ, TNFα and MIP-1 [82]. Thus, overall H-1PV infection has been shown to be favorable for generating an anti-cancer immune response, either through the direct interaction with immune cells or via virus induced cell lysis with trigger anticancer immune responses.

1.3.4 Clinical Evaluation of H-1PV

For the past two decades, H-1PV has been extensively evaluated in a preclinical context in different rodent models of cancer, including melanoma [81, 83, 84], breast cancer [78], glioblastoma [73, 76, 77], pancreatic cancer adenocarcinoma (PDAC) [46, 83]and cervical cancer [79] among others. These studies attested to the promising efficacy of the virus against a repertoire of cancer cells. (Figure 1.5) Two of the noteworthy models for H-1PV have been glioblastoma and pancreatic ductal adenocarcinoma.

Glioblastoma is a fast-growing and aggressive brain tumor with a dismal prognosis and median survival of less than one year [85]. In immunocompetent and immunodeficient rat models of glioblastoma, H-1PV showed specificity and improved survival, with both intravenous as well as intra-tumoral and intra-nasal administration of the virus [72, 76, 77]. These results highlight that systemic delivery of the virus is possible with a fraction of the initial dose of the virus reaching

the tumor site. Probably, also favorited by its small size, H-1PV is capable of crossing the blood brain barrier; the tumor regression observed in immunocompetent rat models was higher as compared to the ones in the immunodeficient ones, and showing the contribution of immune cells to H-1PV mediated anti-cancer activity.

Similar to glioblastoma, PDAC is a form of aggressive disease associated with poor prognosis and quality of life [86]. A single dose of H-1PV in a rat model for PDAC caused a delay in tumor growth and improved survival. As seen in the glioblastoma models, immunocompetent models showed better efficacy than immunocompromised models, once again highlighting the involvement of the immune system in H-1PV mediated therapy. This was attested by H-1PV induced strong release of ICD factor HMGB-1 in PDAC cells [46].

Owing to the success of the preclinical validation, H-1PV was assessed in glioblastoma and PDAC harboring patients in two separate clinical trials were set up to evaluate the safety, toxicity and efficacy of H-1PV in these models.

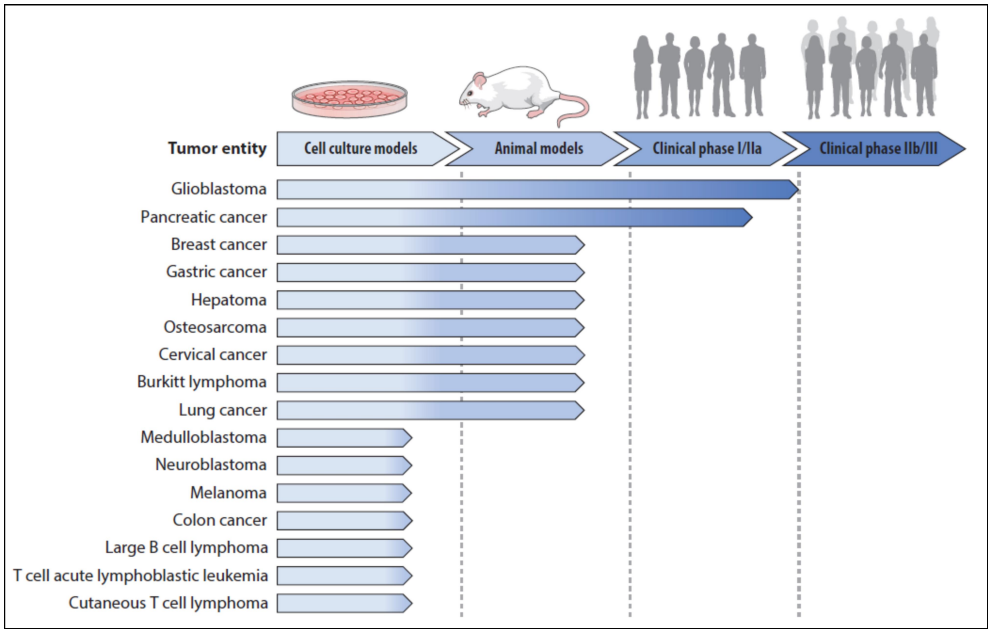

Figure 1.5: *Preclinical and clinical development of H-1PV. Adapted from Hartley, et al.*

In 2015, a Phase I/IIa clinical trial, ParvoORYX01, in recurrent glioblastoma showed that H-1PV was safe, tolerable and non-toxic to the 18 patients enrolled in the trial. The virus was able to cross the blood brain barrier to reach the tumor site and showed preliminary results of efficacy, through an improvement of the progression free survival in the patients in comparison with historical results. The virus therapy was also able to induce a favorable conversion of the tumor immune microenvironment through specific T-cell responses [87].

A second more recent clinical trial, which concluded in 2019, used wild type oncolytic H-1PV to treat inoperable metastatic PDAC. This Phase 2 trial showed H-1PV to be tolerable and non-toxic in all seven patients that were administered the virus treatment. T-cell responses were observed for viral proteins, but an overall favorable immune modulation was also reported for the tumor microen-

vironment, through pronounced infiltration of T-cells with a doubling of the T-cell density post virus treatment. Patients who showed favorable response to the virus treatment also showed increase in pro-inflammatory cytokines such as IL-8, IL-9 and IL-12 [88].

The success of both these Phase IIa trials for H-1PV set a promising precedent for further systemic clinical evaluation of H-1PV.

1.3.5 Caveats and Outlook

Although H-1PV has been one of the extensively studied OVs, it does not come without limitations.

H-1PV cell entry has been recently described and reveals important information about the oncoselectivity of the virus and predilection towards different cell types. However, it is still a matter of perusal as to why certain cell types are sensitive towards H-1PV infection where others remain semi-permissive or completely refractory. This property of the virus may be due to difference in cell signaling pathways, availability of cell entry factors, blocks at the level of replication or just a general block of cell death pathways required for cell lysis. Thus, H-1PV alone cannot be used universally across different cancer cell types.

The clinical evaluation of H-1PV, although met the study endpoints of safety and toxicity, was unable to completely eradicate tumors. Thus highlighting the fact that although H-1PV monotherapy might be effective, it is not sufficient as a standalone therapy. Thus, there is a need for improving H-1PV therapy which can be achieved through various strategies,

- by exploring the virus life cycle and understanding the discrepancies in cell susceptibilities to virus infection.
- by generation of second generation H-1PV mutants, which are better at targeting cancer cells, or show improved oncolysis, show improved immunogenic potential through harboring immunogenic transgenes.
- by combining H-1PV with already available chemotheraputics, radiation therapy and immunotherapeutics for improved oncolysis and immunogenicity.

Studying the virus life cycle is an important approach for improving H-1PV based cancer therapy which will aid in translational applications such as patient stratification based on positive or negative modulators of the virus life cycle. However, this is a time consuming process and may take years of dedicated efforts, to develop high throughput, time effective methods to achieve the objectives. The approach of generating second generation viruses would also require a lot more screening since getting the safety and toxicity of a mutant variant will need thorough investigation from scratch. Thus, the use of combination therapy seems like a logical, time effective approach to improve the potency of wild type oncolytic H-1PV for now.

1.3.6 H-1PV: Combination with Other Chemotherapeutic Drugs

There already have been multiple studies showing the potential of combination therapy in improving H-1PV potency.

The combination of H-1PV with gemcitabine has been reported to improve the cell killing in PDAC cells. This cell death was shown to be immunogenic and H-1PV was able to induce the release of HMGB-1, an important marker for ICD. The combination of H-1PV and Gemcitabine was able to induce ATP release in some PDAC cultures, which was not seen in standalone treatments [46].

H-1PV has also been shown to be effective when combined with checkpoint inhibitor anti-CTLA4 in melanoma cells. This combination was able to induce DC maturation and activation. This combination also enhanced IFNγ and TNFα release by these activated DCs, which concurred with a decrease in anti-inflammatory TGFβ. Furthermore, the combination of H-1PV with checkpoint inhibitors was able to induce the activation of cytotoxic T-cells and cytokine release [84].

H-1PV when combined with HDAC inhibitor Valproic Acid (VPA) was able to synergistically kill a range of cervical and pancreatic carcinoma cells. This cell death was associated with induction of oxidative stress, DNA damage and apoptosis. The study also showed that VPA treatment was able to enhance the acetylation of NS1 protein, thus modulating NS1 mediated transcription and cytotoxicity [79].

Previous work from the lab also shows that the combination of H-1PV with BH3 mimetic ABT-737 was able to enhance virus-mediated oncolysis in 12 glioblastoma cell lines and 19 cell lines derived from mainly pancreatic cancer but also colon, cervical, lung, head and neck and breast cancer. This combination was also effective in upregulating the markers for an immunogenic cell death such as cell surface calreticulin, HMGB-1 and ATP release (unpublished data).

These studies indicate that combination of H-1PV with different pre-existing chemotherapeutics could be beneficial in improving the oncolytic property of the virus and induce a better immune cell activation through a bystander effect. H-1PV can also be used to impart an immunogenic characteristic to a treatment that is otherwise not able to do so.

Chapter 2

Aims of the Project

Based on the previously available data, I decided to set the aim of my PhD project as, "To identify combination therapies based on H-1PV and other drugs against prostate cancer. These combinations should

- have enhanced killing activity than monotherapy (of the drug or H-1PV);
- be able of inducing an immunogenic cell death and engage the immune system components to act against tumor cells

If successful, this study could pave the way for further testing the combination at preclinical level (e.g. in appropriate animal models) and eventually clinical studies as improved therapeutic intervention than H-1PV alone." To achieve the ultimate objective of my project, the following goals were set:

Goals

Goal 1: Identify a drug that potentiate the oncolytic activity of H-1PV.

Prostate cancer as a model

Prostate cancer is the second most commonly diagnosed cancer in men. Although most prostate cancer cases are curable, it can still impend long-term health complications [2]. While a fraction of patients eg. with melanoma or lung cancer, seem to benefit for immunotherapy, this is not the case in prostate cancer and there are clinical studies still ongoing to optimize immunotherapy approaches for prostate cancer [89]. Prostate cancer cells have not been studied extensively with respect to H-1PV infection either and this project would give an opportunity to look into the efficacy of the virus in different prostate cancer cells and potentially identify drugs that could cooperate with H-1PV against this tumor entity. Thus, as a model for screening these combinations, I decided to use prostate cancer cells.

H-1PV in combination with HDAC inhibitors and BH3 mimetics

In this objective, I decided to screen two major classes of drugs:

- HDAC inhibitors: Based on previous data from the lab and ongoing clinical trials in prostate cancer, I decided to screen three different kind of HDAC inhibitors in combination with H-1PV, based on the clinical advancement and class of HDAC inhibitor.
  - VPA: HDAC 1 Inhibitor; in Phase 2 clinical trials for Progressive, Non-Metastatic Prostate Cancer; Synergistic effects with H-1PV [79].
  - Tacedinaline (CI994): selective class I HDAC inhibitor; Phase 2 for advanced myeloma.
  - Pracinostat (SB939): potent pan-HDAC inhibitor; Phase 2 for metastatic prostate cancer.
- BH3 mimetic compounds: Based on previously established efficacy of the combination of H-1PV and ABT-737, I decided to screen two different BH3 mimetic compounds,
  - ABT-737: Inhibits Bcl-xL, Bcl-2 and Bcl-w. Phase 2 for lymphoma and other blood cancers. Synergistic with H-1PV (unpublished data).
  - Venetoclax (ABT-199): Bcl2 selective inhibitor; Phase 3 for Metastatic Castration Resistant Prostate Cancer.

Synergy Assay

In order to test whether the combination of the virus and drug is superior in killing the prostate cancer cells than the treatment of virus or drug alone, I adapted an easy assay as described previously [90]. This assay allows evaluating whether a certain co-treatment under specific experimental conditions and determined concentrations would act in an additive, synergistic or conversely antagonistic manner. Since I wanted to check for oncolytic potential, I decided to use cell viability assay as a readout for this assay. This quick assay would provide me with a sub lethal dose for the virus and drug, as well as aid in identifying the combinations that show a synergistic effect in killing prostate cancer cells. The results obtained in order to achieve this goal have been described in section 3.1 of the Chapter 3

Goal 2: Evaluate whether synergistic combination/s are able to induce the expression of markers for Immunogenic cell death

Since H-1PV has been reported to induce an immunogenic cell death [46, 74, 84], I wanted to see whether the combination/s would be able to retain this effect, enhance it or obliterate it. This objective aimed to look at the general nature of the cell death. I did not intend to deep dive into identifying the mechanism of action for the combination, but rather determine roughly whether a certain kind of cell death was induced and whether this cell death was characterized by the

expression or release of typical markers of ICD, thus aiding in characterizing it as an ICD event. The different ICD markers that I decided to look at were as follows:,

- Cell surface expression of Calreticulin, Hsp70 and Hsp90
- HMGB-1 release
- CXCL-10 secretion
- Extracellular ATP release

The results obtained in order to achieve this goal have been described in section 3.2 of the Chapter 3

Goal 3: Evaluate the overall effect of the combination on immune cells by using functional assays

The main objective of this goal was to see whether H-1PV alone or in combination was able to engage the immune cell populations. This would be beneficial in extrapolating whether the combination/s has the potential for an anti-tumor immune response in case of a clinical setting. The results obtained in order to achieve this goal have been described in section 3.3 and 3.4 of the Chapter 3

Chapter 3

Results

3.1 H-1PV in combination with ABT-737 synergizes in killing prostate cancer derived PC3 cells

3.1.1 Prostate cancer cells show different susceptibility to H-1PV infection

Before exploring combination therapy, I first evaluated the effect of H-1PV monotherapy in prostate cancer cell lines.

Prostate cancer cells, which can be routinely used for therapeutic research, are very difficult to establish as cell lines. There have been numerous efforts in isolating prostate cancer cells from patients and establishing them as cell lines since the past few decades. Owing to these efforts, we now have some cell lines routinely used in prostate cancer research [91, 92]. Based on previous research and literature I decided to evaluate the sensitivity of H-1PV in the following prostate cancer cell lines,

- PC3 cells: These are human epithelial prostate cancer cells, derived from the bone metastatic site of the patient.
- DU145 cells: These are human epithelial prostate cancer cells, derived from the bone metastatic site of the patient.
- LNCaP cells: These are human epithelial prostate cancer cells, derived from the lymph node carcinoma of the prostate.
- VCaP cells: These are human epithelial prostate cancer cells, derived from the vertebral metastatic site of the patient.

For evaluating the sensitivity of the cells to the virus infection, I decided to quantify cell viability using an MTT assay, which relies on metabolically active cells to reduce the tetrazolium dye MTT to a purple colored formazan [93]. This way, I was able to determine the cytotoxic effect H-1PV had on these cells. The cells were treated with increasing virus concentrations ranging from 0.39 to 200

multiplicities of infection (MOI = number of virus particles/cell). 72 hours post infection (hpi) absorbance was read at 570nm. The absorbance values were then calculated as percent cytotoxicity relative to untreated controls. Percent cytotoxicity was then analyzed by non-linear regression curve analysis, to determine the IC_{50} values, or the concentration of the virus able to kill 50% of the cells.

I could clearly see that each cell line responded differently on advent of virus infection (Figure 3.1 A and B). PC3 and DU145 cells were susceptible to H-1PV infection and killed efficiently by the virus with IC_{50} values being less than 15 MOI for both the cell lines. VCaP cell were very resistant to H-1PV infection, with less than 40% cell death incurred at even highest virus concentrations. LNCaP cells on the other hand were completely refractory to the virus infection with almost 90% cells viable at highest virus concentration (Figure 3.1 A and B).

3.1.2 LNCaP cells are resistant to H-1PV infection at the level of virus entry

To understand the disparity in virus susceptibility, we tested the most resistant LNCaP cells to evaluate whether the inhibition to a successful infection was at the level of virus entry or virus replication.

We infected LNCaP cells with a recombinant H-1PV that expressed GFP. This is a replication deficient recombinant H-1PV, with the same capsid as the wild type virus and an EGFP gene under control of the P38 promoter, which is activated by the non-structural NS1 protein [94] (Chapter 1.2).HeLa cells, which are sensitive to H-1PV infection[69], were used as positive control. As seen in Figure 3.2A, there was no GFP expression in LNCaP cells post infection.

After treating the cells with wild type H-1PV, LNCaP cells also failed to show expression of NS1 and the viral capsid protein VP2, as compared to a robust expression in infected HeLa cells, suggesting an early block of virus infection (Figure 3.2B).

We carried out a cell surface binding-entry assay to check whether H-1PV was blocked at the early step of infection. We treated LNCaP and HeLa cells with H-1PV for 4 hours at 37°C. After washing, cells were harvested and the isolated virus genome associated to the cells (as a measure of the fractions of virus particles bound to the cell surface or already inside the cells) calculated by qPCR. As a negative control, cells were also treated with Neuraminidase. Neuraminidase cleaves sialic acid residues on the cell surface, which are known to be critical for facilitating the attachment of virus particles to the cell surface prerequisite for virus entry [35, 95]. Therefore, treatment with this enzyme is anticipated to block virus binding to cell surface and entry.

As seen in Figure 3.2C, it is evident that H-1PV was able to enter the HeLa cells. As expected, the infection was successfully inhibited by Neuraminidase. On the contrary, no virus attachment and entry was observed in the LNCaP cells, demonstrating an early block of virus infection in these cells. These results pro-

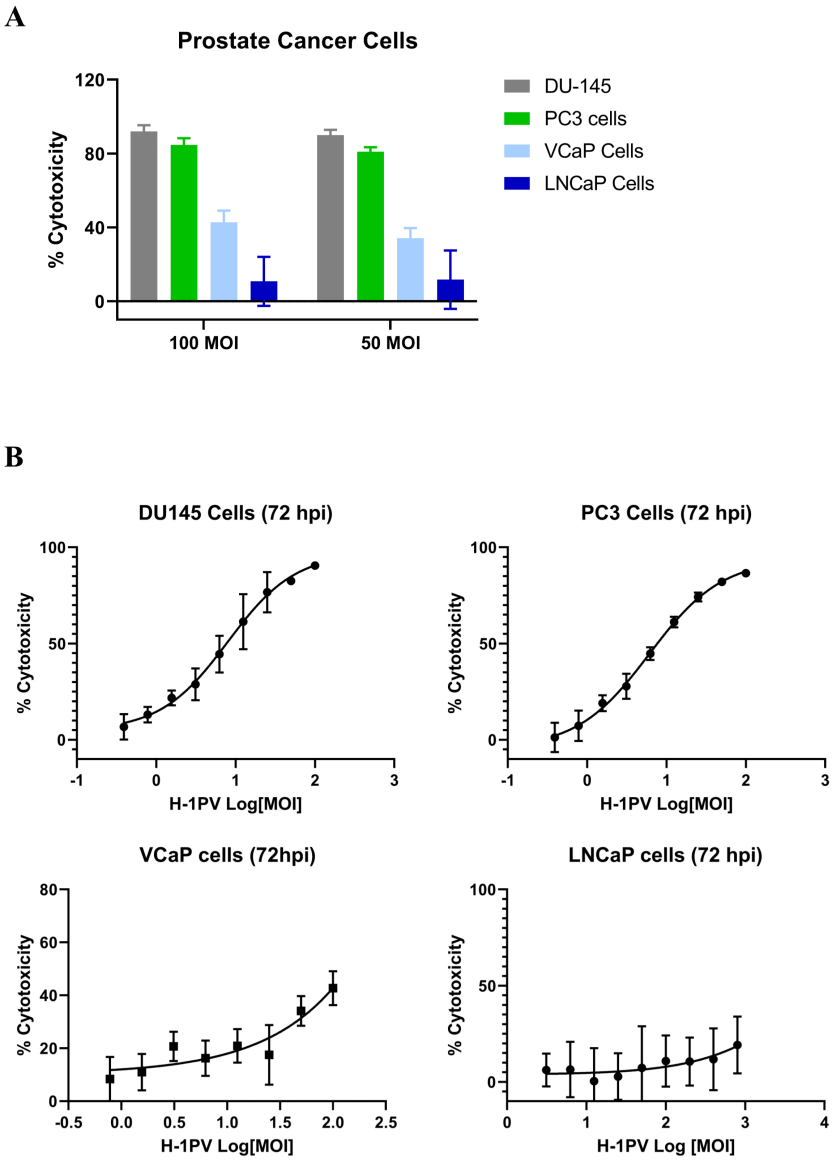

Figure 3.1: ***Prostate cancer cell lines show different susceptibility to H-1PV infection.*** *(A) PC3, DU145, VCaP and LNCaP cell lines were treated with 100 and 50 MOI of H-1PV. 72 hours post infection, percent cytotoxicity was evaluated using an MTT cell viability assay. (B) PC3, DU145, VCaP and LNCaP cells were treated with increasing titers of H-1PV. Cell viability was evaluated 72 hours post infection (hpi) using an MTT cell viability assay. Absorbance values were used to calculate percent cytotoxicity relative to untreated controls and plotted as non-linear regression curves, to obtain* IC_{50} *values. Data are representative of three independent experiments and values are expressed in* $mean \pm SD$ *Statistical significance was calculated using a paired two-tailed t test by GraphPad Prism 9; *$P \leq 0.05$; **$P \leq 0.01$; ***$P \leq 0.001$; ****$P \leq 0.0001$.*

vide insights into the reasons why LNCaP cells are resistant to H-1PV.

H-1PV infection has been recently shown to depend on Galectin-1 and Laminin γ1. These proteins play a role as H-1PV cell attachment factors, and as mediators of virus entry into the host cell [67, 68].In order to evaluate whether the lack of these factors made the LNCaP cells refractory to H-1PV infection, we carried out a western blot for these proteins using total LNCaP cell lysates. HeLa cells were used as a positive control. Western blot analysis show that LNCaP cells are lacking Galectin-1 (Figure 3.2D), which indicates that the LNCaP cells may be resistant to H-1PV infection because they lack this important mediator of virus entry.

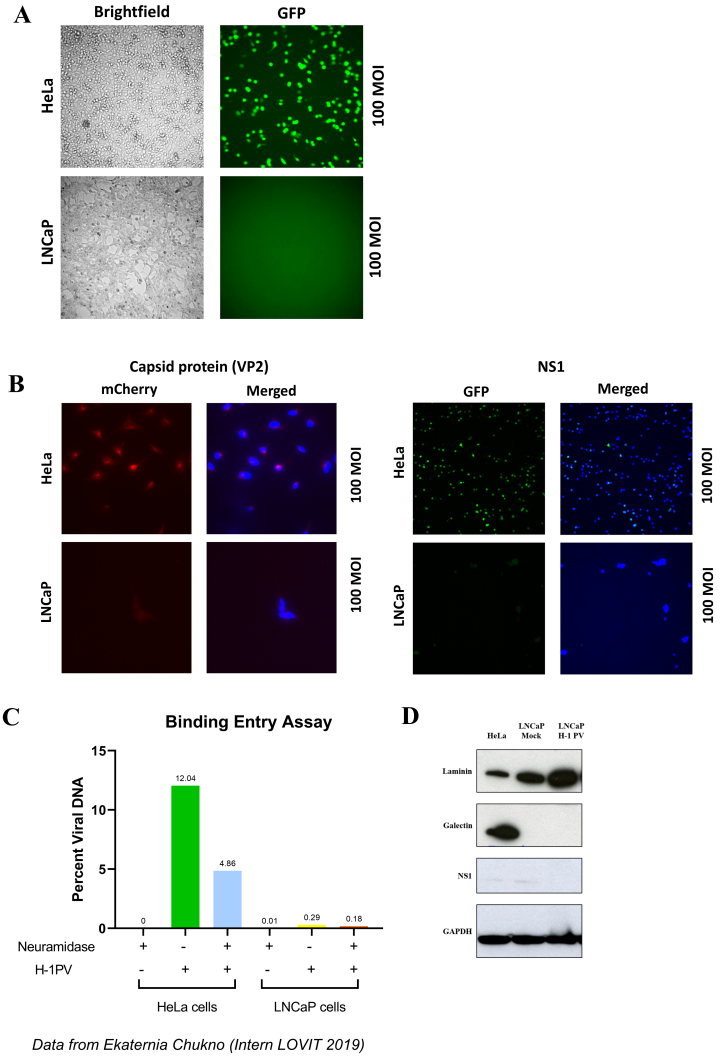

Figure 3.2: ***LNCaP cells are refractory to H-1PV entry and infection most likely for the lack of the Galectin 3, an important factor involved in H-1PV entry.*** *(A) LNCaP and HeLa cells were treated with recombinant H-1PV-EGFP at an MOI of 100 (vp/cell).Images were acquired 48 hours after treatment, at 10X magnification, for bright field and GFP fluorescence. (B) LNCaP and HeLa cells cells were treated with wild type H-1PV (MOI 100) and 24 hours post infection, fixed and stained by immunofluorescence for viral NS1 (mCherry) and VP2 (GFP). (C) LNCaP and HeLa cells were treated with wild type H-1PV (MOI 100) in the presence or absence of Neuraminidase at 37°C for 4 hours. Residual virus was then washed off, the cells were collected and washed, before isolating the total RNA. qPCR was carried out for viral genome DNA. (D) LNCaP cells and HeLa cells were cultured and 24 hours post infection, total proteins were analysed for the content of Laminin-γ chain 1 (Laminin), Galectin-1 (Galectin), NS1 and GAPDH (loading control) by Western blotting. Data are representative of three independent experiments and values are expressed in $mean \pm SD$ Statistical significance was calculated using a paired two-tailed t test by GraphPad Prism 9; *$P \leq 0.05$; **$P \leq 0.01$; ***$P \leq 0.001$; ****$P \leq 0.0001$.*

3.1.3 H-1PV in combination with ABT-737 show a synergistic killing of PC3 cells in a checkerboard assay

In order to evaluate the efficacy of a combination treatment, it is requested that cells are sensitive to the virus infection in the first place. After analyzing different cell types for virus sensitivity, it was apparent that PC3 and DU145 cell lines were the only cell lines available for studying combinatorial treatments since these cells were permissive to virus infection. PC3 cells and DU145 cells both exemplify metastatic prostate cancer, are epithelial in origin and are thoroughly characterized cells in prostate cancer research [92].Thus for the further study I decided to use PC3 and DU145 cells.

Previous studies have evidenced that H-1PV in combination with HDAC inhibitor VPA shows a synergistic effect of cell killing in glioblastoma- as well as pancreatic ductal adenocarcinoma-derived cell lines [79]. It has also been shown that H-1PV in combination with ABT-737, a BH3 mimetic that inhibits anti-apoptotic, pro survival BCL2 family members was synergistic in killing more than 30 different cancer cell types (unpublished data). This combination was also able to induce the expression of some markers for an immunogenic cell death. Thus, this gave me a good rationale to choose the subset of compounds that I could explore in combination with H-1PV in prostate cancer cells. In addition to VPA and ABT-737 these additional drugs were selected:

- BH3 mimetic and selective BCl2 inhibitor ABT-199 (Venetoclax)
- Class I HDAC inhibitor CI994 (Tacedinaline)
- Pan HDAC inhibitor SB939 (Pracinostat)

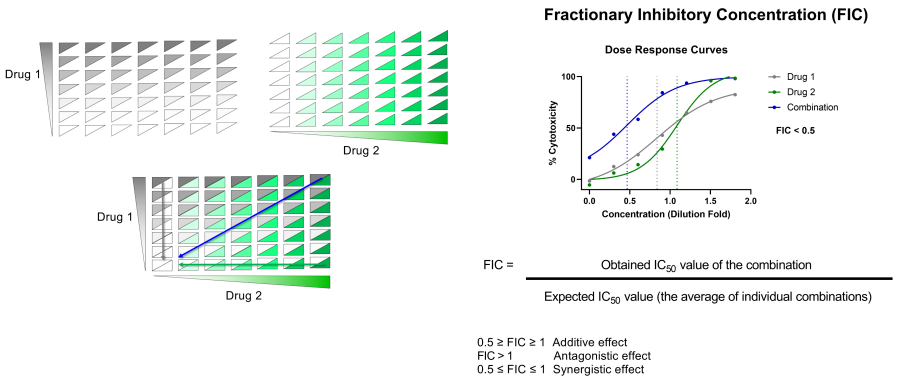

Figure 3.3: ***Adapting a checkerboard assay to evaluate synergy between H-1PV and other drugs.*** *This was protocol was adapted from [90]. (A) Cells were treated simultaneously with increasing concentrations of the virus, the compound and both together, as illustrated. (B) Cell viability was measured using MTT cell viability assay. Absorbance values were converted to percent cytotoxicity, relative to untreated controls. Percent cytotoxicity was then used to calculate IC_{50} values by non-linear regression and Fractional Inhibitory Concentration (FIC) values were calculated as described.*

In order to evaluate the effect of combination on prostate cancer cells, I adapted a checkerboard assay [90]. PC3 and DU145 cells were treated with se-

rial dilutions either of H-1PV titers, selected drugs or of combinations of the virus with drugs (Figure 3.3). 72 hours post treatment, I determined the cell viability using the MTT assay and plotted the percent cytotoxicity (relative to untreated controls) as non-linear regression curves to determine the IC_{50} values for H-1PV alone, the drug alone and the simultaneous combination of H-1PV and the drug. A ratio of these values determines the Fractional Inhibitory Concentration (FIC) index, as described in (Figure 3.3).

- If the FIC value is between 0.5 and 1, it indicates that the average of the IC_{50} values of the drug and the virus is almost equal to the IC_{50} value obtained with the co-treatment. This indicates an additive effect of the combination, where the combination treatment is as good as the sum of individual treatments.
- If the FIC value is more than one, it indicates that the average of the IC_{50} values of the drug and the virus is less than the IC_{50} value obtained with the co-treatment. This indicates an antagonistic effect of the combination, where the combination treatment is worse than the sum of the individual treatments.
- If the FIC value is is less than 0.5, it indicates that the average of the IC_{50} values of the drug and the virus is more than the IC_{50} value obtained with the co-treatment. This indicates a synergistic effect of the combination, where the combination treatment is better than the sum of individual treatments.

In other words, when the values are plotted and represented in the graph, if the the combination of a certain drug and H-1PV would act synergistically, the IC_{50} value would significantly shift to the left on the X-axis, as compared to both the monotherapies.

Using this checkerboard assay, I evaluated the combination of the H-1PV with HDAC inhibitors and BH3 mimetic compounds in PC3 and DU145 prostate cancer cells. The FIC values, in combination with the IC_{50} dose response curves, would be then indicative of whether a certain combination would act synergistically or not, with H-1PV.

As seen in Figure 3.4A, both BH3 mimetic compounds did not show a strong synergistic effect with H-1PV in DU145 cells. This is probably because DU145 cells also harbor a point mutation in the gene encoding for pro-survival BCL2 protein and is unable to express this protein in its functional form [96, 97]. As seen in Figure 3.4B, the combinatorial effect of H-1PV with HDAC inhibitors was almost as effective as the monotherapy treatments with the drugs.

A different scenario was observed in PC3 cells. As seen in Figure 3.5B, consistent with results obtained with DU145 cells, none of the HDAC inhibitors showed a synergistic effect in PC3 cells. On the contrary, the BH3 mimetic compound ABT-737 in combination with H-1PV shows a strong synergistic effect in these

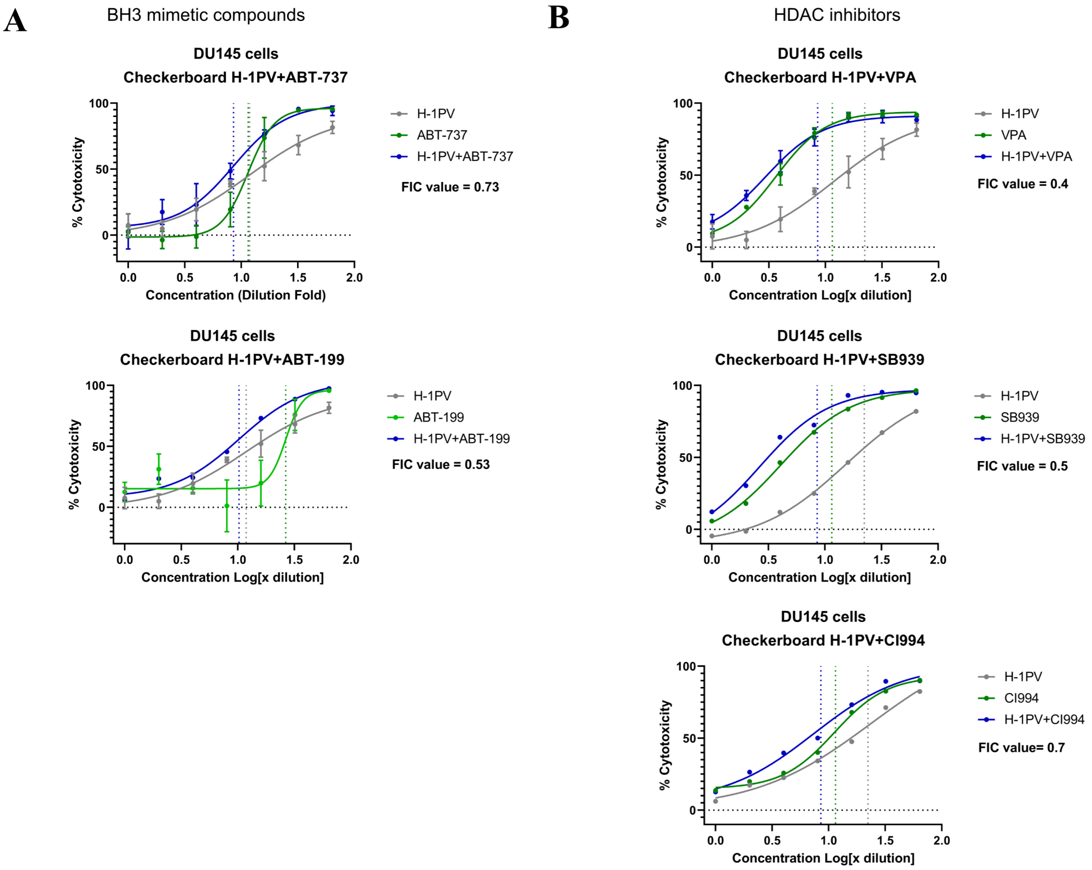

Figure 3.4: ***H-1PV does not seem to show a synergistic effect with any compounds as tested in DU145 cells***. *DU145 cells were treated with increasing concentrations of H-1PV, indicated drug or their combination. 72 hours post infection, cell viability was evaluated using MTT assay. Absorbance values were converted to percent cytotoxicity with relative untreated controls. Dose response curves were plotted for H-1PV alone, drug alone and co-treatment of both, as non-linear regression curves. Checkerboard assay and plots showing non-linear regression curves for DU145 cells showing the* IC_{50} *values indicated by dotted lines on the X-axis. FIC values were calculated for all combination treatments.Data are representative of three independent experiments and values are expressed in* $mean \pm SD$ *Statistical significance was calculated using a paired two-tailed t test by GraphPad Prism 9; **$P \leq 0.05$*; ***$P \leq 0.01$*; ****$P \leq 0.001$*; *****$P \leq 0.0001$.

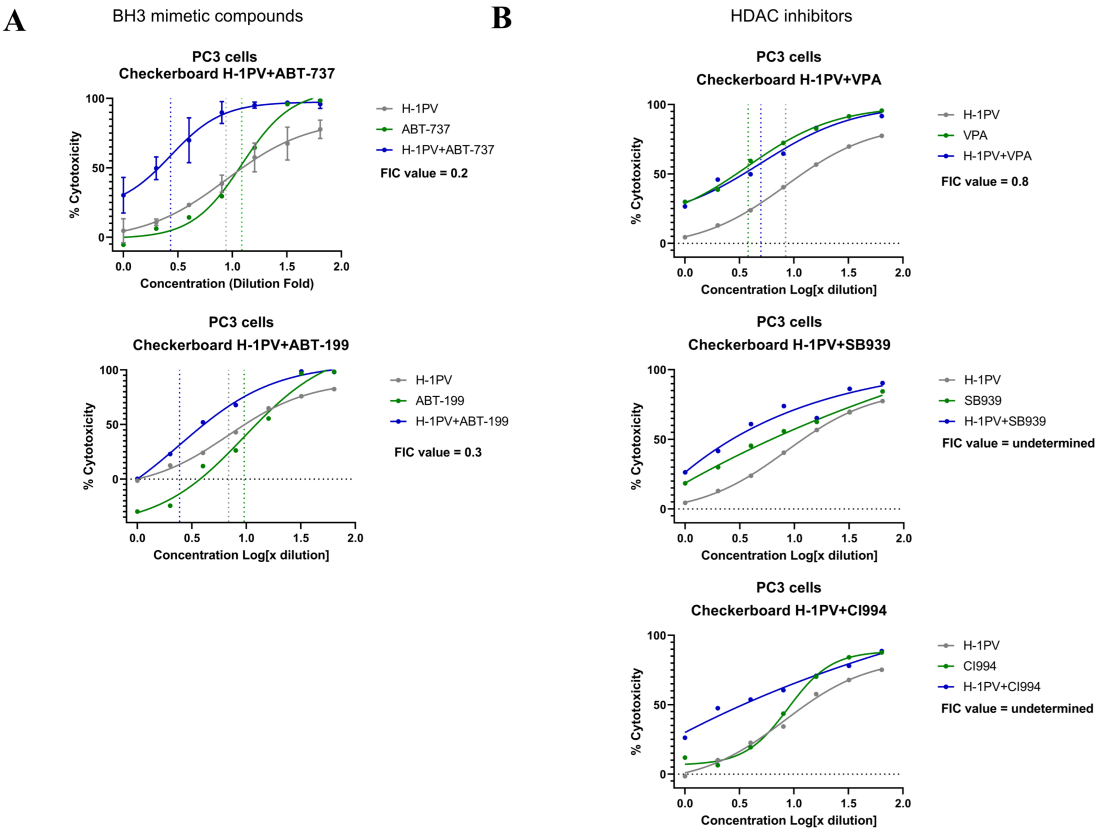

Figure 3.5: ***H-1PV in combination with BH3 mimetic compounds shows a synergistic effect in killing PC3 cells.*** *PC3 cells were treated with increasing concentrations of H-1PV and indicated drugs. 72 hours post infection, cell viability was evaluated using MTT assay. Dose response curves were plot for H-1PV alone, drug alone and co-treatment of both, as non-linear regression curves. Checkerboard assay and lots showing non-linear regression curves for PC3 cells showing the* IC_{50} *values indicated by dotted lines on the X-axis. FIC values were calculated for all combination treatments. Data are representative of three independent experiments and values are expressed in* $mean \pm SD$*. Statistical significance was calculated using a paired two-tailed t test by GraphPad Prism 9; *$P \leq 0.05$; **$P \leq 0.01$; ***$P \leq 0.001$; ****$P \leq 0.0001$.*

prostate cancer cells (Figure 3.5A). Although ABT-199 showed a similar synergistic effect than ABT-737, the IC_{50} value obtained for the compound for these cells was 18.9μM, whereas the IC_{50} value for ABT-737 in PC3 cells was 5.6μM. It is known that ABT-199 and ABT-737, when used at high doses, may induce apoptosis in cytotoxic T-cells, making it toxic for non-cancerous cells [98]. Based on these results, I decided to use ABT-737 to evaluate the functional response of this combination treatment between H-1PV and a BH3 mimetic compound.

3.1.4 H-1PV and ABT-737 co-operate in arresting cell proliferation and increasing oncolysis in PC3 cells

The checkerboard assay shows that the combination of H-1PV and ABT-737 is synergistic in killing PC3 cells. However, it is important to determine whether this synergistic interaction is also validated at lower concentrations of H-1PV and when the drug is used at sub-lethal doses.

PC3 cells were treated with 10 MOI H-1PV and 1μM ABT-737, both concentrations $\leq$ IC_{50} values as seen in Figure 3.6A. 72 hours post infection; the supernatants were evaluated for LDH release, as a marker of cell lysis [93]. As seen in Figure 3.6B, a synergistic increase of LDH release was found in the combination as opposed to treatment alone. Additionally an MTT assay of the same cells, which measures cell viability, confirmed these results.

The cells were also monitored using xCELLigence Real Time Cell Analysis (RTCA) for up to 96 hours post infection. The xCELLigence assay measures cell proliferation in real time by monitoring changes in electrical impedance caused by the growth and spreading of cells on microelectrode arrays[99]. As seen in Figure 3.6C the combination of H-1PV and ABT-737 was significantly more efficient in inhibiting cell proliferation and inducing cell toxicity.

Thus the combination of H-1PV and ABT-737 even at low viral MOI and sublethal doses of the drug, act synergistically in blocking cell proliferation and in killing PC3 cells.

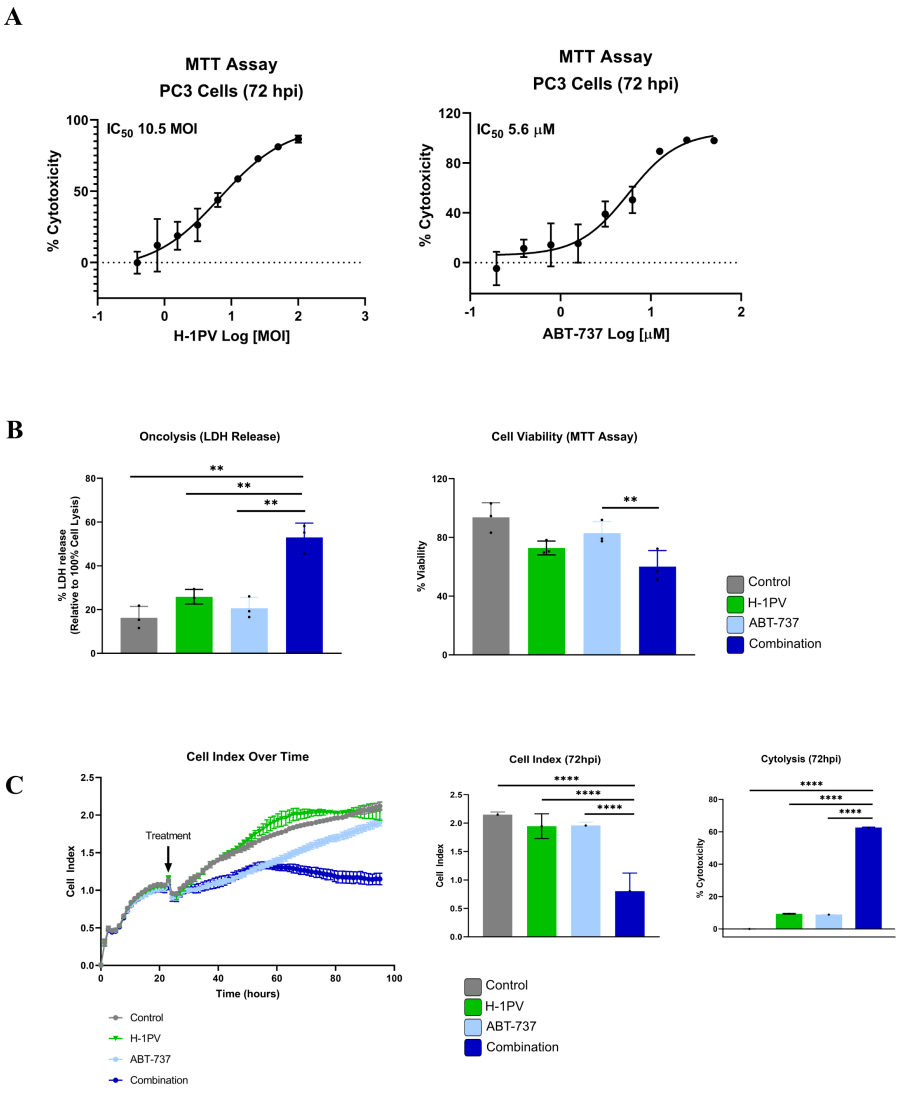

Figure 3.6: ***H-1PV and ABT-737 combination lead to improved oncolysis and reduced cell proliferation in PC3 cells.*** *(A) PC3 cells were grown with or without increasing concentrations of H-1PV and ABT-737. 72 hours post treatment, cell viability was determined using MTT assay and absorbance values converted to percent cytotoxicity (relative to untreated controls) which were plotted as non-linear regression curves to calculate the* IC_{50} *values. PC3 cells were infected with 10 MOI H-1PV and grown with or without sub-lethal concentrations of ABT-737 (1*μ*M). 72 hours post treatment, supernatants were analysed for LDH release as marker of cell lysis and the cells were analysed for cell viability by MTT assay (C)PC3 cells were grown as described in panel B. Cell growth was monitored in real time using the xCELLigence RTCA system for up to 96 hours post treatment. Data are representative of three independent experiments and values are expressed in* $mean \pm SD$ *Statistical significance was calculated using a paired two-tailed t test by GraphPad Prism 9;* $*P \leq 0.05$*;* $**P \leq 0.01$*;* $***P \leq 0.001$*;* $****P \leq 0.0001$*.*

3.2 The combination of H-1PV and ABT-737 induces an immunogenic form of apoptosis

3.2.1 H-1PV in combination with ABT-737 induces markers for apoptosis

Since ABT-737 is a pro-apoptotic drug, it was crucial to see whether the cell death triggered by the combination treatment was apoptotic or not. Apoptosis is a form of programmed cell death, mediated by caspase proteins, especially caspase 3 and 7. Caspase 3 and caspase 7 are known as effector caspases, which upon proteolytic cleavage become active and cleave cellular targets, initiating the cell degradation process which includes DNA degradation and membrane blebbing [100]. Along with caspase 3/7, accumulation of Annexin V at the cell membrane is also a marker of apoptosis. As the cells start dying, the plasma membrane gets compromised and, the otherwise concealed phospholipid, phosphatidylserine (PS) is exposed to the surface. Annexin V has an affinity to bind to these PS residues and is a direct indication of a compromised plasma membrane during apoptosis [100]. As cells undergo apoptosis, the mitochondrial membrane potential is perturbed and the membrane becomes permeable. Thus, a loss in mitochondrial membrane potential, characterized as mitochondrial outer membrane permeabilization (MoMP) is another gold standard marker for apoptosis [101]. Previous literature has also shown that H-1PV is capable of inducing caspase 3/7 cleavage along with a loss in mitochondrial membrane potential in glioblastoma cells and PDAC cells. [46, 72]. Thus keeping this in mind, I decided to evaluate whether the combination of H-1PV and ABT-737 was able to affect these markers, thus causing the cell death via apoptosis.

PC3 cells, post treatment with H-1PV and ABT-737, were analyzed in real-time using the Incucyte Real time imaging S3 system, with fluorescently labelled probes for detecting caspase 3/7 and Annexin V. Activated caspase-3/7 recognition motif (DEVD) is coupled here with a DNA intercalating dye. As it is added to the medium, the inert non-fluorescent substrate is transported into the cell. Here, activated caspase, if present, will cleave the substrate, thus releasing the DNA dye and showing green fluorescence [102]. The Annexin V Dye has a high affinity for phosphatidylserine (PS). If the cells are apoptotic and show a compromised cell membrane, the Annexin V dye binds to the exposed PS and then generates a stable fluorescent red signal [102].

As seen in Figure 3.7, there was a clear upregulation of activated caspase 3/7 and Annexin V in the combination treatment in comparison with treatment with single agents. Thus, it was evident that the cells treated with the combination of H-1PV and ABT-737 were apoptotic, showing the expression of activated caspase 3/7 and a compromised cell membrane.

The treated cells were also analyzed for MoMP using a flow cytometry based

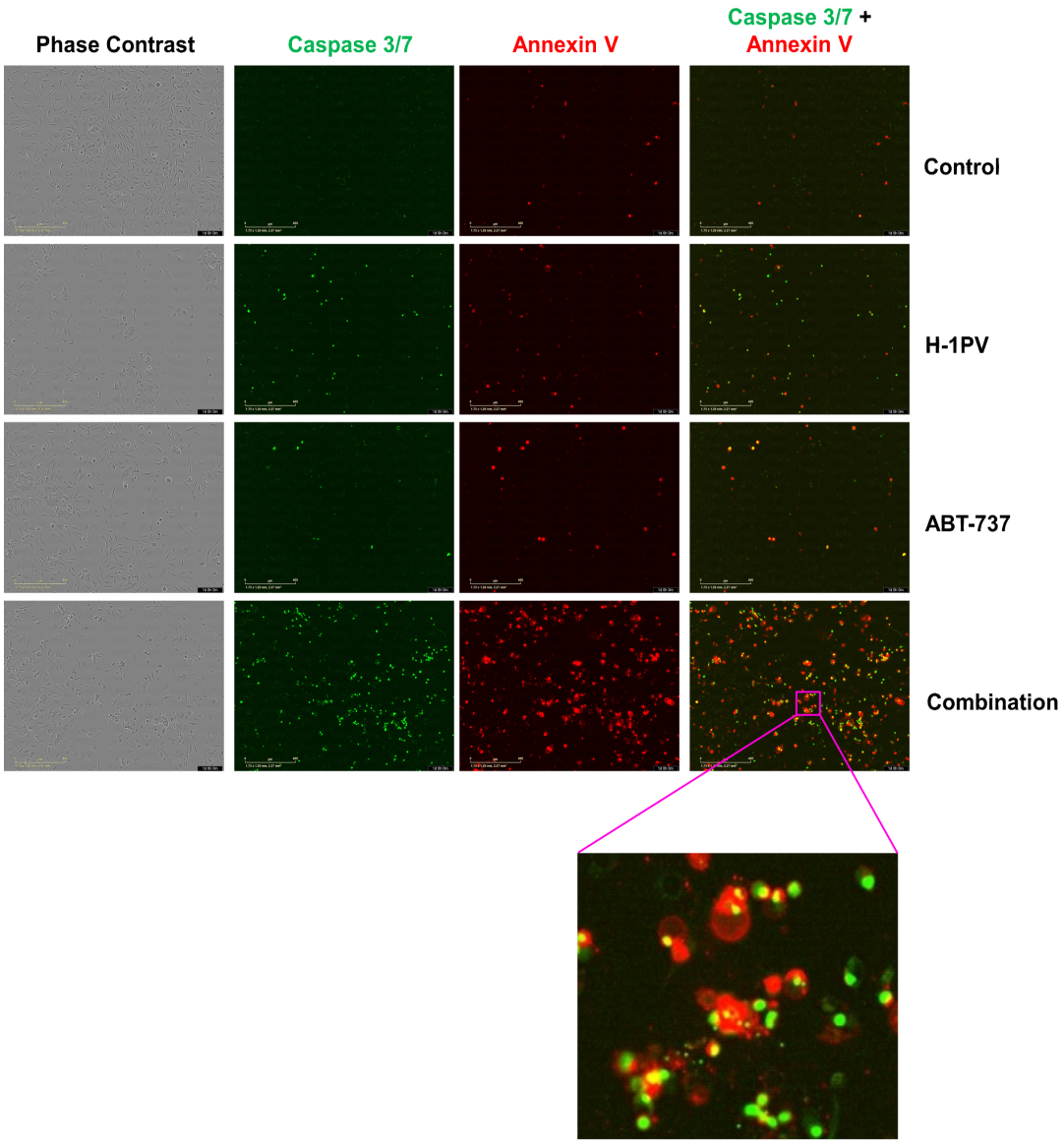

Figure 3.7: ***H-1PV in combination with ABT-737 upregulates activated caspase 3/7 and Annexin V in PC3 cells.*** *PC3 cells were grown with or without H-1PV and ABT-737, alone or combination of the agents. (A) Incucyte real-time imaging was used to evaluate the expression of apoptosis markers, activated caspase 3/7 and Annexin-V for up to 72 hours post treatment, using fluorescence probes specific for the markers.*

fluorescence dye, MitoTracker Deep Red. This cell permeable fluorescent probe, passively diffuse across the plasma membrane to and accumulate in the mitochondria. The signal intensity for the red fluorescence depends highly on the mitochondrial membrane potential and a loss in fluorescence is attributed to MoMP [103]. An increase in MoMP was observed at 48h, with the combination of H-1PV and ABT-737. At 72h post treatment, the effect was observed only with H-1PV alone, but not with the combination with ABT-737, most likely because the co-treated cells were already disrupted and dead (Figure 3.8A). At both time points, the increase in MoMP was significantly higher in the combination treated cells as compared to the untreated cells.

The Annexin-V/Propidium Iodide (PI) assay is a standard method of evaluating the different apoptotic and necrotic populations within the subset of dying cells. Annexin-V is a marker for early apoptosis, and cells exclusively positive for Annexin-V could be described as early apoptotic cells. PI uptake is an indicator of a permeable membrane and thus disorganized cell death such as necrosis. Thus cells exclusively positive for PI could be described as necrotic cells. Apoptotic cells that show membrane blebbing will also show PI staining and thus cells positive for both Annexin-V and PI could be described as late apoptotic events [104]. As seen in Figure 3.8B, I could see a strong increase of both early and late apoptotic cells positive for Annexin V and Annexin V and PI, respectively when treated with the combination of H-1PV and ABT-737.

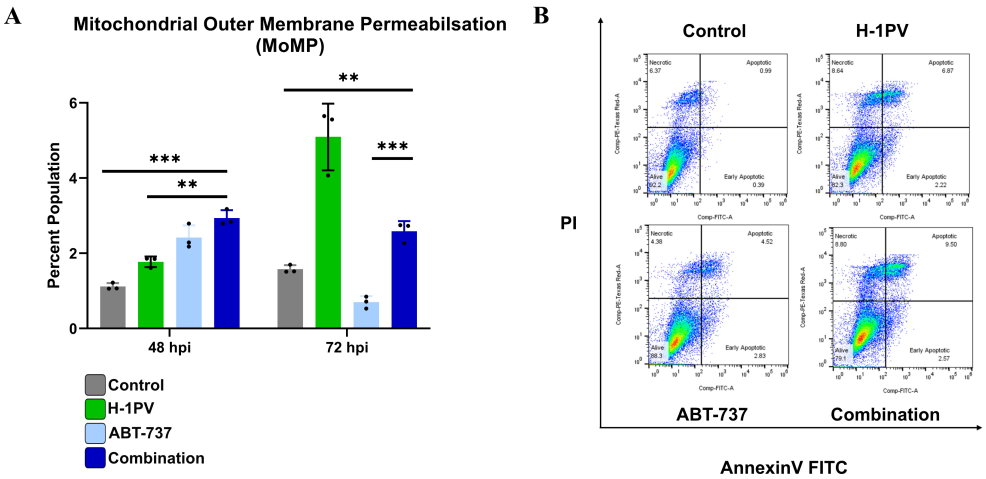

Figure 3.8: ***H-1PV in combination with ABT-737 induces Mitochondrial outer membrane permeablization (MoMP) in apoptotic PC3 cells.*** *PC3 cells were grown with or without 10 MOI H-1PV, 1μM ABT-737, alone or combination of the agents. (A) 48 and 72 hours post infection cells were collected and stained for MitoTracker Red CMXRos. The stained cells were then analysed by flow cytometry. (B) 72 hours post treatment, PC3 cells were stained with Annexin-V-FITC and PI. These cells were then analysed using flow cytometry. Dot plot showing ungated cells for Annexin-V-FITC and PI. Data are representative of three independent experiments and values are expressed in* $mean \pm SD$ *Statistical significance was calculated using a paired two-tailed t test by GraphPad Prism 9; *$P \leq 0.05$; **$P \leq 0.01$; ***$P \leq 0.001$; ****$P \leq 0.0001$.*

H-1PV has been shown to induce apoptosis, cell death through the lysosomal accumulation of cathepsins in glioma cells [46, 72], thus indicating that H-1PV is capable to inducing multiple kinds of cell death pathways, depending on cell

type. Based on this information, I investigated whether the combination of H-1PV and ABT-737 is able to induce a cell death that is "exclusively" apoptotic or is associated with other forms of cell death.

A marker of non-apoptotic cell death is the loss of lysosomal membrane potential due to lysosomal membrane permeabilization (LMP). Various forms of cellular stress such as ER stress or activation of Bax, can trigger LMP [105], which is associated with the release of cathepsins as well as lytic enzymes from the lysosomes into the cell environment causing a cell death process. As seen in Figure 3.9A, there was a significant upregulation of the lysosomal membrane permeabilization, in treated PC3 cells. This effect was time dependent and we saw a maximum effect at 72 hours post infection.

As loss in LMP can be associated with accumulation of Reactive Oxygen Species [105]. Accumulation of reactive oxygen species (ROS) is also largely evidenced in many different forms of cell death pathways such as necrosis, necroptosis, autophagy as well as apoptosis [105]. Thus, I evaluated whether the H-1PV/ABT-737 co-treatment in addition to LMP was also associated with ROS accumulation as a marker of oxidative stress. As seen in Figure 3.9B there was no significant change observed in the accumulation of Reactive Oxygen Species, with any kind of treatment. However, there was significant ROS accumulation in the combination treated cells, as compared to the untreated controls.

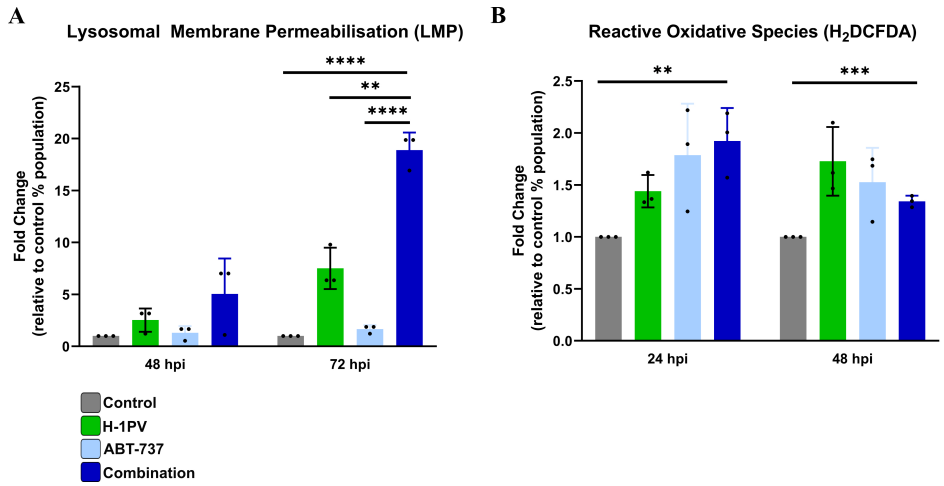

Figure 3.9: ***H-1PV and ABT-737 combination induces markers for non-apoptotic cell death.*** *PC3 cells were grown with or without 10 MOI H-1PV, 1μM ABT-737, alone or the combination of both the agents. (A) Flow cytometry analysis of Lysosomal Membrane Permeabilization (LMP). 24, 48 and 72 hours post infection, PC3 cells were stained with a fluorescence based LysoTracker Yellow and analysed using flow cytometry. (B)PC3 cells were grown with or without H-1PV and ABT-737 alone or the combination of both the agents. 24 and 48 hours post infection, the cells were loaded with CM-H2DCFDA and ROS-dependent CM-H2DCF (DCF) fluorescence was measured by flow cytometry. Data are representative of three independent experiments and values are expressed in* $mean \pm SD$ *Statistical significance was calculated using a paired two-tailed t test by GraphPad Prism 9;* *$P \leq 0.05$*;* **$P \leq 0.01$*;* ***$P \leq 0.001$*;* ****$P \leq 0.0001$.

Although LMP is not a typical marker for apoptosis, it is often times observed in an apoptotic cell because of a dysregulated cell metabolism [105, 106]. Thus, in order to see whether the combination of H-1PV and ABT-737 was killing the cells

exclusively via apoptosis or an alternative cell death pathway as well, I decided to inhibit apoptosis using the pan caspase inhibitor Z-VAD-FMK. Previous literature shows that 50μM Z-VAD-FMK is capable of inhibiting apoptosis in PC3 cells without harming the health of these cells [105]. Hence, this concentration of the compound was used to evaluate the effect of cell death pathways.. I treated the cells with the combination of H-1PV and ABT-737, in the presence of Z-VAD-FMK. I also added the caspase 3/7 dye in order to ensure that apoptosis was inhibited. As seen in Figure 3.10, treatment of the cells with Z-VAD-FMK inhibited apoptosis and protected the H-1PV/ABT-737 co-treated cells from dying providing important evidence that apoptosis is mainly responsible for the cell death observed.

3.2.2 Multiple markers for immunogenic cell death are expressed upon cell death in the combination

There are certain danger associated molecular patterns (DAMPs) which are expressed by a dying cell. These DAMPs are essentially characterized by expression of certain proteins on the surface of cells or secretion of certain proteins by the dying cell, which are not usual for a healthy cell. These DAMPs act as a beacon to attract immune cells, trigger pattern recognition receptors (PRRs) on these cells and eventually elicit an immune response to help and identify dying/infected cells, and clear them out of the cell environment. A cell death capable of inducing an immune cell response is thus termed as an “Immunogenic cell death” (18). Upon immunogenic cell death, calreticulin (CALR) translocates to the surface of the cell and acts as co-stimulatory “eat me” signal for infiltrated immune cells. The expression of CALR on the cell surface is one of the gold standard markers for ICD in malignant disease (19). Similar to CALR, cell surface expression of heat shock proteins (Hsp70 and Hsp90) are also DAMPs, which aid in triggering the function of antigen presenting cells (APCs) (20). Thus, I decided to evaluate whether the dying PC3 cells were expressing calreticulin and Hsp70/90 on their cell surface. As seen in Figure 3.11, there was a significant upregulation of CALR (A), Hsp70 (B) and Hsp90 (C) in H-1PV/ABT-737 co-treated PC3 cells. This expression was significantly higher than that of the monotherapy of H-1PV and ABT-737. The expression of CALR was, increasing in function of the time. A similar trend was also observed for Hsp70 and Hsp90, which also accumulated on the surface of the H-1PV/ABT-737 co-treated PC3 cells in a time dependent manner.

There are also other DAMPs released by the dying cells that act as co-stimulatory “find me” signals and trigger the infiltration of immune cells for clearance. Extracellular ATP released by dying cells acts as an important “find me” DAMP [40]. Similarly, High mobility group protein-1 (HMGB-1) released by dying cells is a co-stimulatory DAMP for the activation of APCs[107]. Another important cellular cascade in the context of ICD is IL-1β/CXCL-10 secretion. CXCL-10 is a proinflammatory cytokine, which will trigger the activation and recruitment of leukocytes such as T-cells, NK cells. TLR-3 dependent Type I IFN cascade is

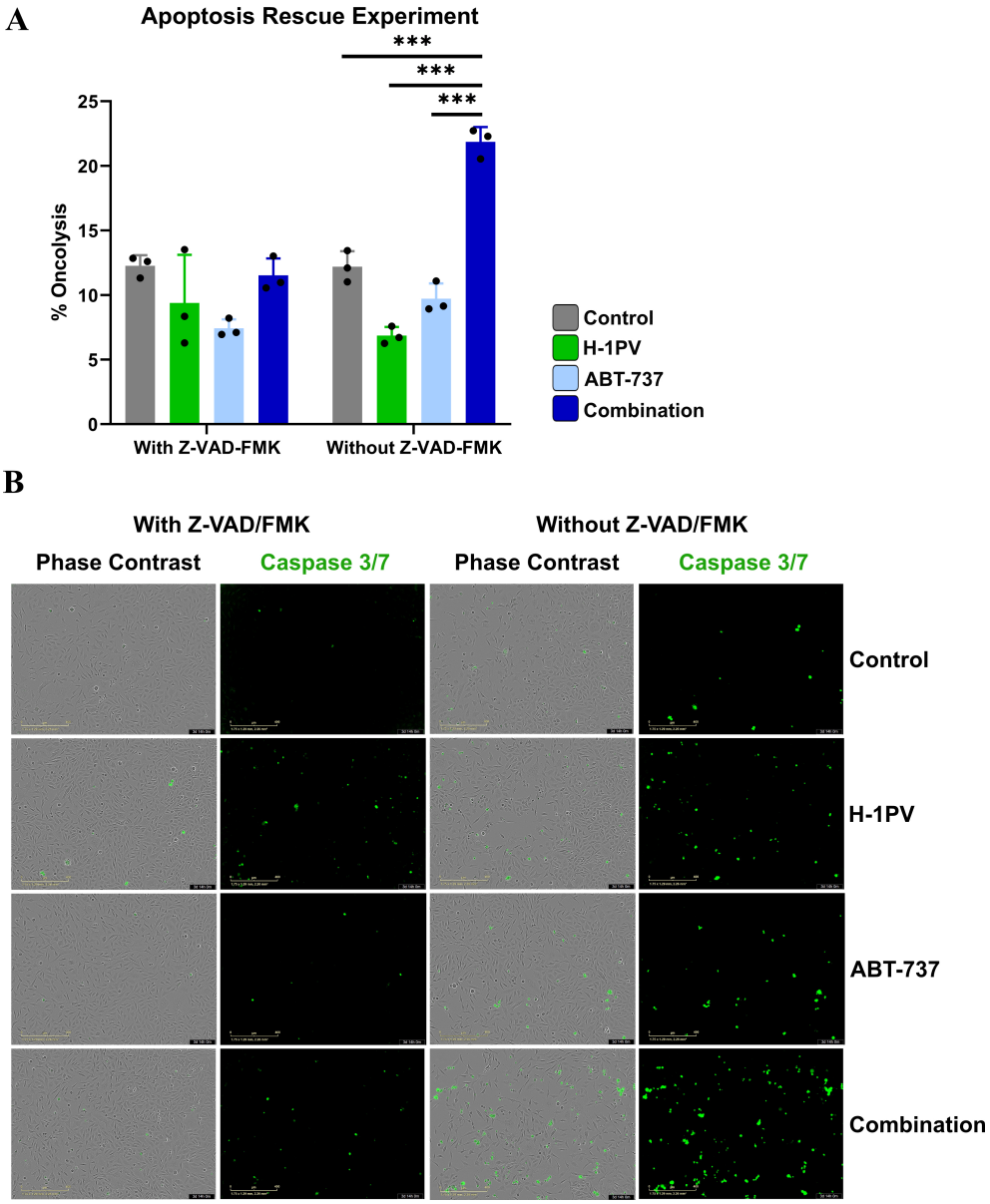

Figure 3.10: *H-1PV and ABT-737 combination induces an apoptotic cell death in PC3 prostate cancer cells. PC3 cells were grown with or without 10 MOI H-1PV, 1μM ABT-737, alone or combination of the agents, in the presence or absence of 50μM Z-VAD-FMK. (A) 72 hours post infection oncolysis was evaluated using LDH assay and plot as fold change relative to untreated controls (B) The cells were monitored in real time using Incucyte SX3. Incucyte images showing caspase 3/7 expression in green, at 72 hpi. Data are representative of three independent experiments and values are expressed in* $mean \pm SD$ *Statistical significance was calculated using a paired two-tailed t test by GraphPad Prism 9;* *$P \leq 0.05$*;* **$P \leq 0.01$*;* ***$P \leq 0.001$*;* ****$P \leq 0.0001$*.*

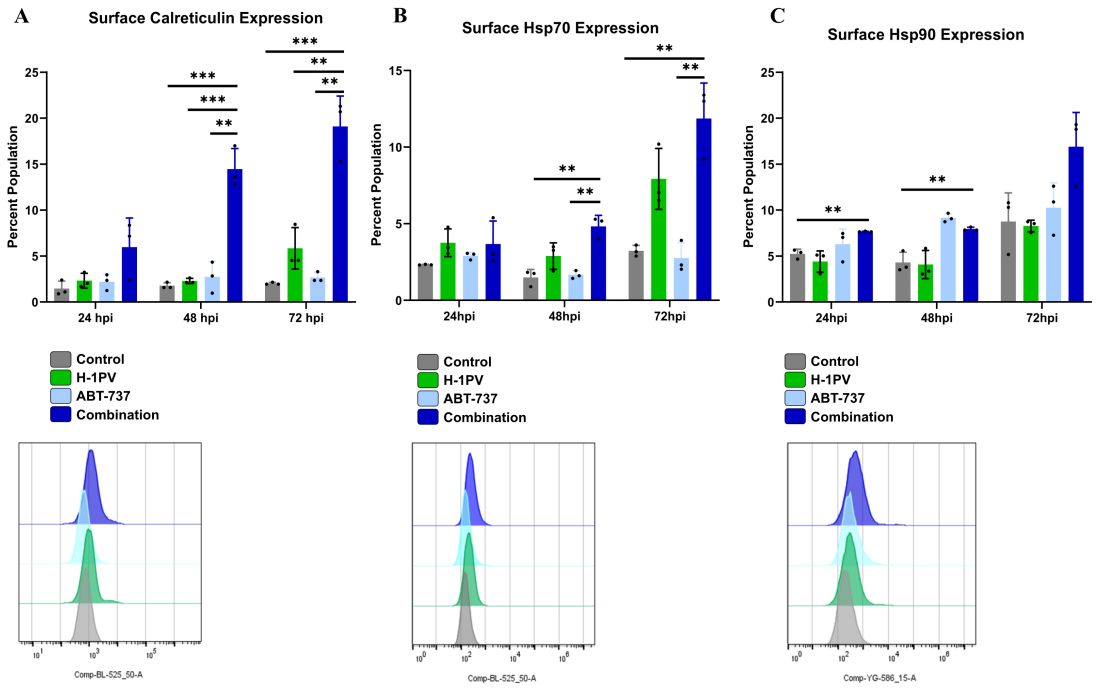

Figure 3.11: ***H-1PV/ABT-737 treatment induces expression of cell surface markers for Immunogenic Cell Death (ICD) in PC3 prostate cancer cells.*** *PC3 cells were grown with or without 10 MOI H-1PV, 1μM ABT-737 alone or the combination of the two agents. 24, 48 and 72 hours post infection cells were stained for cell surface expression of calreticulin-AF488 (A), Hsp70-AF488 (B) and Hsp90-PE (C) and cells were analysed using flow cytometry. Data are representative of three independent experiments and values are expressed in* $mean \pm SD$ *Statistical significance was calculated using a paired two-tailed t test by GraphPad Prism 9;* $*P \leq 0.05$*;* $**P \leq 0.01$*;* $***P \leq 0.001$*;* $****P \leq 0.0001$*.*

usually predominantly triggered by RNA viruses, however ICD induction using chemotherapeutics such as anthracyclines has also shown to trigger the production of Type I IFN/CXCL-10 [41]. Thus, it was of interest to see whether the treated PC3 cells were able to secrete any of these factors. The combination of H-1PV and ABT-737 was able to trigger a time sensitive extracellular ATP release at 24 hpi (Figure 3.12A), majorly because of virus infection. However, there was no effect on HMGB-1 and CXCL-10 release (Figure 3.12B and C), by treatments neither alone nor with combination.

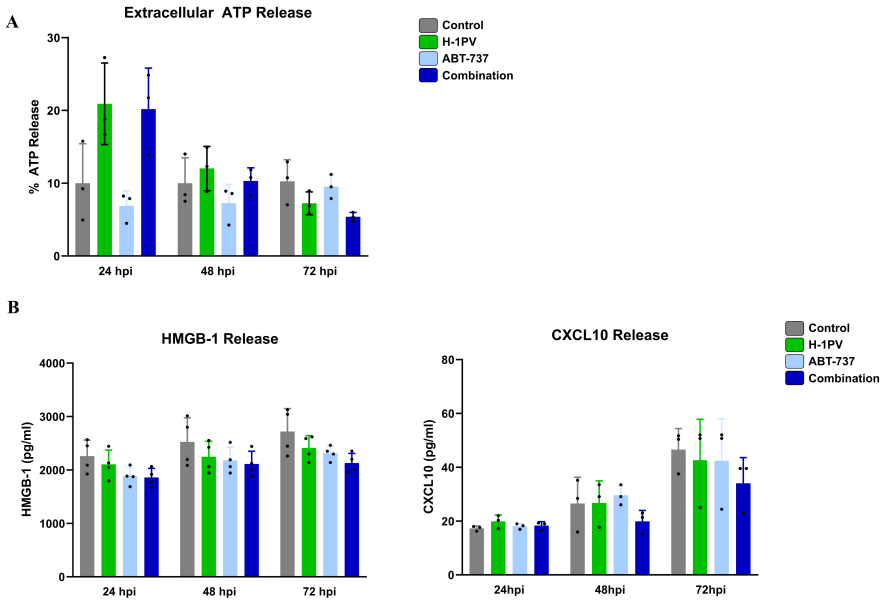

Figure 3.12: *H-1PV and ABT-737 induces the extracellular release of some but not all proteins associated with ICD. PC3 cells were grown with or without 10 MOI H-1PV, 1μM ABT-737 alone or in combination. 24, 48 and 72 hours post infection cell supernatants were collected and evaluated for ATP release using luminescence based Cell Titer Glo (A), and ELISA for (B) HMGB-1 release and (C) CXCL-10 secretion. Data are representative of three independent experiments and values are expressed in* $mean \pm SD$ *Statistical significance was calculated using a paired two-tailed t test by GraphPad Prism 9; *$P \leq 0.05$; **$P \leq 0.01$; ***$P \leq 0.001$; ****$P \leq 0.0001$.*

3.3 H-1PV and ABT-737 co-treatment triggered Immunogenic cell death is able to induce the Dendritic cell (DC)/T-cell axis in PC3 cell based co-cultures

3.3.1 Establishment of a co-culture assay to study dendritic cell activation and maturation

Immunogenic cell death may result in the activation of a functional immune response via DAMPs and PAMPs, which in turn may enable the priming of the adaptive immune response. For instance, expression of Hsp70 and Hsp90 proteins have been associated with improved APC activation and antigen presentation [41]. Since the H-1PV/ABT-737 combination induces an upregulation of both calreticulin and the Heat shock proteins in PC3 cells, I investigated whether this would result in the activation of Antigen Presenting Cells (APCs). To this end, it was necessary to adapt previously used protocols to establish an assay.

A number of studies have shown that oncolytic virus-mediated cell lysis may result in the activation of Dendritic cells (DCs) [45, 84, 108]. In the context of an anti-tumor immune response, DCs are potent professional antigen presentation cells, which would drive an adaptive immune cell response.

Based on previously conducted studies, I decided to set up a co-culture as-

say using PC3 prostate cancer cells and primary DCs. Human Peripheral Blood Mononuclear cells (PBMCs) contain 10-20% CD14+ monocytes. These monocytes can potentially be differentiated into immature DCs (iDCs) using IL-4 and GM-CSF [59]. These iDCs are then suitable for evaluating the effect of ICD on

- DC Maturation
- DC Activation
- DC mediated Phagocytosis

CD14+ monocyte-derived iDCs upon maturation and activation express a repertoire of characteristic cell surface markers. These markers are,

- CD40
- CD80
- CD83
- CD86
- HLA-DR

As described in Chapter 1.2.4, mature DCs eventually would be able to activate T-cell responses. However, for evaluating specific T-cell activation, T-cells need to have an antigen specific TCR to engage with a target cell antigen.

In my model, since I was using healthy donor T-cells, the probability of finding a prostate antigen specific T-cell was low and a very complex and time-consuming process. Thus, I decided to use a known antigen and a complementary antigen-specific TCR, which would enable the evaluation of specific T-cell responses, also limiting the donor-to-donor variability to some extent. For this purpose, I selected the New York esophageal squamous cell carcinoma 1 (NY-ESO1). NY-ESO1 is a well-known cancer-testis antigen (CTAs) which is expressed in multiple cancer types. The amino acid sequence 157-165 of NY-ESO1 is shown to be an active epitope able to be presented by human leukocyte antigen HLA-A2 to induce TCR specific favorable clinical responses [109–111].

Thus, in collaboration with Alice De Roia from Dr. Richard Harbottle's lab we generated a stable recombinant PC3-derived cell line, expressing the NY-ESO1 protein as well as the MHC I molecule HLA-A2, required for presenting this antigen. For establishing this cell line, we used two different vectors expressing dTomato/NY-ESO1 and GFP/HLA-A2 (Refer to Chapter 5 for more details). After transfecting with both vectors, the cells were sorted by FACS to isolate a double positive population, corresponding to those PC3 cells expressing both the NY-ESO1, HLA-A2 transgenes (dTomato and GFP positive cells) (Supplementary Figure 6.1).

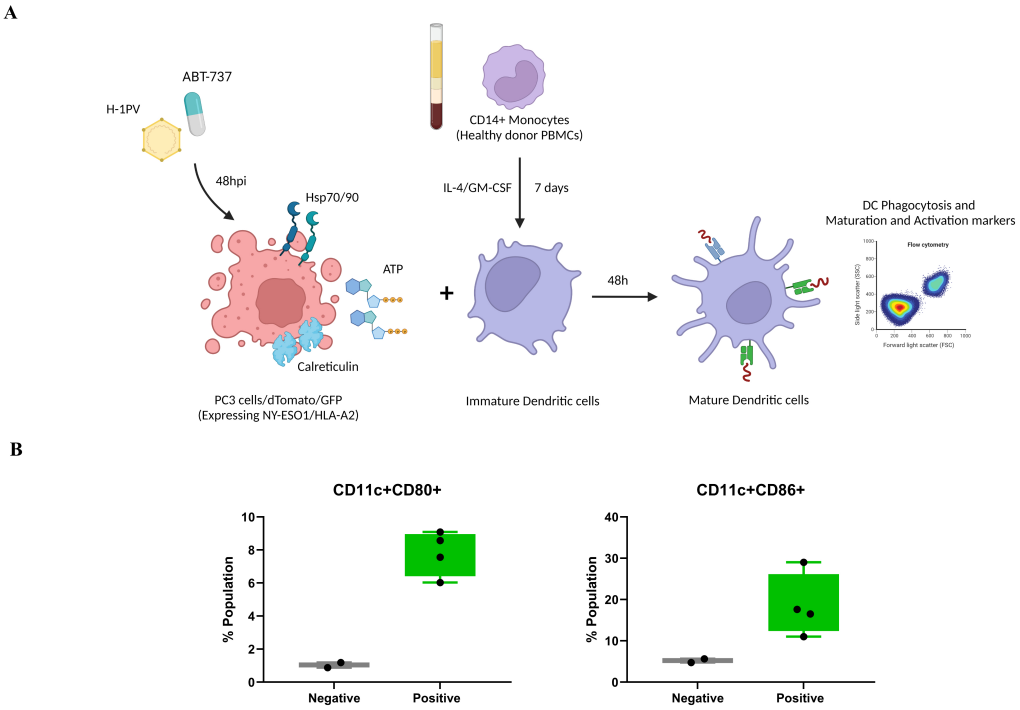

Figure 3.13: ***Establishment of a co-culture assay using PC3 cells and primary DCs, to evaluate DC activation and maturation.*** *(A) (A) Graphical representation of the co-culture assay to study DC Maturation/Activation. CD14+ Monocytes were isolated from healthy donor PBMCs and cultured in IL-4/GM-CSF for 7 days to obtain CD209+ immature dendritic cells (iDCs). PC3 cells expressing NY-ESO1 and HLA-A2 were grown in the presence or absence of 10 MOI H-1PV, 1μM ABT-737, alone or a combination of the two agents. 24h post treatment, isolated iDCs were then co-cultured with these treated cells. 48 hours post co-culture cells were collected and evaluated for cell surface expression of markers for DC maturation/activation. (B) Bar graphs showing establishment of the assay through CD80/CD86 flow cytometry. As negative controls I used cells grown in a cultural media containing IL-4 and GM-CSF which prevents DC maturation where as positive controls I used DCs grown in a cultural media containing a maturation cocktail including IL-6, TNFα and IL-1β. Each dot corresponds to a different donor. A total of 4 donors were used for the establishment of the assay. Values are expressed in $mean \pm SD$ Statistical significance was calculated using a paired two-tailed t test by GraphPad Prism 9; *$P \leq 0.05$; **$P \leq 0.01$; ***$P \leq 0.001$; ****$P \leq 0.0001$. Illustration was created with BioRender.com.*

3.3.2 H-1PV in combination with ABT-737 upregulate the markers for dendritic cell activation and maturation

Immature dendritic cells are phenotypically different from matured/activated DCs. Mature and activated DCs lose the expression of CD209 and gain the expression of CD11c along with increased expression of CD40, CD80, CD83 and CD86. Moreover, CD86+ HLA-DR+ DCs are functionally active and are able to carry out phagocytosis and antigen presentation [59].

As seen in Figure 3.14, after a co-culture assay as described in Figure 3.13, there was a significant upregulation of CD40, CD80, CD83, CD86 as well as HLA-DR, induced by the combination of H-1PV and ABT-737 as compared to the standalone treatments. Although many of these cell surface receptors were upregulated also in the case of H-1PV infection alone, upregulation was statistically higher with the combination of H-1PV/ABT-737 for CD40, CD83 and HLA-DR. It is also important to note that the upregulation of all these markers is significant as compared to untreated controls.

These results indicated that the combination treatment was able to induce the activation and maturation of DCs, better than the monotherapies. The upregulation of CD80, CD86 and HLA-DR also indicated that these activated DCs might be capable of acting as APCs to trigger the co-stimulation of T-cells.

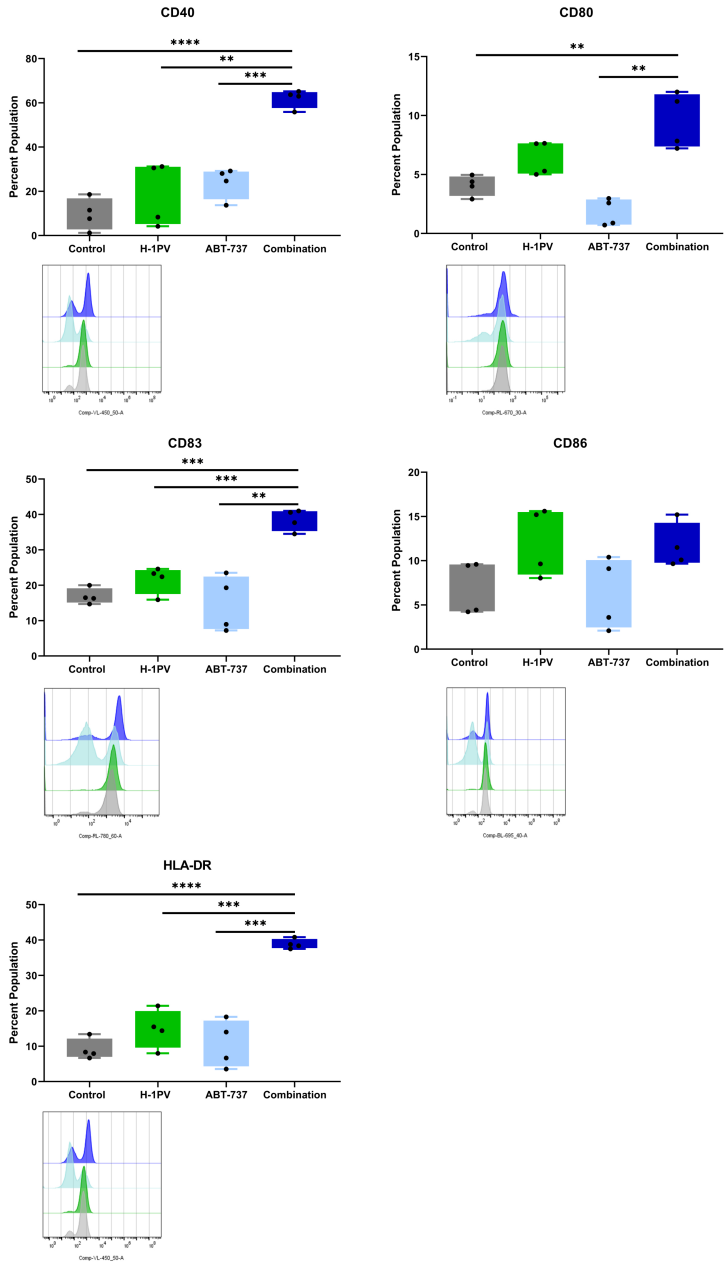

Figure 3.14: ***H-1PV and ABT-737 combination treatment of PC3 cells induces DC activation and maturation in the co-culture assay.*** *PC3 cells expressing NY-ESO1 and HLA-A2 were grown in the presence or absence of 10 MOI H-1PV, 1μM ABT-737, alone or in combination for 24 hours. iDCs isolated and enriched from healthy donors were overlaid on the treated PC3 cells. After 48 hours of co-culturing, dendritic cells were collected and evaluated for cell surface expression of DC maturation/activation markers by flow cytometric analysis. Bar graphs show the percent population of CD11c+ DCs cells expressing CD40, CD80, CD83, CD86 and HLA-DR. Each dot corresponds to a different donor. A total of 4 donors were used for the establishment of the assay. Values are expressed in $mean \pm SD$ Statistical significance was calculated using a paired two-tailed t test by GraphPad Prism 9; *$P \leq 0.05$; **$P \leq 0.01$; ***$P \leq 0.001$; ****$P \leq 0.0001$.*

3.3.3 H-1PV and ABT-737 combination triggers the production of various pro-inflammatory cytokines in dendritic cell based co-cultures of PC3 cells

Dendritic cells are crucial antigen presentation cells, which may directly activate T-cells via co-stimulatory signals essential for cytotoxic T-cell activation. However, an important function of activated DCs is also to secrete pro-inflammatory cytokines for T-cell priming and activation, NK cell recruitment and activation and in general to create an overall pro-inflammatory tumor microenvironment primed for an anti-tumor immune response [45, 59]. Thus, I asked whether the DCs activated through the combination treatment of H-1PV and ABT-737 were able to produce pro-inflammatory cytokines.

The supernatants from the co-cultures analyzed for expression of co-stimulatory molecules (Figure 3.14) were collected and evaluated for an array of multiple cytokines using the BioLegend LegendPLEX platform. As seen in Figure 3.15, I could see a differential expression of cytokines with the treatment of the virus and its combination with ABT-737. IL-1β, IL-6 and TNFα upregulation was observed with the combination as well as the virus treatment. These cytokines are associated with DC maturation and activation and therefore corroborate previous results (Figure 3.14) showing that the combination treatment of PC3 with H-1PV/ABT-737 by inducing an ICD can activate DCs. Furthermore, the H-1PV/ABT-737 co-treatment was also associated with upregulation of IL-2, which is involved in T-cells priming, and activation and IL-12p40, which is a cytokine aiding in a cytotoxic T-cell responses [60]. Interestingly, IL-12p40 is also involved in NK cell activation and proliferation [58].

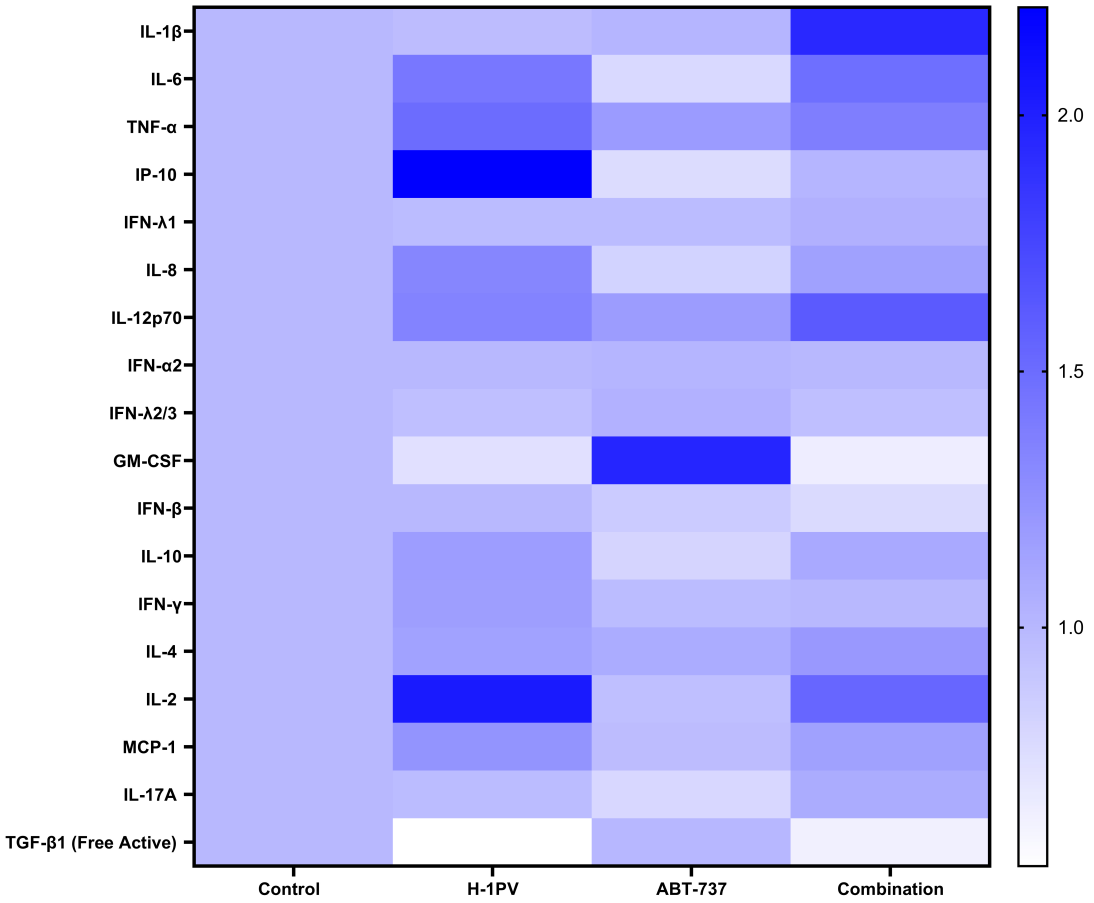

Figure 3.15: ***H-1PV and ABT-737 combination treatment of PC3 cells is associated with cytokine production when PC3 cells are co-cultured with DC cells.*** *PC3 cells expressing NY-ESO1 and HLA-A2 were grown in the presence or absence of 10 MOI H-1PV, 1μM ABT-737, used alone or in combination for 24 hours. iDCs isolated and enriched from healthy donors were overlaid on the treated PC3 cells. After 48 hours of co-culturing, supernatants were collected and assayed for their content of for the indicated cytokines using flow cytometry and the bead based BioLegend LegendPLEX multiplex array. Heatmap shows the fold change for the different cytokines, from 3 donors, relative to the untreated control samples.*

3.3.4 Activated dendritic cells generated as a result of H-1PV/ABT-737 co-treatment are capable of phagocytosis

In the event of an ICD event, the PRRs on DCs are engaged. Further, tumor associated or pathogen associated antigens are captured by DCs through phagocytosis, processed and presented to the T-cells in a MHC-I dependent manner [59, 60].

PC3 cells expressing NY-ESO1 and HLA-A2, also express dTomato and GFP (Supplementary Figure 6.1). Thus, if the DCs are capable of carrying out phagocytosis of a fraction of the dead cells, they will express dTomato or GFP, associated with the cells.

Thus, I repeated the same co-culture assay described in Figure 3.13 , and I checked whether mature CD86+ DCs would also be positive for GFP, as an indication of DC phagocytosis. As seen in Figure 3.16, the combination of H-1PV and ABT-737 was indeed showing a significantly higher population of CD86+GFP+ cells than H-1PV or ABT-737 alone.

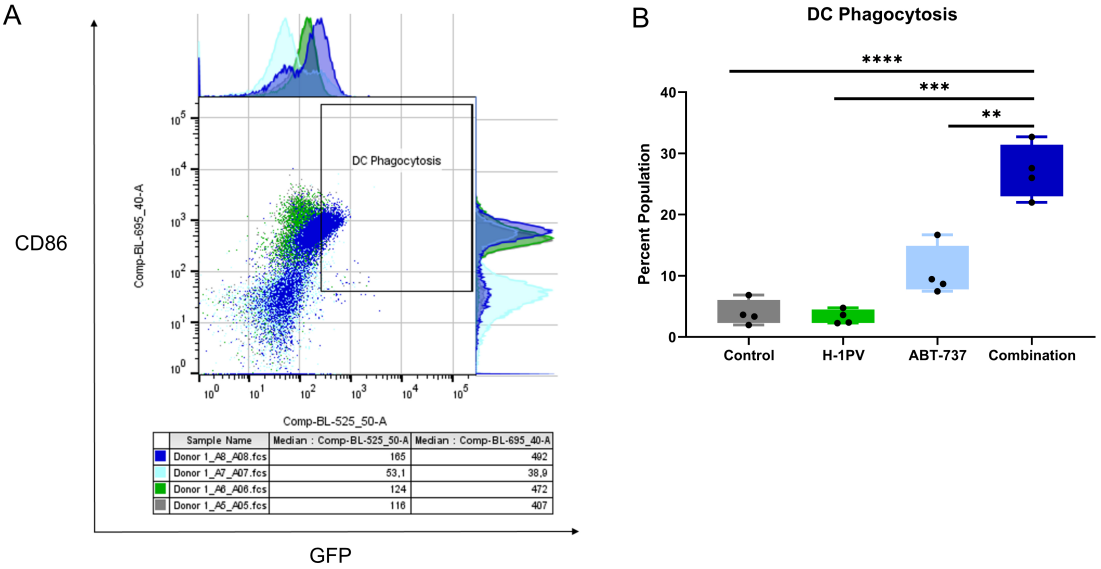

Figure 3.16: ***H-1PV in combination with ABT-737 is capable of inducing phagocytosis of dead PC3 cells by activated DCs.*** *PC3 cells expressing NY-ESO1, HLA-A2 (as well as dTomato and GFP) were grown in the presence or absence of 10 MOI H-1PV, 1μM ABT-737, alone or in combination for 48 hours. iDCs isolated and enriched from healthy donors were overlaid on the treated PC3 cells. (A) Representative dot plot from one donor showing CD86+GFP+ cells, 48 hours post co-culture. CD86+GFP+ dendritic cells were considered as the fraction of DCs capable of phagocytosis. Only CD86+ DCs were used as control for gating. (B) Bar Graph showing the CD86+GFP+ populations from 4 donors. Each dot is a donor. Values are expressed in $mean \pm SD$ Statistical significance was calculated using a paired two-tailed t test by GraphPad Prism 9; *$P \leq 0.05$; **$P \leq 0.01$; ***$P \leq 0.001$; ****$P \leq 0.0001$.*

3.3.5 Functionally active dendritic cells generated through a co-treatment of H-1PV and ABT-737, are able to induce T-cell activation in a PC3 cell based co-culture model

To explore DC-mediated T cell activation against PC3 cells expressing NY-ESO1, I established a T-cell based co-culture extended as shown in Figure 17. As PC3 cells

were expressing the NY-ESO1 antigen, T-cells purified from PBMCs of healthy donors (as discussed in 5) were transiently transfected with S/MAR-DNA vectors encoding the NY-ESO1 TCR, in collaboration with Alice De Roia from Dr. Richard Harbottle's lab (Supplementary Figure 6.5) . These transfected T-cells were then co-cultured with DCs from the previous assay (Figure 3.13). CD69 cell surface expression was evaluated on these T-cells, 16 hours post co-culture with DCs.

As seen in Figure 3.17, a significant upregulation of CD69 was seen when PC3 cells were treated with the combination of H-1PV and ABT-737, as compared to both the mono-therapies.

Thus, I could see that the cascade of DC/T-cell activation, which was started with an immunogenic cell death and expression of DC priming factors by the (co)treated PC3 cells, was completed with a successful T-cell activation. This effect was much stronger when PC3 cells were co-treated with oH-1PV and ABT-737 together.

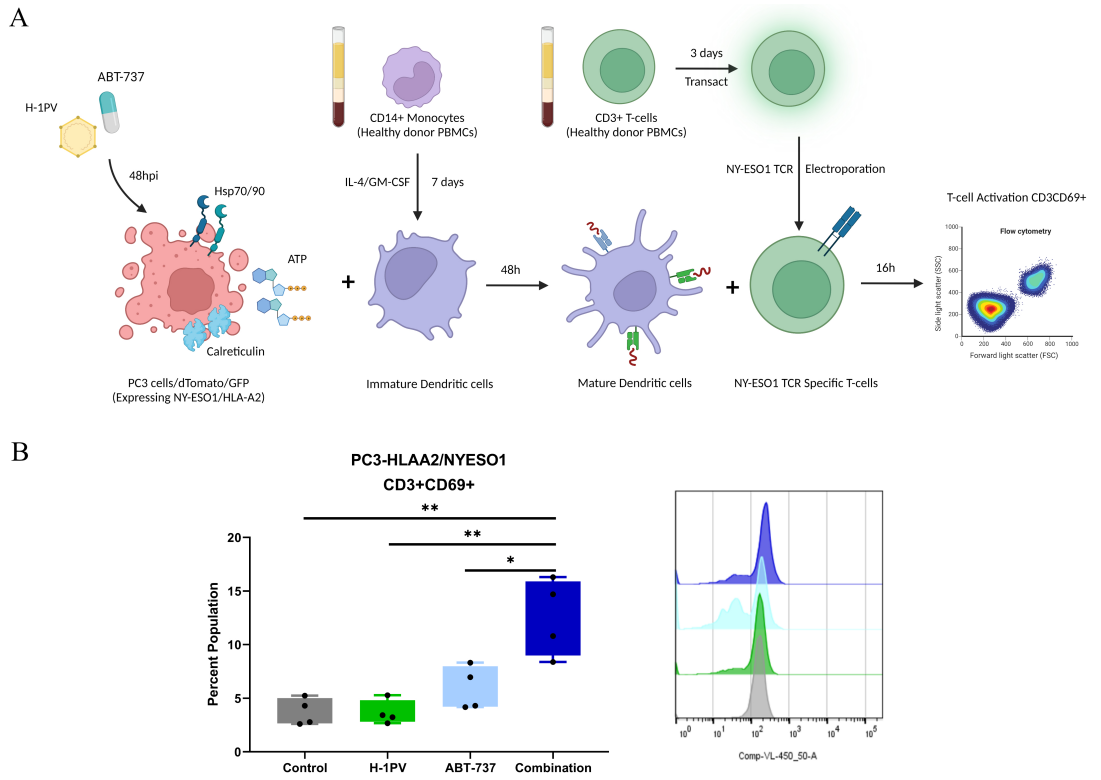

Figure 3.17: *H-1PV/ABT-737 induced matured DCs were capable of activating T-cell activation in PC3 cells based co-cultures. Pictograph showing the DC/T-cell based co-culture model. PC3 cells expressing NY-ESO1 and HLA-A2 were used to generate matures DCs as described in Figure 3.13. NY-ESO1 specific TCR T-cells were generated by transient transfection with S/MAR vectors (Supplementary Figure 6.7) and co-cultured with these mature DCs. T-cell activation was then analysed using CD69 flow cytometry. (B) PC3 cells expressing NY-ESO1 and HLA-A2, were treated with 10 MOI H-1PV, 1μM ABT-737, individually or combined for 24 hours, and then co-cultured with iDCs for additional 48 hours. These DCs were then collected and further co-cultured with NY-ESO1-TCR transfected T-cells. 16 hours post co-culture the T-cells were collected and evaluated for CD69 expression using flow cytometry. Each dot is a donor. Values are expressed in $mean \pm SD$ Statistical significance was calculated using a paired two-tailed t test by GraphPad Prism 9; *$P \leq 0.05$; **$P \leq 0.01$; ***$P \leq 0.001$; ****$P \leq 0.0001$. Illustration was created with BioRender.com.*

3.4 H-1PV in combination with ABT-737 triggers the activation of Natural Killer (NK) cells and accelerates the NK cell mediated killing of PC3 cells

3.4.1 PC3 cells express pro-cytotoxicity Natural Killer cell ligands upon co-treatment of H-1PV and ABT-737

One of the important factors in a virus-induced immune response is the activation of NK cells and other factors for innate immunity. Previous reports show that H-1PV is able to induce NK cell function, resulting in NK cell mediated cytotoxicity of infected cells [65, 82]. NK cell mediated cytotoxicity is very dynamic and is modulated by the intricate signaling pathways and receptor interactions on NK cells as well as target cells. There are inhibitory interactions e.g. HLA-A, B or C (on target cells)-KIR (on NK cells) which block the activity of NK cells or activating interactions such as MICA/MICB (on target cells)-NKG2D (on NK Cells) which induce NK cells mediated cytotoxicity [112]. Although constitutively expressed in normal cells, the expression of these ligands are upregulated in the event of stress, which then acts as a stimulatory signal for NK cells to be engaged and induce NK-mediated cytotoxicity [113, 114]. Previous reports suggest that H-1PV treatment alone could upregulate some of the NK-activating ligands on pancreatic cancer cells [65, 82].

Thus, I asked whether H-1PV alone or the combination of H-1PV with ABT-737 was able to induce any changes in some of these ligands on the cancer cells.

Based on previous literature, CD155 (PVR) and CD112 (Nectin-2) were selected as binding ligands for DNAM-1, a pro-cytotoxicity ligand on NK cells. MICA/MICB and ULBP-2/5/6 were selected as binding ligands for NKG2D, another important pro-cytotoxicity ligand on NK cells. Lastly, HLA-A, B and C were selected as ligands for KIR, an inhibitory ligand on NK cells. I treated PC3 cells with H-1PV and ABT-737, individually or in combination, and evaluated the expression of these ligands using flow cytometry.

As Figure 3.18 shows, the combination of H-1PV and ABT-737 was able to significantly upregulate CD155, MICA/MICB and ULBP 2/5/6 which bind to the NK cell receptors triggering cytotoxic effects. Treatment with the H-1PV/ABT-737 combination was also associated with the downregulation of the expression of HLA-A, B and C, ligands known to bind to KIR on NK cells inhibiting NK cell based cytotoxicity.

Altogether these results indicate that the combination of H-1PV and ABT-737-more efficiently, than single treatment, able to alter the expression of NK cell associated ligands on PC3 cells that may induce NK cell mediated cytotoxicity.

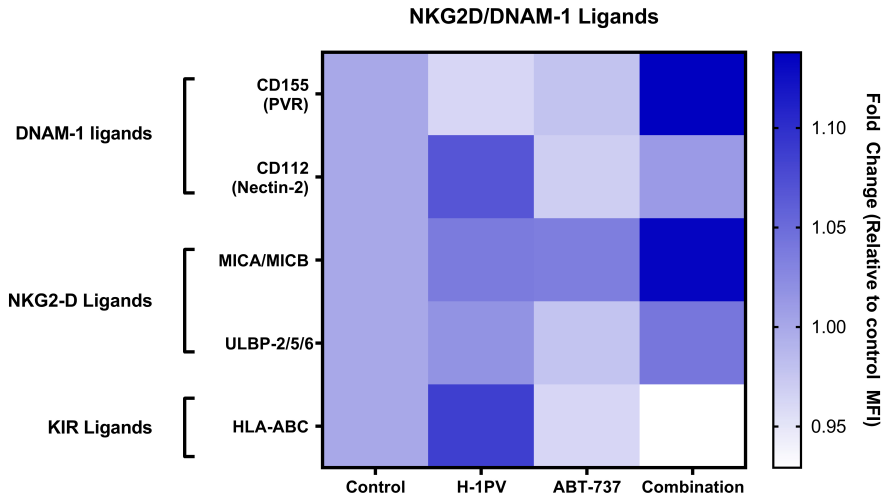

Figure 3.18: ***H-1PV in combination with ABT-737 is able to upregulate the pro-cytotoxicity NKG2D/DNAM-1 and down regulate inhibitory KIR ligand on PC3 cells.*** *PC3 cells were grown with 10 MOI H-1PV, 1μM ABT-737, alone, or in combination. 48 hours post treatment, cells were harvested and assessed for the expression of CD155, CD112, MICA/MICB, ULBP-2/5/6 and HLA-A,B,C by flow cytometry. Heatmap shows the fold change for the different cytokines, from 3 independent experiments expressed as mean, relative to the untreated control samples.*

3.4.2 H-1PV and ABT-737 combination induces Natural Killer (NK) cell activation and NK cell based cytotoxicity

As there was an upregulation of multiple activating ligands and downregulation of inhibitory ligands on H-1PV/ABT-737 co-treated PC3 cells, I investigated whether these changes would be sufficient to trigger the activation of NK cells and eventually induce NK mediated cytotoxicity against cancer cells.

To this end, it was first necessary to establish a proper assay to see whether NK cells were activated by the (co)-treated PC3 cells, using NK cells and target PC3 cells. Based on previous literature [65, 115], total PBMCs were overlaid on top of (co)-treated PC3 cells (Figure 3.19A). After testing multiple time points, and based on the time point in which the different expression of ligands was demonstrated in Figure 3.18, I selected 48 hours of – H-1PV and ABT-737 co-treatment- as the time for evaluating whether the co-treated PC3 cells would induce NK cell activation (data not shown). After these 48 hours, the treated PC3 cells were then co-cultured with PBMCs for 6 hours after which cells were stained for the T-cell marker CD3, NK cell lineage marker CD56 and degranulation marker CD107a.

CD107a is upregulated on the surface of NK cells when engaged with target cells and its expression is correlated to cytokine secretion and NK cell mediated lysis of target cells [112].

Cells stimulated with a cocktail of PMA/Ionomycin used in this experiment as a positive control were able to show an upregulation of the above-cited markers as seen in Figure 3.19 . With the use of protein transport inhibitor Brefeldin-A, intracellular cytokines were contained within the cell and it was possible to also detect intracellular IFNγ.

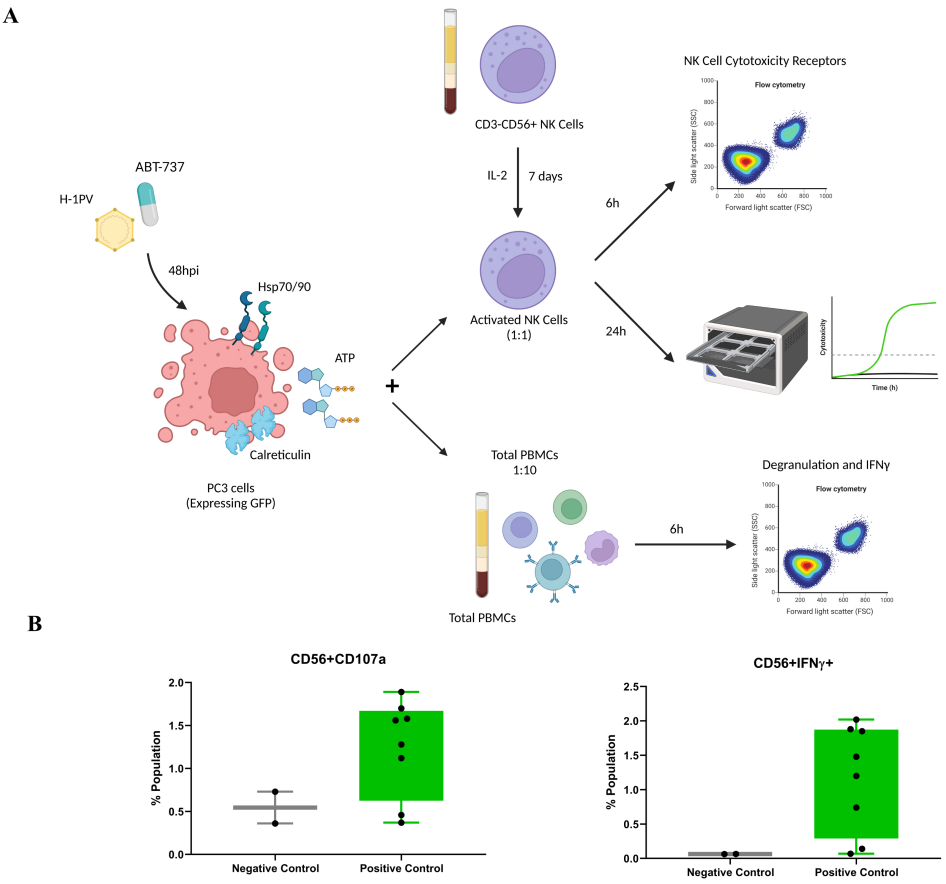

Figure 3.19: ***Establishment of natural killer cell based co-culture assay with PC3 cells.*** *(A) Pictograph showing the NK based co-culture assay. PC3 cells were grown with or without 10 MOI H-1PV, 1μM ABT-737, alone or in combination. 48 hours post treatment, total PBMCs isolated from healthy donors were overlaid on top of the PC3 cells in a 1:10 ratio (1 PC3 cell:10 PBMCs). 1 hour post co-culture protein transport inhibitor Brefeldin-A was added to the culture. After additional6 hours of co-culture, cells were evaluated for cell surface expression of CD107a and intracellular IFNγ. (B) Untreated PBMCs were used as negative controls to establish baseline expression where as PMA/Ionomycin was used a positive control to establish the assay. Each dot is a donor. Values are expressed in $mean \pm SD$ Statistical significance was calculated using a paired two-tailed t test by GraphPad Prism 9; *$P \leq 0.05$; **$P \leq 0.01$; ***$P \leq 0.001$; ****$P \leq 0.0001$. Illustration was created with BioRender.com.*

After having established the assay, PC3 cells treated with H-1PV and ABT-737 alone and in combination were co-cultured with total PBMCs from multiple donors. As seen in Figure 3.20, when gated on CD3-CD56+ cells (NK cells), there was a significant upregulation of the degranulation marker CD107a as well as intracellular IFNγ with respect to the combination treated cells as opposed to the stand alone treatments with H-1PV or ABT-737. This effect is in line with the upregulation of NKG2D/DNAM-1 associated ligands and downregulation of HLA-ABC, KIR associated ligand on PC3 cells described before (Figure 3.18)

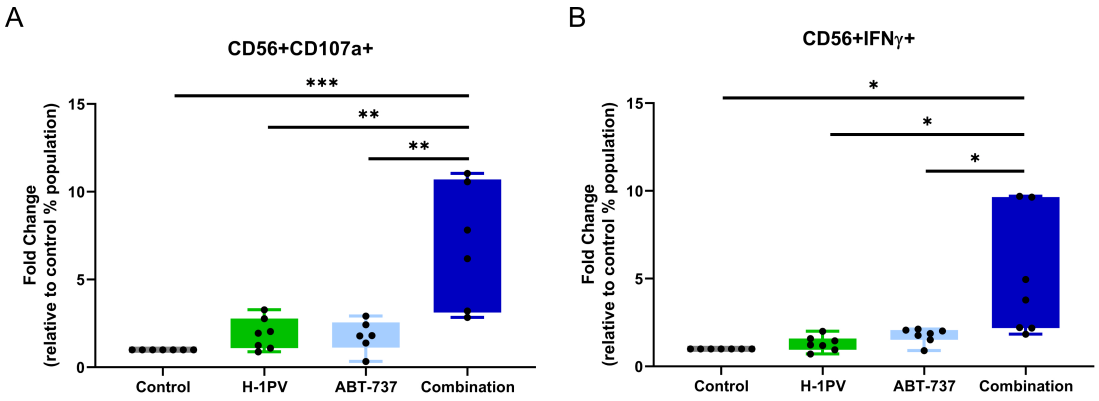

Figure 3.20: ***H-1PV in combination with ABT-737 induces upregulation of degranulation marker CD107a and intracellular IFNγ gated on NK cells.*** *. PC3 cells were grown with or without 10 MOI H-1PV, 1μM ABT-737 alone or in combination. 48 hours post treatment, total PBMCs isolated from healthy donors were overlaid on the treated cells. 1 hour post treatment Brefeldin-A was added to the cells. After a total of 6 hours of co-culture, cells were collected and analysed for CD107a and intracellular IFNγ using flow cytometry. Each dot is a donor. Values are expressed in $mean \pm SD$ Statistical significance was calculated using a paired two-tailed t test by GraphPad Prism 9; *$P \leq 0.05$; **$P \leq 0.01$; ***$P \leq 0.001$; ****$P \leq 0.0001$.*

The results above provide evidence of H-1PV-ABT-737 co-treatment of PC3 cells may result in the activation and degranulation of NK cells by using lineage markers in flow cytometry for a bulk PBMC population. To evaluate whether the NK cells express cytotoxic activity, I established a cytotoxicity-based assay using isolated primary NK cells. However, after multiple attempts isolated NK cells did not seem to survive by themselves in a culture without the addition of cytokines. After screening of the literature, I adapted a protocol in which, NK cells were grown in the presence of IL-2 for a week [65, 115].

By using PC3 cells expressing GFP, it was possible to set up a cytotoxicity assay using the real time imaging system, Incucyte S3. PC3-GFP cells were treated with H-1PV and ABT-737, alone or in combination. 48 hours post treatment, primary NK cells (IL-2 activated) from healthy donors were overlaid on these treated cells, in the ratio 1:1.

Cell growth and GFP signal was monitored for up to 48 hours of co-culture. The Incucyte S3 software was used to calculate cell confluence.

As seen in Figure 3.21A, the combination of H-1PV and ABT-737 was able to accelerate the cytotoxicity brought about by NK cells. This was also verified by an increase in LDH release at 24 hours post co-culture, in the PC3 cells co-treated

with H-1PV/ABT-737 (Figure 3.21B). The pro-cytotoxicity cell surface receptors present on NK cells, which are associated with the cancer cell ligands tested in Figure 3.14, were also upregulated by the combination treatment of H-1PV and ABT-737 (Figure 3.21C).

Thus, altogether these experiments demonstrate that co-treatment of PC3 cells with H-1PV and ABT-737 is associated with changes in the expression of pro-stimulatory NK cell associated ligands, that indeed induce the activation of NK cells which participate in the killing of cancer cells.

3.4.3 H-1PV in combination with ABT-737 triggers cytokine production in Natural Killer cells

Similar to DCs, active NK cells also produce an array of cytokines [112]. Thus, I checked whether the treatment of PC3 cells with the H-1PV/ABT-737 combination would result in cytokine production by NK cells. Supernatants from the co-culture assay as described in Figure 3.21, were collected, 24 hours post co-culture and evaluated for an array of multiple cytokines using the BioLegend LegendPLEX platform. As seen in Figure 3.22, several cytokines were found in the supernatant of PC3/NK co-cultures when PC3 cells were infected with H-1PV. However, upregulation of IL-12p40 was specifically observed only when PC3 cells were co-treated with H-1PV/ABT-737 combination. This cytokine is associated with NK cell activation and therefore corroborates previous results (Figure 3.21) showing that the H-1PV/ABT-737 combination treatment by inducing an ICD may activate NK cells. Co-treatment of PC3 cells was also associated with a significant upregulation of IL-4, IL-17A and TGF-β1. IL-4 and IL-17A are crucial for inflammation and IL-17A plays an important role in recruitment of neutrophils to the site of inflammation.

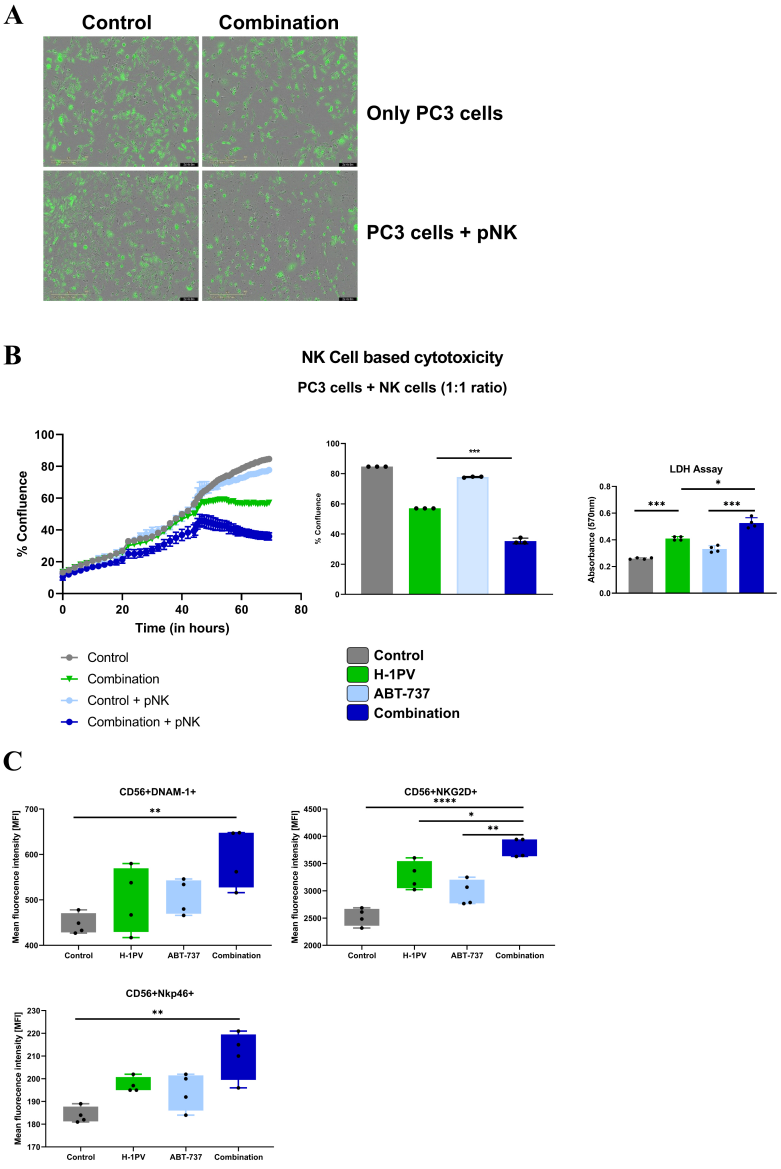

Figure 3.21: ***Treatment of PC3 with the H-1PV and ABT-737 combination accelerates NK cell mediated killing of PC3 cells and induces activation markers associated with NK cell based cytotoxicity on PC3 cells.*** *PC3 cells were grown with, without H-1PV, ABT-737 alone, or in combination. 48 hours post treatment, primary NK cells (cultured in IL-2 for one week) isolated from healthy donors were overlaid on the treated cells. The cells were monitored in Incucyte S3 for upto total 72 hours post treatment. (A) Incucyte images showing PC3 cells expressing GFP with or without H-1PV, ABT-737 alone or in combination. (B) Cell confluence over time for PC3 cells with or without NK cells. Bar graph shows confluence values at 24 hours post co-culture. LDH assay was carried out with the supernatants 24 hours post co-culture. (B) 6 hours post co-culture NK cells were collected and the NK cell population (CD56+) was evaluated for NKG2D and DNAM-1 expression using flow cytometry. Each dot is a donor. Values are expressed in* $mean \pm SD$ *Statistical significance was calculated using a paired two-tailed t test by GraphPad Prism 9;* $*P \leq 0.05$*;* $**P \leq 0.01$*;* $***P \leq 0.001$*;* $****P \leq 0.0001$.

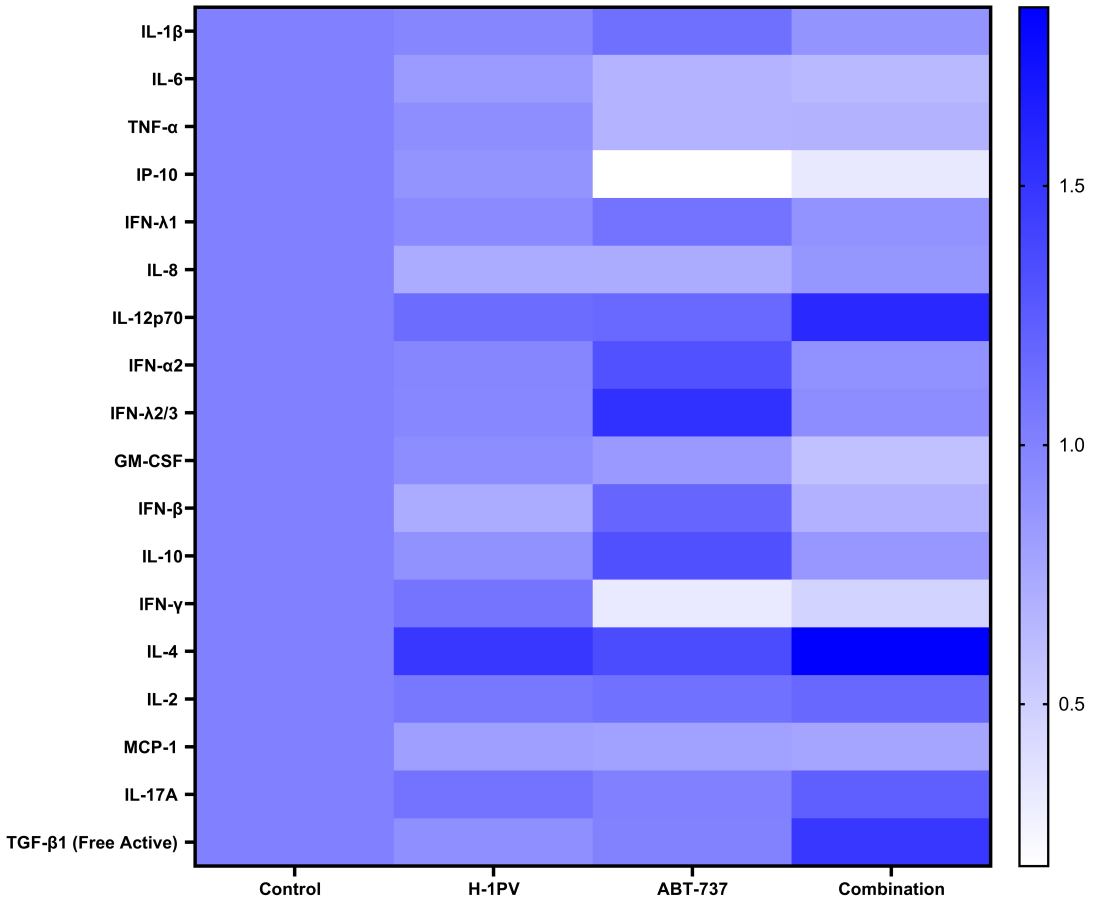

Figure 3.22: ***H-1PV and ABT-737 combination treatment of PC3 cells is associated with cytokine production by co-cultured NK cells.*** *PC3 cells expressing GFP grown in the presence or absence of 10 MOI H-1PV, 1μM ABT-737, alone or the combination of the two agents. 48 hours post treatment NK cells (IL-2 activated) were co-cultured with these treated PC3 cells. After 24 hours of co-culture supernatants were collected and assayed for their content of cytokines through flow cytometry using the bead based BioLegend LegendPLEX multiplex platform. Heatmap showing the fold change for different cytokines, for 3 donors, normalised to the untreated control.*

3.5 H-1PV in combination with ABT-737 is capable of synergistically killing patient-derived prostate cancer cell cultures

The lack of suitable cell lines for screening the efficacy of the combination was one of the major limiting factors throughout the project. Thus, I decided to validate the treatment in patient-derived primary prostate cancer cell cultures as clinically relevant models. I obtained patient derived LuCaP 136 and LuCaP 147, which are patient derived spheroid cultures, from Dr. Johannes Linxweiler in UKS Homburg. I first tested whether these cultures were sensitive to parvovirus infection by using recombinant H-1PV expressing GFP. As seen in Figure 3.23, I could see that both these spheroid cultures were susceptible to virus infection.

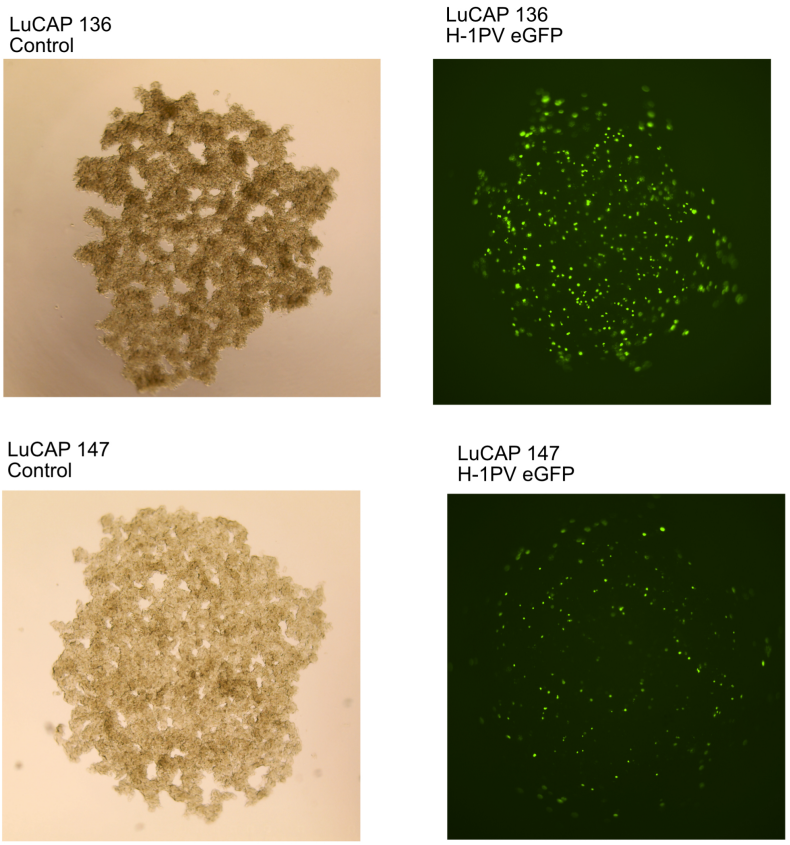

Figure 3.23: *H-1PV is able to infect patient-derived LuCaP 136 and LuCaP 147 spheroid cultures. LuCaP 136 and LuCaP 147 cells were grown in the presence of replication incompetent H-1PV expressing GFP. Images were captured on a Nikon Confocal Microscope showing spheroid cultures with H-1PV (green).*

I decided to treat the cells with varying concentrations of the virus and ABT-737, alone or in combination. I could see that at 50 MOI H-1PV and 1μM ABT-737, there was a very strong synergistic effect in LuCaP 147 cells and a mild one in LuCaP 136 cells (Figure 3.24). Thus, these results confirmed in primary spheroid cultures derived from patients with prostate cancer that the addition of ABT-737

potentiates the killing activity of H-1PV.

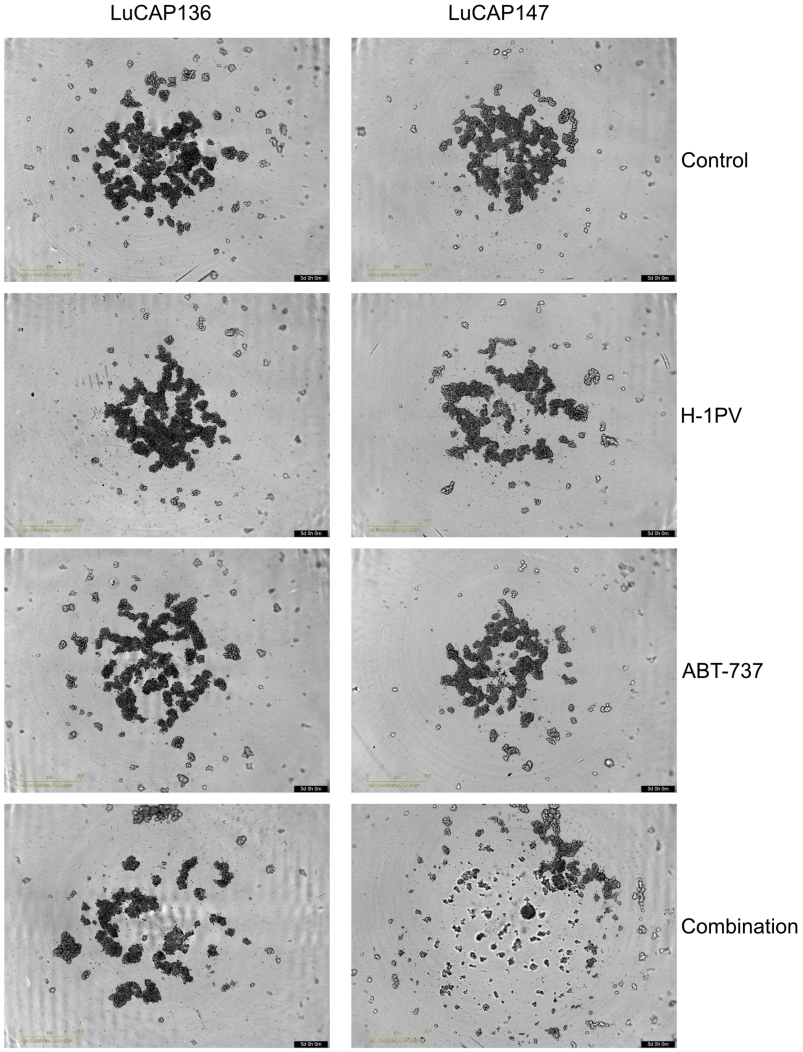

Figure 3.24: *H-1PV in combination with ABT-737 induced cytotoxicity of prostate derived spheroid cultures. LuCaP 136 and LuCaP 147 cells were grown with or without 50 MOI H-1PV, 1µM ABT-737, alone or in combination. Cells were monitored in real time on an Incucyte SX3. Image above showing representative images 72 days after treatment.*

Chapter 4

Conclusions and Outlook

Oncolytic virotherapy is a fast evolving field in cancer research. As with any other therapy, it has its own challenges and advantages. Phase I and IIa clinical trials in glioma and pancreatic carcinoma patients showed that H-1PV treatment, although safe, well tolerated and associated with some signs of efficacy, is still insufficient as a monotherapy to completely eradicate tumors. Thus, the goal of my thesis was to potentiate the oncolytic activity of the virus, through combination therapy in prostate cancer. I was able to show that there is potential in combining H-1PV with chemotherapeutics such as pro-apoptotic BH3 mimetic drug ABT-737 in prostate cancer cells. These results substantiated the previous findings from the lab where ABT-737 was found to be effective in combination with H-1PV against multiple cancer cell types, including glioma and pancreatic cancer cells. In this thesis, the use of the drug, even at sub-lethal doses is able to boost the oncolytic activity of H-1PV in a synergistic manner in a prostate cancer PC3 cells. This cell death induced by the combination is apoptotic and shows signs of an immunogenic cell death (ICD). This ICD is further capable of engaging dendritic cells, T-cells, and NK cells, thus hinting towards a favorable anti-tumor immune response against prostate cancer cells (Figure 4.1).

4.1 Prostate cancer cells showed different susceptibility to H-1PV infection.

Prostate cancer cells have been studied sparsely in the context of H-1PV infection. In PC3 prostate cancer cells, both *in vitro* and in a rat xenograft model [18, 116, 117], it was demonstrated that an H-1PV mutant expressing CDK9 silencer shRNA exhibited superior oncolytic potential compared to the wild-type H-1PV. These findings also revealed that the use of wild-type H-1PV as a monotherapy had only a marginal therapeutic effect on PC3 xenografts *in vivo*. This highlighted the issue of insufficiency of the monotherapy, also in prostate cancer cells. Furthermore, this provided me a rationale to investigate different combination therapies to potentiate H-1PV therapy in prostate cancer cells.

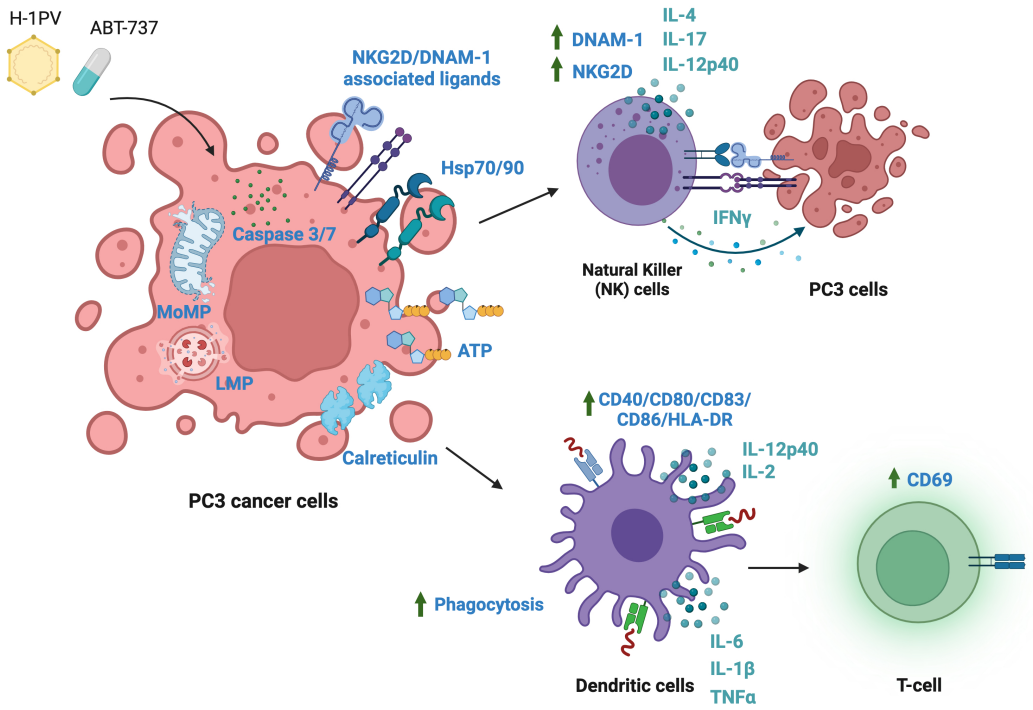

Figure 4.1: ***Graphical Abstract showing the mode of action for H-1PV and ABT-737 co-treatment in prostate cancer PC3 cells and the effect of the treatment on primary immune cells.*** *The combination of H-1PV and ABT-737 exhibits a synergistic effect in the selective destruction of PC3 cells. This cell death process is linked to an increase in Lysosomal Membrane Permeabilization (LMP) and induction of apoptosis as revealed by increase of Mitochondrial outer membrane permeabilization and activation of caspase3/7. H-1PV/ABT-737 combination is also associated with increased levels of cell surface calreticulin, Hsp70, Hsp90, and release of extracellular ATP. These molecular changes are indicative of immunogenic cell death (ICD). Consequently, the ICD triggers the activation and maturation of dendritic cells (DCs), which are capable of phagocytosing antigens and serving as antigen-presenting cells (APCs). This, in turn, leads to the stimulation of T-cell activation. Furthermore, the co-treatment of H-1PV and ABT-737 upregulates the expression of pro-cytotoxicity ligands associated with natural killer (NK) cells on PC3 cells. As a result, the activation of primary NK cells is enhanced, leading to increased killing of PC3 cells treated with H-1PV/ABT-737 by NK cells. Illustration was created with BioRender.com.*

I discovered that H-1PV was able to efficiently infect only 2 out of 4 prostate cancer cell lines that were tested. Oncolytic viruses are strictly dependent on cell host factors for their life cycle which include availability of cell surface receptors and soluble factors for enabling the process of cell entry, need of cellular factors for viral replication and cell lysis [118]. Unsuccessful or a non-productive infection may occur at every step of the virus life cycle, from entry to egress. For instance, reovirus requires the junctional adhesion molecule 1 (JAM-1), an integral tight junction protein, as a cell surface receptor to enter cells. It was shown that induction of JAM-1 expression could enable reovirus infection in otherwise non-permissive cells [119]. Recent studies demonstrate that H-1PV requires Laminin $\gamma 1$ and Galectin-1 for cell entry, along with sialic acid residues. Depletion of both Laminin $\gamma 1$ and Galectin-1, in otherwise permissive HeLa and NCH125 cells, could inhibit H-1PV cell entry and thus a successful infection [67, 68]. Thus emphasizing the importance of host cellular factors for virus entry.

I found that H-1PV is unable to infect the LNCaP prostate cancer cell line and this is most likely because these cells do not present Galectin-1 on their surface. This could potentially explain the inability of the virus to enter these cells. This data is indicative of the fact that in a clinical setting, it would be important to screen the patient cancer cells for factors that are needed for the virus for a productive infection. Unfortunately, many of these factors remain to be identified in the case of H-1PV.

Testing cancer cells for H-1PV infection is not the sole limiting factor; it is also imperative to assess the effectiveness of the drug intended for use in the combination study in patient cancer cells. The efficacy of the drug, whether used alone or in conjunction with H-1PV, can differ among various cell types. For example, VPA, a drug previously shown to synergize with H-1PV in eliminating pancreatic and cervical cancer cells [79], is less effective in prostate cancer cells, as shown in this study.

The adapted synergy assay based on Cokol-Cakamak et al.[90] could provide a suitable platform for testing the efficacy of the virus as well as the compound. This assay effectively assesses the dose response curve of the virus and the drug. It also determines the combined action of the two, indicating whether it is additive, synergistic, or antagonistic.

4.2 The combination of H-1PV and ABT-737 triggers an apoptotic cell death.

H-1PV is known to trigger different cell death pathways in different cancer cell lines. It has been shown in glioblastoma cells, where H-1PV alone is known to kill glioma cells through a cathepsin mediated non-apoptotic cell death [73]. However, it was also previously shown that a combination of H-1PV with ABT-737 was able to trigger an apoptotic cell death in glioma and pancreatic cancer cells (unpublished results). Thus, I wanted first to confirm whether H-1PV/ABT-737 co-treatment also induces apoptosis in prostate cancer cells.

In case of the prostate cancer cells, I could see a very significant upregulation of activated caspase 3/7 and Annexin V and changes in mitochondrial outer membrane permeabilization (MoMP), all markers for apoptosis. The treatment of apoptosis inhibitor ZVAD/FMK was able to successfully block apoptosis and rescue PC3 cells from H-1PV/ABT-737 mediated cell death, which confirmed the likelihood that H-1PV in combination with ABT-737 triggers an apoptotic cell death. These results indicated that pro-apoptotic drug ABT-737 was probably able to potentiate the oncolytic activity of H-1PV, by enabling apoptosis in these cells. Inhibition of apoptosis by cancer cells, is also a very fundamental process in cancer initiation and progression. Thus, many cancer cells harbor defects in apoptotic cell death factors. For instance, a functional p53 is essential to trigger apoptosis in tumor cells. More than 50% of human cancer cells have been shown to have a p53 mutation, which also has been shown to be prognostic of a poor response to chemotherapy [120, 121]. Thus, considerable efforts are employed in devising promising and new approaches for treatment for cancer through exploitation of apoptosis [106]. In prostate cancer cells as well, there have been numerous studies which have shown multiple pathways for apoptosis being defected causing a block in apoptosis. For instance, metastatic prostate cancers show a p53 mutations [122] as well as over-expression of anti-apoptotic BCL2 proteins [123]. Thus it is possible that ABT-737 mediated apoptosis could be co-related to the inhibition of BCL2 proteins by this drug in PC3 cells, as seen in the study.

A very significant upregulation of Lysosomal Membrane Permeabilization (LMP) was also observed upon treatment of PC3 cells with H-1PV and ABT-737. LMP is often associated with a non-apoptotic cell death. However, recent studies have also shown LMP in late apoptotic cells [105, 124]. LMP is caused by a plethora of different factors occurring in the event of cell death. DNA Damage, activation of Bax protein, induction of Reactive Oxygen Species are some of the different factors which induce LMP [105, 124]. Oncolytic H-1PV is capable of inducing many of these factors during oncolysis [31, 79, 125]. Thus, the induction of LMP could be attributed as a standalone event, caused by the virus infection or it could also be a part of an apoptotic process.

It is important to note that cell death processes can be complex, and cells may

engage multiple death pathways simultaneously or sequentially, depending on the specific conditions and stimuli involved. The classification of cell death induced by oncolytic viruses is an active area of research, and our understanding of the diverse mechanisms and their interplay continues to evolve.

4.3 H-1PV and ABT-737 induce the markers for an immunogenic cell death (ICD)

Conventionally, apoptotic cell death is a programmed function of cell metabolism, which ensures formation of apoptotic bodies (small aggregated packages of cell remains encased in the cell membrane). These apoptotic bodies are then phagocytosed by macrophages as a way of clearing cell debris. This ensures that the cell material, largely released in the extracellular space, is effectively cleared out and thus an elaborate inflammation response is specifically avoided, making the cell death tolerogenic [126, 127]. On the contrary, a classical feature of non-apoptotic cell death is compromised cell membrane, a "leaky" membrane, eventually puncturing the cell and releasing all cell material into the extracellular space. This cell material triggers an immune response and causes infiltration of immune cells to clear the debris and other affected cells [11, 126, 127].

However, this conformist outlook about apoptosis has been criticized for being an oversimplification of the process [127]. Recent reports also suggest an immunogenic apoptosis can be triggered by chemotherapy and oncolytic virotherapy. Doxorubicin, a well-known ICD inducing anthracycline, was shown to induce immunogenic cell death dependent on caspase activation in colon carcinoma cells. This immunogenic cell death was able to activate DCs and T-cells and showed tumor regression in a syngeneic mouse model for colon carcinoma [128]. It has also been shown that apoptotic cells are capable of presenting antigens to dendritic cells through an MHC-I dependent manner. Especially in the case of stressful events such as viral infections, this was shown to be relevant in mouse models [129]. Significantly, the heat shock proteins (Hsp) and calreticulin have been observed to bind with recently processed cytosolic-derived epitopes in a dying cell. Furthermore, when introduced *in vivo*, they effectively activate cytotoxic T lymphocytes through cross-priming [130–132]. Heat shock proteins are generally induced in the events of stressful events such as virus infection. Otherwise acting as molecular chaperones which aid in proteasome-mediated degradation of proteins as well as aid the cells in overcoming stress induced cell death, in the event of certain triggers, these molecules translocate to the cell surface and act as DAMPs to activate the immune cells. Hsp70 and Hsp90 are known to trigger immune cell differentiation and maturation [106, 132]. Previously too H-1PV, as a standalone treatment was able to induce the expression of Hsp72 in melanoma cells [80]. Accordingly, we hypothesized that expression of surface calreticulin, Hsp70 and Hsp90 in the H-1PV/ABT-737 co-treated PC3 cells could result in im-

mune cell maturation and activation as a consequential downstream of the immunogenic cell death observed. However, this was not obvious considering other immunogenic cell death markers.

Although I saw a significant expression of cell surface DAMPs, the expression of extra-cellular DAMPs, namely HMGB-1 release, CXCL-10 secretion and extracellular ATP, seemed to be less significant in H-1PV and ABT-737 treated PC3 cells. I saw an increase in extracellular ATP at early time points with H-1PV infection. Although this was not enhanced when the virus was used in combination with ABT-737, it is crucial to note that this effect was retained in the combination treatment and was still higher than untreated cells. In PC3 cells treated with H-1PV alone or in combination with ABT-737, I did not see HMGB-1 release at any given time point. Although HMGB-1 release is one of the characteristic markers for ICD, its expression alone cannot be necessarily associated as a reliable sign of immunogenicity. There have been discordant reports of HMGB-1 expression being able to induce immune activation as a standalone DAMP molecule [39].

Like HMGB-1 release, I did not see IFNα2 secretion or it's downstream CXCL-10 secretion with the virus treatment alone or in combination with ABT-737. H-1PV has been recently shown to shut down type I IFN responses in pancreatic cancer cells. Exogenous IFN was unable to rescue the cells from infection; however, H-1PV infection still led immune cells to produce IFNγ [133]. Thus, the fact that I did not see IFNα2 or CXCL-10 production by PC3 cells treated with H-1PV (with or without ABT-737) could be attributed to the silencing of innate immune signaling by H-1PV in prostate cancer cells as well. However, further experiments are required to shed light on this aspect in PC3 prostate cancer cells.

Classification of an immunogenic cell death also does not require the expression of all DAMPs. Depending on triggers and type of cell death, the markers for immunogenic cell death vary largely. For instance, it has been shown that treatment of cancer cells with anthracyclines such as doxorubicin have been shown to trigger eIF2 phosphorylation which leads to the expression of cell surface CRT, release of HMGB-1 and ATP in breast cancer cells [134]. In another study, it was shown that treatment with Bortezomib was able to induce cell surface expression of CRT and HSP70 in lymphoma cells, but no HMGB-1 and ATP release [135]. However, both the treatments, independently, were shown to be engaging immune cells to induce an anti-cancer immune response, despite expressing different DAMPs [134, 135].

Thus, cell surface expression of CRT, Hsp70 and Hsp90 along with ATP release could be sufficient to characterize H-1PV-ABT-737 triggered cell death as immunogenic. If the expression of said markers was indeed adequate to define the cell death as immunogenic, it would reflect in the ability of these cells to induce the activation of immune cells. Thus, I decided to look at different immune cell populations to see whether PC3 cells treated with H-1PV and ABT-737, were able to induce any form of a functional immune response.

4.4 H-1PV/ABT737 co-treatment mediated immunogenic cell death was further able to engage the adaptive as well as innate immune cell function.

Recapitulating a functional immune response *in vitro* has always been a challenge for immunologists. The requirement of specific haplotypes in human immune cells, limited capabilities to replicate distal and proximal signals occurring under physiological conditions are some of the major factors that somehow hinder the true study of functional immune cell based responses outside of physiological conditions [136]. Thus, I had to primarily adapt screening assays, based on literature, to set proper functional models for testing the effect of a H-1PV based treatment on immune cells.

Dendritic cell-based assays have been established and used in immunotherapy research since a few years now [137, 138]. Based on available literature for using dendritic cells and in particularly, with H-1PV virotherapy, I was able to optimize the conditions for PC3 cells and replicate these assays to evaluate the status of dendritic cells upon co-treatment of H-1PV and ABT-737 [84, 138, 139]. Based on my results, it was clear that the killing of PC3 by H-1PV/ABT-737 combination was able to induce, on DCs, the upregulation of cellular markers associated with their maturation and activation. The presence of co-stimulatory markers CD80, CD86 and HLA-DR is a key property, which enables T-cell engagement and activation. These markers were not expressed at the same levels when PC3 cells were treated with single agents. These results support that H-1PV in combination of ABT-737 can induce a cell death in PC3 that leads to a more efficient engagement of DCs. Generation of functional DCs is the first step in initiating an anti-tumor immune response. These results confirm previous observations that oncolytic viruses, including H-1PV induce potent immune responses and can enhance tumor-associated antigens presentation by DCs [30, 84, 140].

In order to evaluate the engagement of T-cells, I utilized NY-ESO1 as a model antigen, known for its expression in various cancers, including prostate, and its ability to elicit robust immune responses [109, 141]. I first established an *in vitro* assay to evaluate TCR specific T-cell responses using donor specific DCs as APCs. I found that, the functionally active DCs generated upon H-1PV/ABT-737 co-treatment of PC3 cells, were able to also upregulate the activation of NY-ESO1 TCR specific T-cells, thus confirming the completion of the DC/T-cell axis. My results suggest that when applied to an immunologically cold tumor, the co-treatment of H-1PV and ABT-737 could serve as an adjuvant therapy, further boosting T-cell responses. It would be however important to see whether these activated T-cells are functional in killing cancer cells themselves. It was unfortunately not possible to investigate this using the established assay. Further work remains to be carried out to characterize T-cell response.

As adaptive immune cell responses are important in tumor immunotherapy,

natural killer (NK) cells also play a crucial role in promoting an effective anti-tumor immune response especially in association with oncolytic virotherapy. Their ability to target and eliminate cancer cells, modulate the immune response, and counteract immune evasion mechanisms makes them valuable tools in the fight against cancer. It has already been shown previously that H-1PV is able to trigger NK cell mediated killing of pancreatic cells through upregulation of NK cell mediated pro-cytotoxicity ligands [65].

I could see that H-1PV/ABT-737 co-treatment had the remarkable ability to significantly enhance the activation of NK cells, a critical component of the body's innate immune system. This effect was significantly higher in the combination treatment than in stand-alone treatment with the virus and the BH3 mimetic. This enhanced activation led to a superior NK cell-mediated cell death, where NK cells effectively targeted and eliminated PC3 cancer cells, providing further evidence of the ability of the H-1PV/ABT-737 co-treatment of reinforcing immune responses in this context.

Thus, overall, H-1PV in combination with ABT-737 kill cancer cells more efficiently inducing an immunogenic form of cell death. This results in the activation of multiple immune cell populations. So sublethal doses of ABT-737 not only act as a booster of H-1PV oncotoxicity but also may reinforce H-1PV's ability to engage the immune system and to elicit anti-cancer immune responses. The results obtained also provides preliminary indication for the further application of this combination therapy as adjuvant therapy for immunological interventions, with respect to DCs, T-cells as well as NK cells in cancer immunotherapy.

4.5 Validation of combination using patient derived cell cultures: LuCaP 136 and LuCaP 147

The major part of this thesis is dedicated towards elucidating the nature of H-1PV/ABT-737 co-treatment in only PC3 cell line. The clinical relevance of PC3 cells lies in their ability to recapitulate many features of aggressive prostate cancer in patients, making them a valuable tool for studying the molecular mechanisms underlying prostate cancer progression and for developing new therapeutic strategies. Researchers can use PC3 cells to test the efficacy of various drugs or other therapeutic agents, including chemotherapy, radiation therapy, immunotherapy, and targeted therapies, to identify potential therapeutic targets and to elucidate the molecular pathways involved in tumor growth and metastasis [142]. Furthermore, PC3 cells have been used to model the bone metastasis that commonly occurs in advanced prostate cancer, providing insights into the mechanisms that promote cancer cell homing, adhesion, and growth in the bone microenvironment [92]. In summary, PC3 cells have shown significant clinical relevance in prostate cancer research and have contributed to the development of new therapeutic approaches for the treatment of advanced prostate cancer.

Although this is true, the biggest limitation of this study remains the use of only one cell type to characterize the effect of H-1PV/ABT-737 combination treatment. Thus, it was important to evaluate the efficacy of the combination treatment in relevant clinical models, such as other patient derived cells. In this context, I was able to find two different types of patient derived established cell cultures for prostate cancer.

LuCaP prostate cancer cultures are a series of cell culture models derived from human prostate cancer tissues. These cultures have been established and maintained in laboratory settings to study various aspects of prostate cancer biology, including tumour growth, response to treatments, and molecular characteristics. The LuCaP series typically refers to a collection of prostate cancer cell lines derived from individual patients. Each cell line within the LuCaP series is assigned a specific number, such as LuCaP 136, which represents the particular patient from whom the cells were obtained [143–145]. I was able to obtain LuCaP 136 and LuCaP 147 for validating the effect of this combination.

As seen with other cell types, it was important to first verify whether H-1PV can infect these cells. Both LuCaP 136 and LuCaP 147 were responsive to virus treatment. I further tested whether the combination of H-1PV and ABT-737 was effective in these cells. The combination was indeed able to show a synergistic effect in both these cell cultures. This experiment proved significant as it demonstrated the effectiveness of the combined treatment of H-1PV and ABT-737 in multiple cell types. Although the synergistic effect seen in LuCaP 147 was far more effective than that of LuCaP 136 cells, the combination treatment was still more effective than monotherapies alone.

Testing treatment regimens in various patient-derived cells is an essential step in advancing precision medicine, improving treatment outcomes, understanding drug resistance, and accelerating the development of novel therapies. It brings research closer to the individual patient and increases the potential for successful clinical interventions [146]. LuCaP 136 and LuCaP 147, especially are very relevant models for translational prostate cancer research as they have largely retained the immunophenotype and genetic fidelity of the original patient xenograft. Secondly, these cultures are 3D spheroid cultures, which have been shown to be better suited models for translational research. It has been shown that drug responses can vary between 2D cell line based models and 3D spheroid cultures. Drug responses to 3D models have been shown to be more similar to the *in vivo* responses, proving to be a better tool for cancer research [147]. For instance, Eder et al. cultured prostate cancer cells using the hanging drop technique, and co-cultured the cancer cells with cancer-associated fibroblasts [148]. The results demonstrated a higher count of cancer cells relative to fibroblasts within the spheroids, which accurately mirrors what is typically observed *in vivo*. By utilizing this approach, the researchers successfully circumvented the issue of non-representative cell type ratios often encountered in 2D models.

Thus, overall the results obtained from this experiment were very promising and indicative of the fact that the co-treatment of H-1PV and ABT-737 may work in enhancing oncolytic as well as immunogenic potential of H-1PV, across different cell types. However further studies need to be done in order to see whether this synergistic killing of spheroid cultures is associated with the expression of markers for immunogenic cell death and whether this combination is able to induce a favourable anti-cancer immune cell activation, across different cells types as well.

4.6 Final Comments and Outlook

Investigating the immune system *in vivo* can be difficult, so researchers often resort to *in vitro* and *ex vivo* assays to simplify the system. However, when using these approaches, important factors relevant to therapeutic intervention are often overlooked. For example, the potency of a compound may differ significantly between *in vitro* and *in vivo* settings due to its shelf life and pharmacokinetic clearance *in vivo* [149]. Additionally, the behavior of immune cells is strongly influenced by both proximal and distal signaling, which can impact their ability to infiltrate tumor tissues and carry out their functions efficiently [150, 151].

The lack of any pre-clinical data using immunocompetent mouse models is one of the major limitations of this study. To address this issue, we tested TRAMP-C1 mouse prostate cancer cells. Unfortunately, these cells were not permissive to H-1PV infection 6.8 which created a roadblock in furthering this study. To address this challenge, a crucial next step would involve investigating alternative mouse prostate cancer cells like RM-1, which find common application in immunotherapy and pre-clinical studies for prostate cancer [152, 153].

Additionally, exploring various rat cell lines such as AT-2 and AT-3 [154] for H-1PV infection could be considered for testing the efficacy of the H-1PV/ABT-737 combination therapy. Syngeneic rat models employing these cells have also been extensively utilized in evaluating the therapeutic effectiveness of diverse treatments [155, 156]. Furthermore, H-1PV efficacy has been already examined in various orthotopic rat models, including glioma (RG2 based rat model), offering preliminary insights into the potential of using rat models for H-1PV intervention studies [32, 77].

Nevertheless, the investigation lays the foundation for a combination therapy integrating H-1PV and the BH3 mimetic ABT-737. The findings presented in this thesis hold promise as a predictive indicator for potential clinical outcomes for future clinical studies using H-1PV and ABT-737 in prostate cancer. Particularly noteworthy is the research's demonstration of H-1PV sensitivity and its effectiveness when combined with ABT-737 in prostate cancer cells. Furthermore, the study further corroborates the immunogenic effects of H-1PV therapy, especially when used in conjunction with the BH3 mimetic drug.

Chapter 5

Materials and Methods

5.1 Cell lines

Prostate cancer derived PC3, DU145, LNCaP, VCaP and TRAMPC1 cells [91, 92] were were grown in Rosewell Park Memorial Institute (RPMI) 1640 (Sigma Aldrich R8758) supplemented with 10%FBS (GIBCO 26140079) and 1% Penicillin Streptomycin (GIBCO 15140122). The cervical carcinoma derived HeLa cells were cultured in Dulbecco's Modified Eagle's Medium (DMEM) (Sigma Aldrich D6429) supplemented with 2mM Glutamine, 10%FBS (GIBCO 26140079) and 1% Penicillin Streptomycin (GIBCO 15140122). NB324K cells were grown in Mimimal Essential Media (MEM) (Sigma Aldrich M4655) supplemented with 5%FBS (GIBCO 26140079) and 1% Penicillin Streptomycin (GIBCO 15140122).

5.1.1 Plasmids

- S/MAR-NYESO1-dTomato (Figure 6.1)
- S/MAR-HLA-A2-GFP (Figure 6.1)
- S/MAR-NYESO1-TCR (Figure 6.5)

5.2 Viruses

5.2.1 Wild Type H-1PV

Wild type H-1PV was produced,purified and titrated as previously described [94, 157]. In brief, NB324K cells were infected with virus stocks. When the cytopathic effect of the virus was apparent (5-7 days post infection), cells were harvested and subjected to three freeze-thaw cycles. Cell extracts were then treated with 50U/mL Benzonase nuclease ultrapure (Sigma Aldrich E8263) for 30 min at 37°C. viral particles were then purified through an iodixanol discontinuous gradient. Viral titers were quantified using a plaque assay.

5.2.2 recH-1PV-EGFP

Recombinant H-1PV with the green fluorescent protein-encoding gene(recH-1PV-EGFP) was produced,purified and titrated as previously described [94, 157]. In brief, virus stocks were amplified by infecting NB324K cells with recH-1PV-EGFP and Ad-VP-helper [94]. When the cytopathic effect of the virus was apparent (5-7 days post infection), cells were harvested and subjected to three freeze-thaw cycles. Cell extracts were then treated with 50U/mL Benzonase nuclease ultrapure (Sigma Aldrich E8263) for 30 min at 37°C. viral particles were then purified through an iodixanol discontinuous gradient. Viral titers were quantified using a plaque assay.

5.2.3 Plaque Assay to determine virus titer

Viral titres were quantified by plaque assay as previously described in [94]. In short, NBK324K cells were infected with serial dilutions of purified H-1PV for 1 hour, followed by replacement of virus suspension with an overlay of 0.68% Bacto Agar (BD Biosciences 214010) in MEM (Sigma Aldrich M4655) supplemented with 5% FBS (GIBCO 26140079). At five days post-infection, plaque formation was detected by incubating cells with 0.18% neutral red containing 0.85% Bacto Agar diluted in 1X DPBS (Sigma Aldrich D8537). Plaques were counted from duplicates and titres were expressed as plaque forming units (pfu) per mL.

5.3 Methodology

5.3.1 Cell Viability Assays

Oncolysis was calculated using LDH release and cell viability was calculated using MTT (Sigma Aldrich M5655) cell viability assay. 2000 PC3 cells were seeded in 96 well plates. 8-10 hours post seeding, cells were treated with or without 10 Multiplicities of Infection (MOI)(10 virus particles per cell) H-1PV, 1μM ABT-737 (Selleckchem S1002) , alone or in combination. Cells were incubated at 37°C, 5%CO_2.

LDH Assay:

- 72 hours post infection, 50 μL cell supernatant was collected and the cells were taken for MTT assay
- LDH assay was carried out using LDH assay kit (Promega G1780) as per manufacturer's instructions.
- 100% cell lysis controls were used to calculate relative percent lysis for all samples. The values were expressed as percent oncolysis.

MTT Assay:

- 5μg/mL MTT (Sigma Aldrich M5655) reagent was added to each well and cells were incubated with MTT (Sigma Aldrich M5655) for 2-3 hours
- Media was removed and plates were dried, upside down at 37°C, overnight
- 100 μL of 100% Isopropanol (Sigma Aldrich I9516) was added to the wells
- Shake at 200rpm for 15-20 min
- Absorbance was recorded at 595nm and calculate percent viability relative to untreated cells as 100% viable.

5.3.2 Diagonal Assay to evaluate synergy

This protocol was adapted from [90]. 2000 PC3 cells were seeded in 96 well plates. 8-10 hours post seeding, cells were treated with or without serially diluted titers of H-1PV ranging from 100MOI to 0.38MOI, serially diluted concentration of ABT-737 (Selleckchem S1002), ABT-199 (Selleckchem S8048), VPA (Selleckchem S1168), Pracinostat/SB939 (Selleckchem S1515) and Tacedinaline/CI994 (Selleckchem S2818) ranging from 100μM to 0.38μM , alone or in combination (as shown in Figure 3.3). Cells were incubated at 37°C, 5%CO_2.

- 72 hours post treatment, 5μg/mL MTT (Sigma Aldrich M5655) reagent was added to each well and cells were incubated with MTT reagent for 2-3 hours
- Media was removed and plates were dried, upside down at 37°C, overnight

- 100 μL of 100% Isopropanol (Sigma Aldrich I9516) was added to the wells
- Shake at 200rpm for 15-20 min
- Absorbance was recorded at 595nm and calculate percent viability relative to untreated cells as 100% viable.
- X-values (concentration of treatment) were transformed to log values
- Non-linear regression curves (four parameters) were plot to calculate the IC_{50} values for H-1PV alone, drug alone and combination of the virus and the drug

5.3.3 Cell Proliferation using Real Time Cell Analysis (RTCA) xCELLigence

7000 PC3 cells were seeded in 96 well E-Plate (Roche). 8-10 hours post seeding, cells were treated with or without 10 MOI H-1PV, 1μM ABT-737 (Selleckchem S1002) , alone or in combination. Cells were incubated at 37°C, 5%CO_2. Cell proliferation was monitored every 30 min in real time. Data are expressed as "Cell index" (n = 3) calculated by the RTCA software 1.2.1 (Agilent) as a measure of cell adhesion and, therefore, cell viability. Cell index at 72 hours post treatment was used to calculate percent cytotoxicity (cytolysis) relative to untreated control.

5.3.4 Binding Entry Assay for H-1PV in LNCaP cells

This is a method to detect cell-associated virus more precicely – by doing a qPCR on its DNA. The experiment is done in triplicates in a 24 well plate, 20000 cells/well. HeLa cells were used as a reference for LNCaP. Seed 20000 cells in 24 well plates. 8-10 hours post seeding treat the cells with 100 MOI H-1PV.Tubes with H-1PV containing media were used as input for DNA extraction as 100% virus.

- Cells were incubated for 2 hours – shaken every 5-10 minutes
- Virus solution was removed and cells were washed twice with 1X DPBS (Sigma Aldrich D8537)
- Cells were harvested and and frozen together with the control input media at -80°C
- Three freeze-thaw cycles were done using liquid nitrogen and 37°C water bath. Samples were throuroughly between the cycles.
- Qiagen Mini Elute Virus Spin kit was used to extract the viral DNA
- qPCR was performed as described in [67]

The primers (purchased from Applied Biosystem) used for recognising the NS1 region are

forward primer: 5'-GCGCGGCAGAATTCAAACT-3'

reverse primer: 5'-CCACCTGGTTGAGCCATCAT-3'

5.3.5 Western Blotting for Galectin and Laminin in LNCaP cells

Western blotting was performed as described previously [67, 68]. Immunoblotting was carried out with the following antibodies: rabbit polyclonal anti-galectin-1 (HPA000646) at 1:1000 dilution, (Sigma Aldrich) at 1:4000 dilution; rabbit polyclonal anti-laminin gamma 1 (Thermo Fisher Scientific PA5-36300) at dilution 1:1000; rabbit anti-NS1 SP8 antiserum [158] and rabbit anti-VP1/2 antiserum [159] at 1:5000 dilution. The membrane was then incubated with horseradish peroxidase-conjugated secondary antibodies (Santa Cruz) used at 1:1000 dilution.

5.3.6 Immunofluorescence of NS1 and VP2

20000 LNCaP and HeLA cells were seeded in 24 well plates. 8-10 hours post seeding cells were treated with 100 MOI H-1PV and incubated for 24 hours at 37°C, 5%CO_2.

- Cells were harvested using trypsin-EDTA (Sigma Aldrich SM-2003) before fixing with 3.7% Paraformaldehyde (PFA)
- Cells were washed thrice with 1X DPBS (Sigma Aldrich D8537) before permeabilizing in 0.2% TritonX100 (Sigma Aldrich T8787) for 4 minutes
- Cells were washed thrice with 1X DPBS (Sigma Aldrich D8537). Cells were blocked with 20% FBS (GIBCO 26140079) for 30 min.
- Cells were washed thrice with 1X DPBS (Sigma Aldrich D8537) before incubating with primary antibodies (anti-NS1 and anti-VP2 as described in [35]) for 45 minutes to 1 hour. Nuclei were stained using 10μL DAPI (Sigma Aldrich D9542).
- Cells were washed thrice with 1X DPBS (Sigma Aldrich D8537) before analysing under 10X magnification using a Nikon confocal microscope.

5.3.7 Detection of Apoptosis

Incucycte based analysis of Caspase 3/7 and Annexin V

2500 PC3 cells were seeded in 96 well plates (Nunc). 8-10 hours post seeding, cells were treated with or without 10 MOI H-1PV, 1μM ABT-737 (Selleckchem S1002), alone or in combination at 37°C, 5%CO_2. At this point caspase 3/7 green (Sartorius 4440) and Annexin V red (Sartorius 4641) were added, diluted 1:4000, as per manufacturer's instructions. Cells were monitored from seeing upto 72 hours

post treatment in the Incucyte SX3, with images being captured every hour for phase contrast, green and red fluorescence at 10X magnification. Cell confluence and image analysis was done using the Incucyte SX3 software.

Mitochondrial outer Membrane Permeabilization and Lysosomal Membrane Permeabilization

62500 PC3 cells were seeded in 12 well plates. 8-10 hours post seeding, cells were treated with or without 10 MOI H-1PV, 1μM ABT-737 (Selleckchem S1002), alone or in combination at 37°C, 5%CO_2.

- 24, 48 and 72 hours post treatment, media was collected in 15mL tubes (Corning Falcon CLS352096). Cell supernatants were centrifuged at 350g to collect all debris and cell material.
- Cells were harvested using cell dissociation buffer (Thermo 13151014) and collected in the same tube as the cell debris and cell material from the previous step. Cells were centrifuged at 350g for 5 min at room temperature.
- Supernatants were discarded and cells were washed with 1X DPBS (Sigma Aldrich D8537)
- Cells were stained with Zombie Green cell viability solution (BioLegend 423111) for 15 min in dark, at room temperature. Cells were washed with 1X FACS Buffer (1X PBS+2%FBS).
- Cells were then stained with MitoTracker CMXRos (ThermoFisher Scientific M46752) and LysoTracker yellow HCK-123 (ThermoFisher Scientific L12491) as per manufacturer's instructions.
- Cells were incubated at 37°C for 1 hour and centrifuged at 350g for 5 min at room temperature. The pellet was washed with 1X FACS Buffer (1X DPBS + 2%FBS + 2mM EDTA)
- Unstained cells and compensation controls were used and at least 20000 cells were acquired on a BD LSR Fortessa
- Samples were analyzed by gating live cells (Zombie negative) followed by gating for green and red fluorescence (Figure 6.2)
- Percent population as well as Mean Fluorescence Intensities (MFI) were exported for the samples. Percent population was plot from 3 different experiments done independently.

Detection of Reactive Oxygen Species

62500 PC3 cells were seeded in 12 well plates. 8-10 hours post seeding, cells were treated with or without 10 MOI H-1PV, 1μM ABT-737 (Selleckchem S1002), alone or in combination at 37°C, 5%CO_2.

- 24 and 48 hours post treatment, media was removed and cells were incubated with 10μM H_2DCFDA substrate (ThermoFisher Scientific D399) for 1 hour at 37°C
- Cells were then grown for an additional 30 min after removing the H_2DCFDA substrate.
- Cells were harvested using cell dissociation buffer (Thermo 13151014) and collected. Cells were centrifuged at 350g for 5 min at room temperature.
- Supernatants were discarded and cells were washed with 1X DPBS (Sigma Aldrich D8537)
- Unstained cells were used and at least 20000 live cells were acquired on a BD LSR Fortessa
- Samples were analyzed by gating live cells followed by gating for the green fluorescence (Supplementary Figure 6.2)
- Percent population as well as Mean Fluorescence Intensities (MFI) were exported for the samples. Percent population was plot from 3 different experiments done independently.

5.3.8 Evaluation of Immunogenic Cell Death

62500 PC3 cells were seeded in 12 well plates. 8-10 hours post seeding, cells were treated with or without 10 MOI H-1PV, 1μM ABT-737 (Selleckchem S1002), alone or in combination at 37°C, 5%CO_2.

Extracellular ATP Release, HMGB-1 release and CXCL-10 secretion

- 24, 48 and 72 hours post treatment, media was collected in 15mL tubes (Corning Falcon CLS352096). Spin the cell supernatants at 350g to remove debris and cell material. Supernatant was collected for further analysis.
- 100μL of media was used for HMGB-1 detection through ELISA (Assay Genie HUFI00660) as per manufacturer's instructions
- 100μL of media was used for CXCL-10 detection through ELISA (BioLegend 439904) as per manufacturer's instructions
- 50μL of media was used for detection of extracellular ATP using Cell Titer Glo (Promega G7571) as per manufacturer's instructions

Flow Cytometry based analysis of cell surface proteins

- 24, 48 and 72 hours post treatment, media was collected in 15mL tubes (Corning Falcon CLS352096). Cell supernatants were centrifuged at 350g to collect all debris and cell material.

- Cells were harvested using cell dissociation buffer (Thermo 13151014) and collected in the same tube as the cell debris and cell material from the previous step. Cells were centrifuged at 350g for 5 min at room temperature.
- Supernatants were discarded and cells were washed with 1X DPBS (Sigma Aldrich D8537)
- Cells were stained with Zombie Red cell viability solution (BioLegend 423110) for 15 min in dark, at room temperature. Cells were washed with 1X FACS Buffer (1X PBS+2%FBS).
- The pellet containing cells was incubated in 1X FACS Buffer containing the staining antibodies for AlexaFluor 488-Calreticulin (R&D Systems), AlexaFluor 488-HSP70 (Enzo Life Sciences ADI-SPA-830PE-D) and AlexaFluor 647-HSP90 (Enzo Life Sciences ADI-SPA-820-488-E) separately since two of the antibodies were of the same fluorochrome
- Cells were incubated on ice for 1 hour and centrifuged at 350g for 5 min at 4°C. The pellet was washed with 1X FACS Buffer (1X DPBS + 2%FBS + 2mM EDTA)
- Unstained cells and compensation controls were used and at least 20000 cells were acquired on a BD LSR Fortessa
- Samples were analyzed by gating live cells (Zombie negative) followed by gating for the respective antibodies (Supplementary Figure 6.2)
- Percent population as well as Mean Fluorescence Intensities (MFI) were exported for the samples. Percent population was plot from 3 different experiments done independently.

5.3.9 Co-culture Assays

Isolation of PBMCs from buffy coats

Use all sterile reagents and perform the protocol under aseptic conditions.

- Buffy coats were obtained from consenting donors at the Blutspendezentrale IKTZ Heidelberg.
- Blood was diluted 1:1 with plain RPMI 1640 media. 3M EDTA (GIBCO 15575020), pH 8.0, was added to avoid platelet aggregation.
- 15mL Histopaque 1077 (Sigma Aldrich 10771-100mL) was added to the Leucosep tubes (Greiner Bio 227289) and the tubes were centrifuged at 800g for 1 min to collect the Histopaque below the filter
- The media/blood mixture was added to the leucosep tubes, above the filter.

- The tubes were then carefully centrifuged at 800g for 30 min, room temperature (RT), without brake and acceleration
- The blood mixture was separated into distinct layers,
  - Erythrocytes and granulocytes precipitated below the filter
  - A layer Histopaque above the erythrocytes and granulocytes
  - A buffy coat layer with lymphocytes and monocytes sandwiched between the Histopaque and the plasma layer
  - Plasma at the very top of the mixture
- The plasma layer was removed (till about 1 cm above the buffy coat) using a pipette
- The remaining supernatant (above the filter) was collected into a fresh 50mL tube (BD)
- 10mL 1X DPBS (Sigma Aldrich D8537) was added to the supernatant and centrifuged at 350g for 10 min, room temperature, with brake and acceleration set at default henceforth
- The supernatant was discarded and pellet was suspended in 10mL 1X DPBS (Sigma Aldrich D8537). The tube was centrifuged at 350g for 10min, room temperature, to wash away any remaining plasma.
- Supernatant was discarded and the pellet was suspended in 3mL of ACK Lysis Buffer (Gibco A1049201),to be incubated at RT for 5 min, mixing every 2 min. This ensured that any remaining Red Blood Cells (RBCs) were lysed.
- ACK Lysis buffer was neutralised by adding 8 mL plain RPMI 1640 media to the cells. Cells were then centrifuged at 350 g for 10 min, room temperature.
- Supernatants were discarded and the pellet was suspended in 5 mL complete RPMI 1640 media. Cells were centrifuged at 350 g, 10 min at room temperature to remove any remaining ACK lysis buffer.
- Supernatants were discarded and the pellet was suspended in 10 mL complete RPMI 1640 media. This cell suspension is the peripheral blood mononuclear cell population (PBMCs), which was evaluated for cell viability and total cell number using viability dye trypan blue (Diluted 1:20 with media and then 1:1 with trypan blue) on the Countessa Cell counter.

Evaluation of DC Maturation, Activation and Phagocytosis using a PC3 based co-culture system

Use all sterile reagents and perform the protocol under aseptic conditions.

- PBMCs were isolated as described in 5.3.9.

- Half of the PBMCs were cryopreserved for further assays, at 50 million cells/cryovial in 85% FBS, 10% DMSO in complete RPMI media.
- CD14+CD16- Monocytes were isolated from PBMCs using the MojoSort Monocyte isolation kit (BioLegend 480048)
- Monocytes were evaluated for cell number and viability using trypan blue on the Countessa Cell counter. Monocytes were then cultured in a 24 well plate (0.1 million cells/well) in 500μL complete RPMI containing 50ng/mL rHu GM-CSF (BioLegend 766106) and 50ng/mL rHu IL-4 (BioLegend 766206), 1% HEPES (GIBCO 15630106), 1% GlutaMAX (GIBCO 35050061), 1% Sodium Pyruvate (GIBCO 11360070).
- On day 3, media was replenished with fresh cytokines.
- Immature DCs were harvested on day 6. Monocytes will detach and float as they differentiate into iDCs.
- Cells were evaluated for CD209, a marker for dendritic cell lineage.
- 25000 PC3 cells expressing NYESO1/dTomato and HLA-A2/GFP (Supplementary Figure 6.1) were seeded per well in a 24-well plate. 8-10 hours post seeding, cells were treated with 10 MOI H-1PV, 1μM ABT-737 (Selleckchem S1002) alone or in combination.
- 24 hours post treatment, isolated iDCs were overlaid on top of the treated PC3 cells in the ratio 1:5 (1 PC3 cell: 5 iDCs).
- The activation and maturation of DCs was determined by using flow cytometry after 48 hours of co-culture cells were harcested and first blocked with FcR Blocking Reagent (Miltenyi Biotec 130-059-901) before being stained for the following markers
  - APC-CD80 (BioLegend 375404)
  - APC-Cyanine 7 CD83 (BioLegend 305330)
  - BV650- CD40 (BioLegend 334338)
  - BV421- HLA-DR (BioLegend 307636)
  - PerCP Cyanine 5.5- CD86 (BioLegend 374216)
  - Zombie Red Cell viability dye (BioLegend 423110)
- Cells were fixed with Cell Fixation Buffer (BioLegend 420801) and acquired within 2 days of staining on a BD LSR Fortessa
- At least 50,000 cells were acquired per sample. Live cells (Zombie Red negative) were gated for fluorescent markers. Percent population and MFI values were exported. Percent population was plot for 4 different donors.

- CD86+GFP+ cells were plot as Phagocytosis fraction of matured DCs (Supplementary Figure 6.2)
- Cell supernatants were collected before staining for cytokine array analysis using BioLegend LegendPLEX platform for the anti-virus panel (BioLegend 740390) as well as essential human immune response panel (BioLegend 740930) as per manufacturer's instruction.
- Maturation of DCs was induced by addition of a cytokine cocktail containing 10 ng/mL TNFα (R&D Systems 210-TA-005), 1,000 IU/mL IL-6 (R&D Systems 206-IL-010), 10 ng/mL IL-1β (R&D Systems 210-LB-005). This served as a positive control for the assay.

Evaluation of T-cell activation using a PC3 based co-culture system

Use all sterile reagents and perform the protocol under aseptic conditions.

- PBMCs were isolated as described in 5.3.9.
- Co-culture assay with DCs was performed as described in 5.3.9
- 5 days before termination of the DC co-culture, T-cells were isolated from corresponding donors (by thawing frozen PBMCs), using MojoSort Pan T-cell isolation kit (BioLegend 480131)
- Isolated T-cells were incubated with IL-7 (Miltenyi Biotec 130-093-937), IL-15 (Miltenyi Biotec 130-093-955) and T-cell Transact (Miltenyi Biotec 130-111-160) in TexMACS Medium (Miltenyi Biotec 130-097-196)
- On day 3, T-cells were counted and electroporated to be transfected using MaxCyte GTx platform, with S/MAR vector for NY-ESO1 TCR (Supplementary Figure 6.5)
- Cells were rested for 2 days in TexMACS without cytokines and transact
- Transfection efficiency was evaluated using flow cytometry (Supplementary Figure 6.5)
- Co-cultured DCs were collected and overlaid on top of the T-cells in a 1:2 ratio (1 DC:2 T-cells)
- 16 hours post co-culture, T-cells were collected and first blocked with FcR Blocking Reagent (Miltenyi Biotec 130-059-901) before being stained for AlexaFluor 700-CD3 (BioLegend 317340), BV421-CD69 (BioLegend 310930) and Zombie Red cell viability dye (BioLegend 423110)
- Cells were fixed with Cell Fixation Buffer (BioLegend 420801) and acquired within 2 days of staining on a BD LSR Fortessa.

- At least 50,000 cells were acquired per sample. Live cells (Zombie Red negative) were gated for fluorescent markers. Percent population and MFI values were exported. Percent population was plot for 4 different donors. (Supplementary Figure 6.6)

Flow Cytometry based analysis of Natural Killer (NK) Cell Ligands

62500 PC3 cells were seeded in 12 well plates. 8-10 hours post seeding, cells were treated with or without 10 MOI H-1PV, 1μM ABT-737 (Selleckchem S1002), alone or in combination at 37°C, 5%CO_2.

- 24, 48 and 72 hours post treatment, media was collected in 15mL tubes (Corning Falcon CLS352096). Cell supernatants were centrifuged at 350g to collect all debris and cell material.
- Cells were harvested using cell dissociation buffer (Thermo 13151014) and collected in the same tube as the cell debris and cell material from the previous step. Cells were centrifuged at 350g for 5 min at room temperature.
- Supernatants were discarded and cells were washed with 1X DPBS (Sigma Aldrich D8537)
- Cells were stained with Zombie Red cell viability solution (BioLegend 423110) for 15 min in dark, at room temperature. Cells were washed with 1X FACS Buffer (1X PBS + 2%FBS + 2mM EDTA).
- The pellet containing cells was incubated in 1X FACS Buffer containing the staining antibodies for APC-MICA/MICB (BioLegend 320908), PE-CD112 (BioLegend 337410), FITC-CD155 (BioLegend 337628), AlexaFluor700-HLA-ABC (BioLegend 311438) and BV421-ULBP 2/5/6 (BD Biosciences 748128)
- Cells were incubated on ice for 1 hour and centrifuged at 350g for 5 min at 4°C. The pellet was washed with 1X FACS Buffer
- Unstained cells and compensation controls were used and at least 20000 cells were acquired on a BD LSR Fortessa
- Samples were analyzed by gating live cells (Zombie negative) followed by gating for the respective antibodies
- Percent population as well as Mean Fluorescence Intensities (MFI) were exported for the samples. Percent population was plot from 3 different experiments done independently. (Supplementary Figure 6.2)

Natural Killer (NK) cell activation using total PBMCs in a PC3 based co-culture model

Use all sterile reagents and perform the protocol under aseptic conditions.

- PBMCs were isolated as described in 5.3.9.
- 25000 PC3 cells were seeded cells per well in a 24-well plate. 8/10 hours post seeding, cells were treated with 10MOI H-1PV, 1μM ABT-737 (Selleckchem S1002) alone or in combination. Cells were then incubated for 48 hours at 37°C, 5% CO2.
- 48 hours post treatment, total PBMCs were overlaid on top of the treated cells in a 1:10 ratio (1 PC3 cell : 10 PBMCs)
- 1 hour post co-culture, 100 units of Brefeldin-A (BioLegend 420601) was added to the cells and cells were incubated for 5 hours further.
- After 6 hours of total co-culture, cells were harvested and first blocked with FcR Blocking Reagent (Miltenyi Biotec 130-059-901) before being stained for APC-CD107a (BioLegend 328620), APC Cyanine 7-intracellular IFNγ (BioLegend 502530), Zombie Red Cell Viability Dye (BioLegend 423110).
- Cells were fixed with Cell Fixation Buffer (BioLegend 420801) and acquired within 2 days of staining on a BD LSR Fortessa.
- At least 50,000 cells were acquired per sample. Live cells (Zombie Red negative) were gated for fluorescent markers. Percent population and MFI values were exported. Percent population was plot for 4 different donors. (Supplementary Figure 6.7)

Natural Killer (NK) cell activation and NK cell based cytotoxicity using IL-2 activated NK cells

Use all sterile reagents and perform the protocol under aseptic conditions.

- PBMCs were isolated as described in 5.3.9.
- Primary CD3-CD56+ NK cells were isolated from total PBMCs using MojoSort NK cell isolation kit (BioLegend 480054). NK cells were cultured in RPMI 1640 supplemented with 5% Cell-Vive™ T-NK Xeno-Free Serum Substitute (BioLegend 420502), 200IU/mL IL-2 (BioLegend 589108) for 7 days. Media was replenished every 3 days with fresh cytokine.
- 2500 PC3-GFP cells were seeded cells per well in a 96-well plate. 8-10 hours post seeding, cells were treated with 10 MOI H-1PV, 1μM ABT-737 (Selleckchem S1002) alone or in combination. Cells were then incubated for 24 hours at 37°C, 5% CO2. Cells were monitored in Incucyte SX3, at 10X magnification, image captured every 2 hours.
- 24 hours post treatment, IL-2 activated NK cells were overlaid on top of the treated cells in a 1:1 ratio (1 PC3 cell : 10 PBMCs). Images were now captured every 30 min.

- Cells were monitored for 24 hours post co-culture.
- After 24 hours of total co-culture, cells were harvested and first blocked with FcR Blocking Reagent (Miltenyi Biotec 130-059-901) before being stained for PE-NKGG2D (BioLegend 320806), PE/Dazzle594-DNAM-1 (BioLegend 338318), APC-Nkp44 (BioLegend 325110) and Zombie Green Cell Viability Dye (BioLgened 423111).
- Cells were fixed with Cell Fixation Buffer (BioLegend 420801) and acquired within 2 days of staining on a BD LSR Fortessa.
- At least 50,000 cells were acquired per sample. Live cells (Zombie green negative) were gated for fluorescent markers. Percent population and MFI values were exported. Percent population was plot for 4 different donors. (Supplementary Figure 6.8)
- Cell supernatants were collected before staining for cytokine array analysis using BioLegend LegendPLEX platform for the anti-virus panel (BioLegend) as well as essential human immune response panel (BioLegend) as per manufacturer's instruction.
- Cell supernatants were also used for LDH analysis as described in 5.3.1
- Real time cell confluence was calculated using the Incucyte SX3 software and plot as percent confluence against time.

5.3.10 Patient derived prostate cancer cell cultures: Culture

Use all sterile reagents and perform the protocol under aseptic conditions. LuCaP 136 and LuCaP 147 cells were kindly provided by Dr. Johannes Linxweiler from Universitätsklinikum des Saarlandes, Germany. LuCaP 136 and 147 cells are derived from serially transplantable patient-derived xenografts (PDXs). These cells were cultured as described previously [143, 144, 160].

5.3.11 Evaluating the effect of H-1PV, ABT-737 (Selleckchem S1002), alone or in combination on patient derived cell cultures

- 10000 LuCaP 136 and LuCaP 147 cells were seeded per well in a 96 well ultra low attachment plates (Corning). 8-10 hours post seeding, cells were treated with 100 MOI H-1PV, 1μM ABT-737 (Selleckchem S1002) alone or in combination. Cells were then incubated for 24 hours at 37°C, 5% CO2.
- Cells were monitored in real time with the Incucyte SX3 at 4x magnification, acquiring images every 2 hours
- Real time cell confluence was calculated using the Incucyte SX3 software and plot as percent confluence against time.

5.3.12 Statistical Analysis

Data are representative of three independent experiments and values are expressed in $mean \pm SD$. Statistical significance was determined by students t-test using GraphPad Prism 9. Only values above p<0.05 were considered significant: p≤0.05 (*), p≤0.01 (**), p≤0.001 (***) and p≤0.0001 (****).

Chapter 6

Supplementary Data

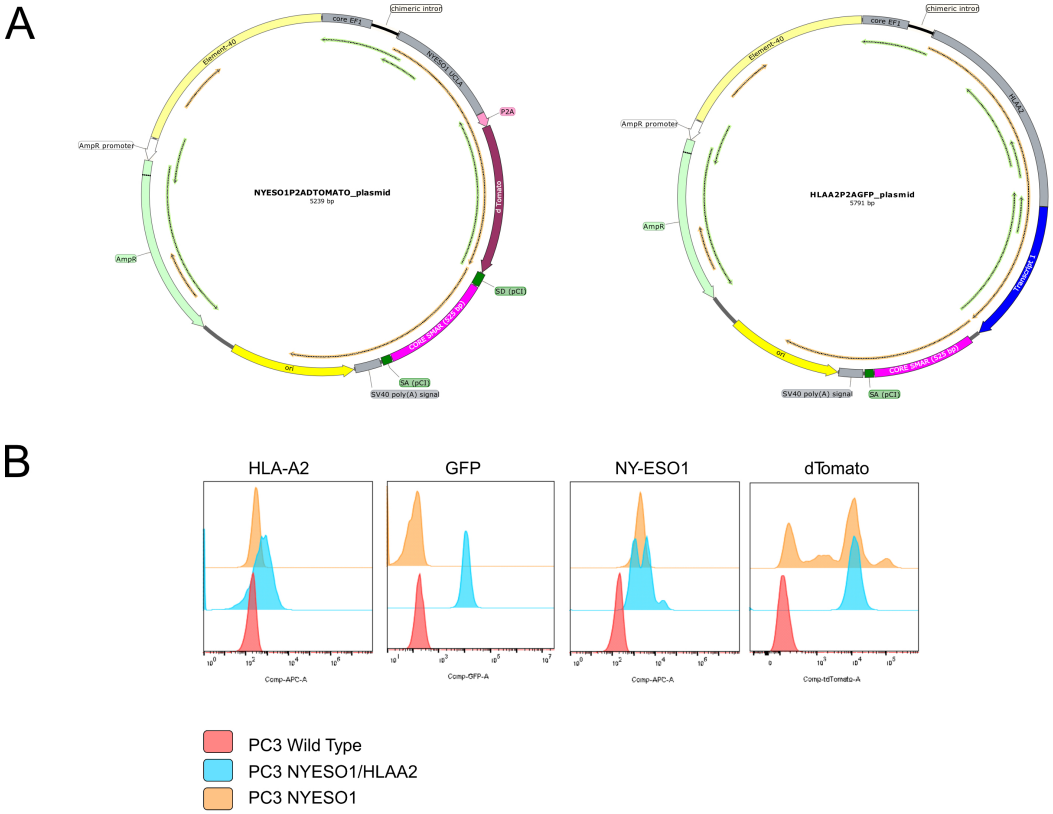

Data generated in collaboration with Alice De Roia from Dr. RIchard Harbottle's lab

Figure 6.1: ***Generation of PC3 stable cell line expressing NY-ESO1/HLA-A2.*** *(A) Plasmid maps for S/MAR based vectors for NY-ESO1 and HLA-A2 transfection. (B) 100000 wild type PC3 cells were simultaneously transfected with S/MAR-dTOMATO-NYESO1 and S/MAR-EGFP-HLAA2. Cells were sorted every 2 weeks for dTomato+GFP+ cells. After 6 weeks, the cell line was established. Flow cytometry histograms showing expression of HLA-A2, NYESO-1, GFP and dTomato, as compared to the wild type PC3 cells.*

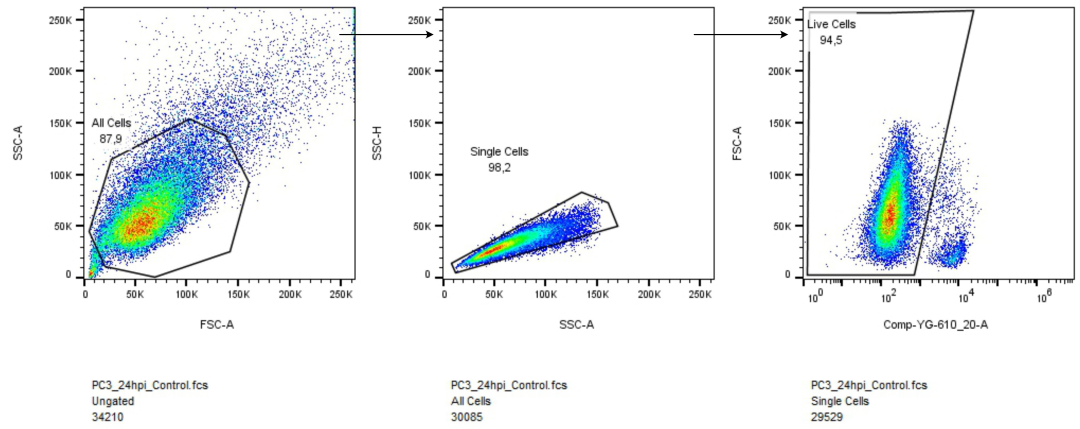

Figure 6.2: *Gating Strategy for flow cytometry of PC3 cells. 30000 PC3 cells were acquired on a BD LSR Fortessa. Healthy live cells were gated on a FSC-A vs SSC-A dot-plot. Doublet discrimination was carried out by gating cells on a SSC-A vs SSC-H dot-plot. Single cells were gated on a live-dead dye (Zombie Red) to obtain Zombie negative live cells. Live cells were used to gate all fluorochrome markers. Unstained and compensation controls were used for final gating.*

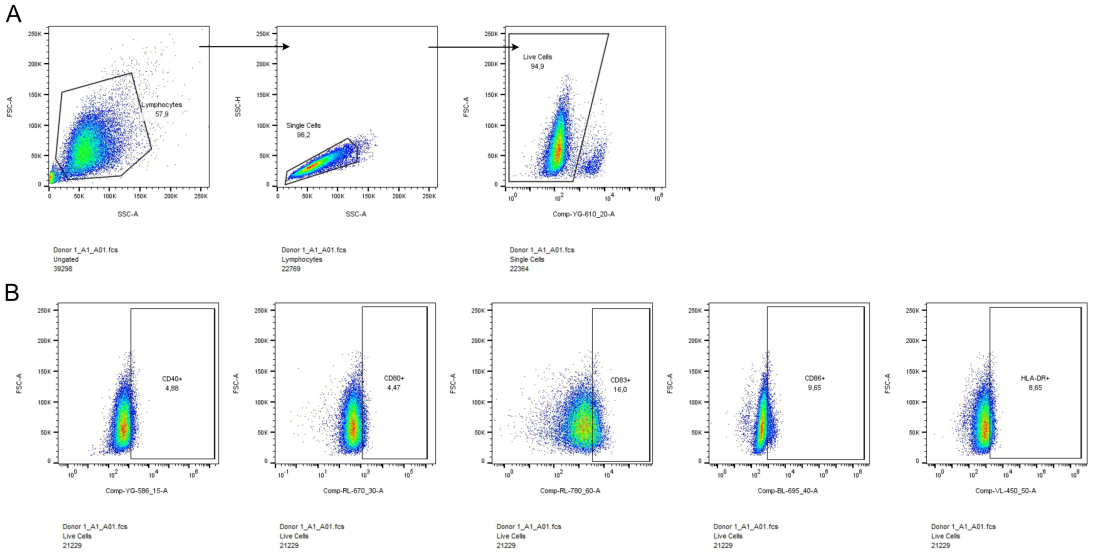

Figure 6.3: *Gating strategy for flow cytometry of dendritic cell activation. (A) 50000 dendritic cells were acquired on a BD LSR Fortessa. Healthy live cells were gated on a FSC-A vs SSC-A dot-plot. Doublet discrimination was carried out by gating cells on a SSC-A vs SSC-H dot-plot. Single cells were gated on a live-dead dye (Zombie Red) to obtain Zombie negative live cells. (B) Live cells were used to gate all fluorochrome markers. Unstained and compensation controls were used for final gating.*

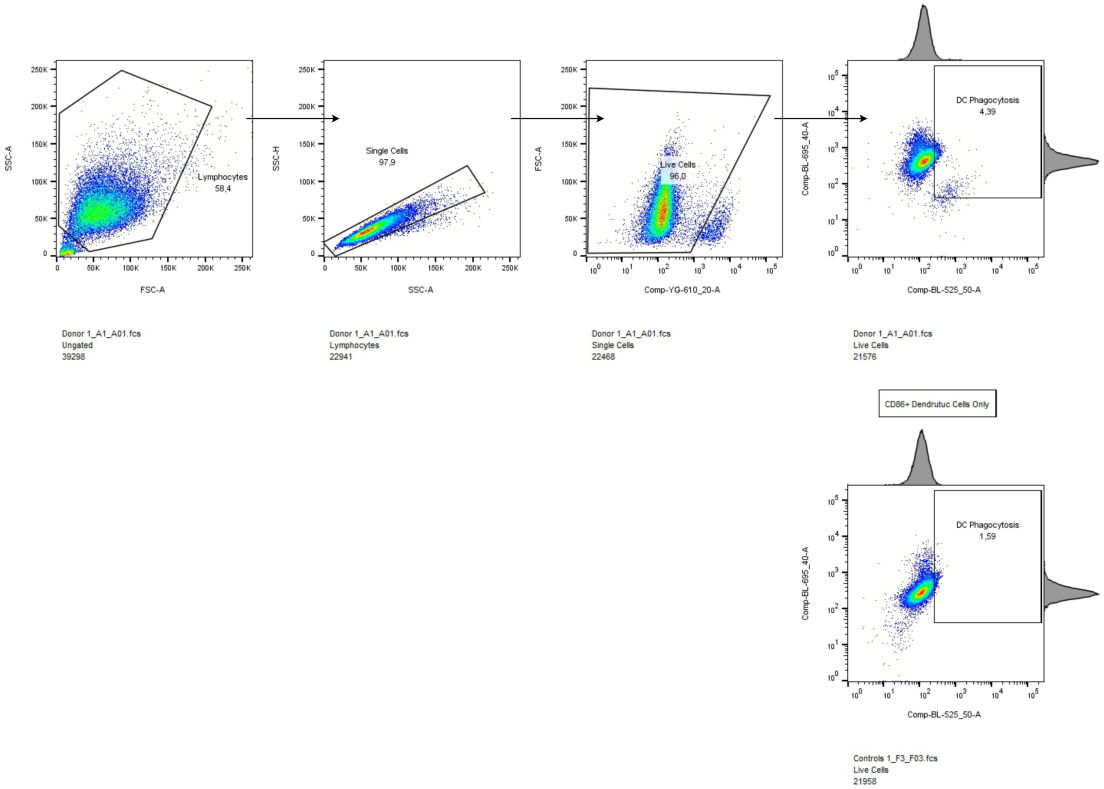

Figure 6.4: *Gating strategy for flow cytometry of phagocytosis by dendritic cells. 50000 dendritic cells were acquired on a BD LSR Fortessa. Healthy live cells were gated on a FSC-A vs SSC-A dot-plot. Doublet discrimination was carried out by gating cells on a SSC-A vs SSC-H dot-plot. Single cells were gated on a live-dead dye (Zombie Red) to obtain Zombie negative live cells. Live cells were used to gate CD86+GFP+ cells. CD86+ only dendritic cells, Unstained and compensation controls were used for final gating.*

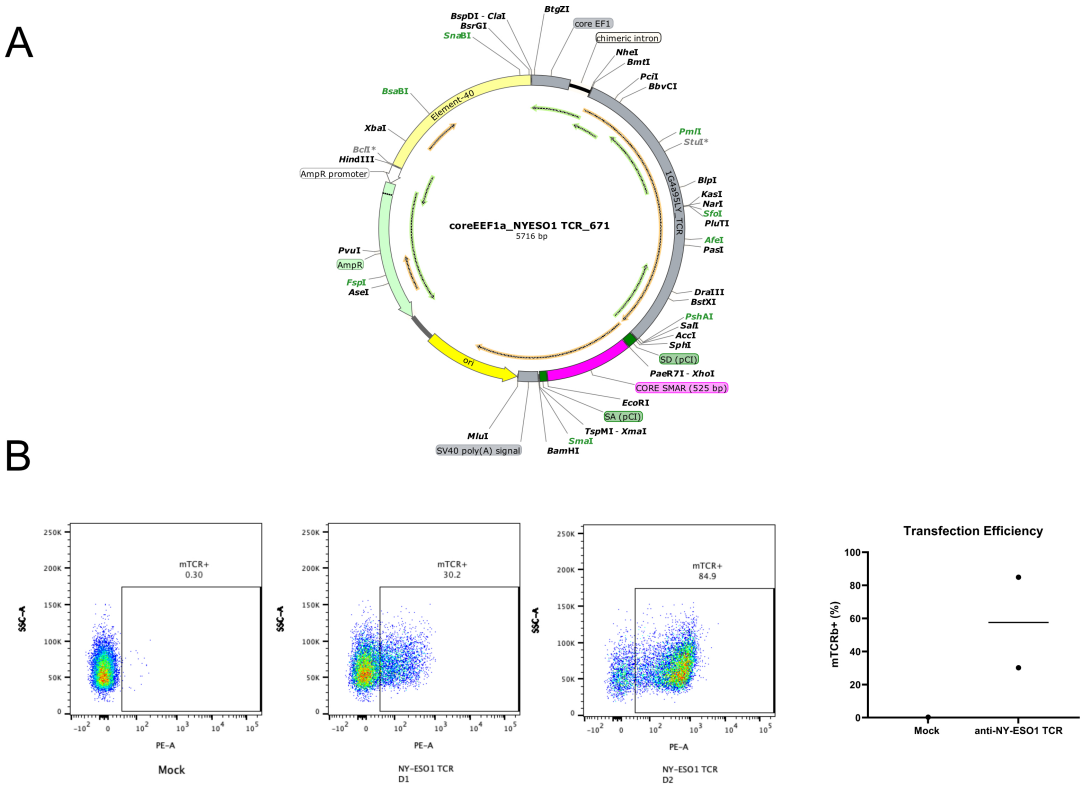

Data generated in collaboration with Alice De Roia from Dr. RIchard Harbottle's lab

Figure 6.5: ***Generation of NY-ESO1 TCR specific T-cells*** *(A) Plasmid map showing S/MAR based vector expressing NY-ESO1 specific TCR (B) CD3+ T-cells were isolated from healthy donors and grown with Transact and IL-7 and IL-15 for 3 days. 100,000 activated T-cells were transfected with NY-ESO1-TCR plasmid from A and rested for 2 days before evaluating transfection efficiency using flow cytometry. Dot plot and bar graph showing transfection efficiency as compared to mock transfected T-cells.*

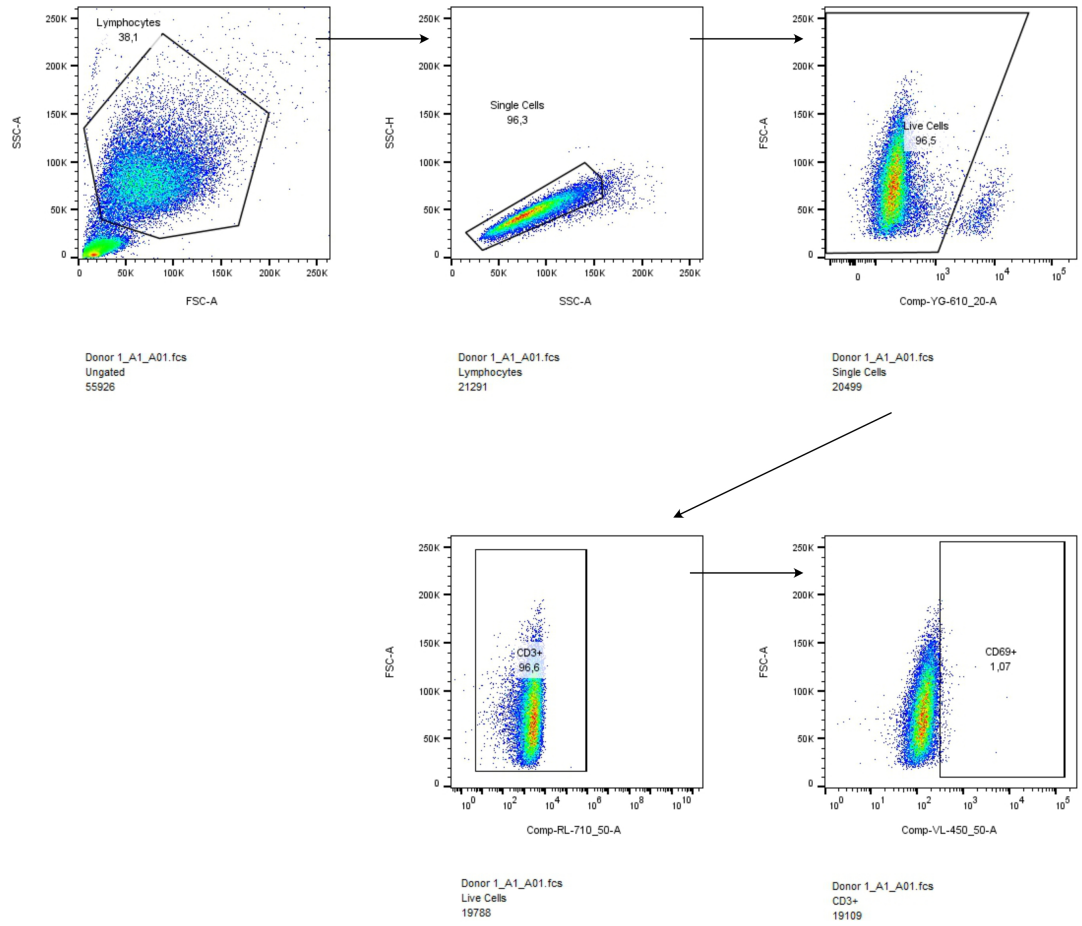

Figure 6.6: *Gating strategy for flow cytometry of flow cytometry of T-cell activation. 50000 T-cells were acquired on a BD LSR Fortessa. Healthy live cells were gated on a FSC-A vs SSC-A dot-plot. Doublet discrimination was carried out by gating cells on a SSC-A vs SSC-H dot-plot. Single cells were gated on a live-dead dye (Zombie Red) to obtain Zombie negative live cells. Live cells were used to gate CD3+CD69+ cells. Unstained and compensation controls were used for final gating.*

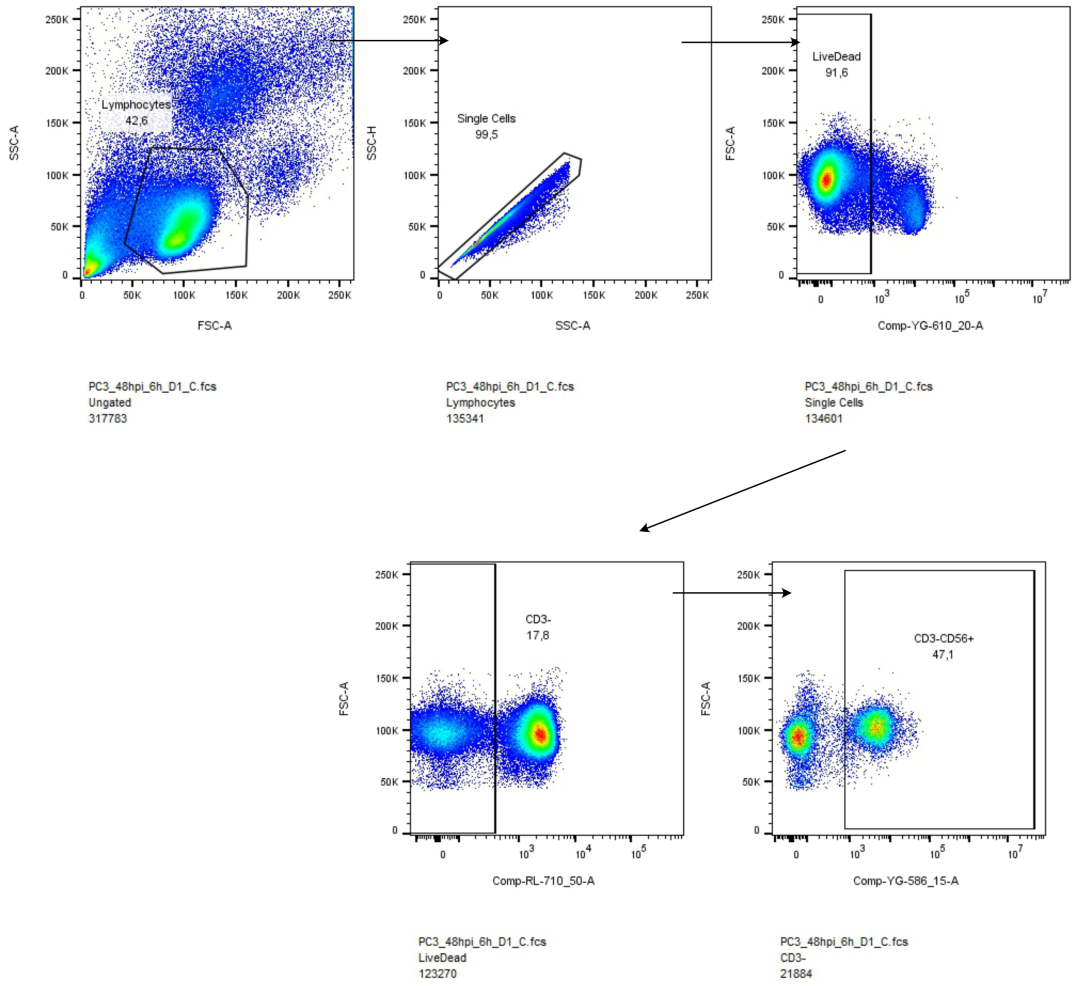

Figure 6.7: *Gating strategy for flow cytometry of Natural Killer Cells from total PBMCs. 50000 CD56+ cells were acquired on a BD LSR Fortessa. Healthy live cells were gated on a FSC-A vs SSC-A dot-plot. Doublet discrimination was carried out by gating cells on a SSC-A vs SSC-H dot-plot. Single cells were gated on a live-dead dye (Zombie Red) to obtain Zombie negative live cells. Live cells were used to gate CD3-CD56+ cells. These cells were then used for further gating. Unstained and compensation controls were used for final gating.*

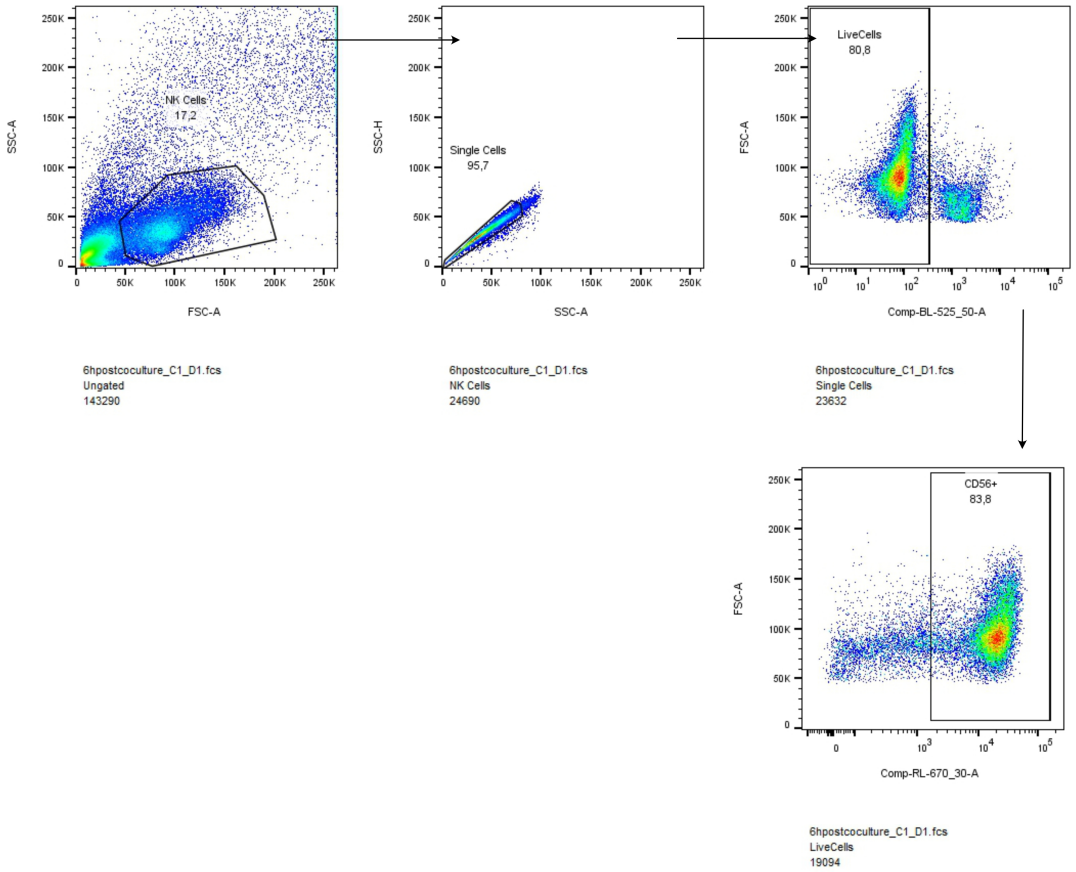

Figure 6.8: *Gating strategy for flow cytometry of Natural Killer Cells from total PBMCs. 50000 cells were acquired on a BD LSR Fortessa. Healthy live cells were gated on a FSC-A vs SSC-A dot-plot. Doublet discrimination was carried out by gating cells on a SSC-A vs SSC-H dot-plot. Single cells were gated on a live-dead dye (Zombie Green) to obtain Zombie negative live cells. Live cells were used to gate CD56+ cells. These cells were then used for further gating. Unstained and compensation controls were used for final gating.*

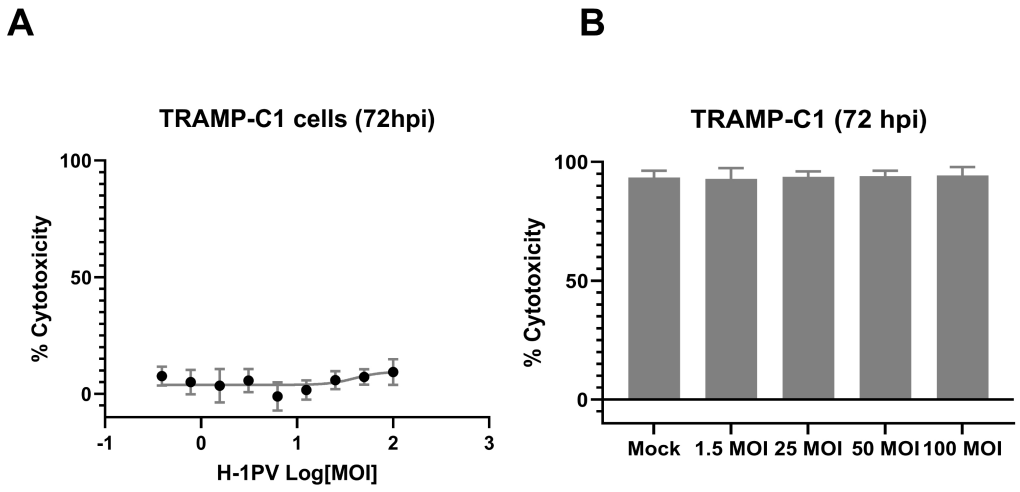

Figure 6.9: ***TRAMPC1 cells are refractory to H-1PV infection.*** *(A) TRAMPC1 cells were treated with increasing titres of H-1PV. Cell viability was evaluated 72 hours post infection (hpi) using an MTT cell viability assay. Absorbance values were calculated as percent cytotoxicity relative to untreated controls and plotted as non-linear regression curves, to obtain IC_{50} values. (B) TRAMPC1 cells were treated with 1.5, 25, 50 and 100 MOI of H-1PV. 72 hours post infection, percent cytotoxicity was evaluated using an MTT cell viability assay. Data are representative of two independent experiments and values are expressed in $mean \pm SD$*

References

(1) Kāle, M. R., *The Hitopadesa of Narayana*; Motilal Banarsidass: 1896 (cit. on p. v).

(2) Siegel, R. L.; Miller, K. D.; Wagle, N. S.; Jemal, A. *CA: A Cancer Journal for Clinicians* **2023**, *73*, 17–48 (cit. on pp. 1, 19).

(3) Hanahan, D. *Cancer Discovery* **2022**, *12*, 31–46 (cit. on p. 1).

(4) Knight, S. R. et al. *The Lancet* **2021**, *397*, 387–397 (cit. on p. 1).

(5) Baskar, R.; Lee, K. A.; Yeo, R.; Yeoh, K.-W. *Int J Med Sci* **2012**, *9*, 193–199 (cit. on p. 1).

(6) Urruticoechea, A.; Alemany, R.; Balart, J.; Villanueva, A.; Viñals, F.; Capellá, G. *Curr Pharm Des* **2010**, *16*, 3–10 (cit. on pp. 1, 2).

(7) Debela, D. T.; Muzazu, S. G.; Heraro, K. D.; Ndalama, M. T.; Mesele, B. W.; Haile, D. C.; Kitui, S. K.; Manyazewal, T. *SAGE Open Medicine* **2021**, *9*, PMID: 34408877, 20503121211034366 (cit. on pp. 1, 2).

(8) Weledji, E. P.; Orock, G. E. *Oncol Rev* **2015**, *9*, 274 (cit. on p. 1).

(9) Sayed, N.; Allawadhi, P.; Khurana, A.; Singh, V.; Navik, U.; Pasumarthi, S. K.; Khurana, I.; Banothu, A. K.; Weiskirchen, R.; Bharani, K. K. *Life Sciences* **2022**, *294*, 120375 (cit. on p. 2).

(10) Huang, Z.; Guo, H.; Lin, L.; Li, S.; Yang, Y.; Han, Y.; Huang, W.; Yang, J. *Journal of Medical Virology* **2023**, *95*, e28729 (cit. on p. 2).

(11) Li, K.; Zhao, Y.; Hu, X.; Jiao, J.; Wang, W.; Yao, H. *Am J Transl Res* **2022**, *14*, 4192–4206 (cit. on pp. 2, 4, 62).

(12) Kelly, E.; Russell, S. J. *Molecular Therapy* **2007**, *15*, 651–659 (cit. on pp. 2, 3).

(13) Pelner, L.; Fowler, G. A.; Nauts, H. C. *Acta Medica Scandinavica* **1958**, *162*, 5–24 (cit. on p. 2).

(14) Hoster, H. A.; Zanes, R. P. J.; Von Haam, E. *Cancer Res* **1949**, *9*, 473–480 (cit. on p. 2).

(15) Cassel, W. A.; Garrett, R. E. *Cancer* **1965**, *18*, 863–868 (cit. on p. 2).

(16) Hastie, E.; Grdzelishvili, V. Z. *Journal of General Virology* **2012**, *93*, 2529–2545 (cit. on p. 3).

(17) Yaghchi, C. A.; Zhang, Z.; Alusi, G.; Lemoine, N. R.; Wang, Y. *Immunotherapy* **2015**, *7*, PMID: 26595180, 1249–1258 (cit. on pp. 3, 9).

(18) Bretscher, C.; Marchini, A. *Viruses* **2019**, *11*, DOI: 10.3390/v11060562 (cit. on pp. 3, 12, 58).

(19) Martuza, R. L.; Malick, A.; Markert, J. M.; Ruffner, K. L.; Coen, D. M. *Science* **1991**, *252*, 854–856 (cit. on p. 3).

(20) Robert-Guroff, M. *Current Opinion in Biotechnology* **2007**, *18*, Chemical biotechnology / Pharmaceutical biotechnology, 546–556 (cit. on p. 3).

(21) Matveeva, O. V.; Guo, Z. S.; Senin, V. M.; Senina, A. V.; Shabalina, S. A.; Chumakov, P. M. *Molecular Therapy - Oncolytics* **2015**, *2*, 15017 (cit. on p. 3).

(22) Aldrak, N.; Alsaab, S.; Algethami, A.; Bhere, D.; Wakimoto, H.; Shah, K.; Alomary, M. N.; Zaidan, N. *Cells* **2021**, *10*, DOI: 10.3390/cells10061541 (cit. on p. 3).

(23) Torres-Domínguez, L. E.; McFadden, G. *Expert Opinion on Biological Therapy* **2019**, *19*, PMID: 30919708, 561–573 (cit. on p. 3).

(24) Alberts, P.; Tilgase, A.; Rasa, A.; Bandere, K.; Venskus, D. *European Journal of Pharmacology* **2018**, *837*, 117–126 (cit. on p. 3).

(25) Liang, M. *Current Cancer Drug Targets* **2018**, *18*, 171–176 (cit. on p. 4).

(26) Harrington, K. J.; Puzanov, I.; Hecht, J. R.; Hodi, F. S.; Szabo, Z.; Murugappan, S.; Kaufman, H. L. *Expert Review of Anticancer Therapy* **2015**, *15*, PMID: 26558498, 1389–1403 (cit. on pp. 4, 5).

(27) Todo, T.; Ito, H.; Ino, Y.; Ohtsu, H.; Ota, Y.; Shibahara, J.; Tanaka, M. *Nature Medicine* **2022**, *28*, 1630–1639 (cit. on p. 4).

(28) De la Nava, D.; Selvi, K. M.; Alonso, M. M. *Frontiers in Immunology* **2022**, *13*, DOI: 10.3389/fimmu.2022.866892 (cit. on pp. 4, 5).

(29) Johnson, P. A.; Wu, A.; Johnson, J. C.; Schauer, Z.; Wu, T.; Fernandes, F.; Schabert, R.; Mardon, A. *Applied Microbiology* **2022**, *2*, 319–329 (cit. on pp. 4, 9).

(30) Engeland, C. E.; Ungerechts, G. *Cancers* **2021**, *13*, DOI: 10.3390/cancers13030544 (cit. on pp. 5, 64).

(31) Marchini, A.; Bonifati, S.; Scott, E. M.; Angelova, A. L.; Rommelaere, J. *Virology Journal* **2015**, *12*, 6 (cit. on pp. 5, 61).

(32) Allaume, X.; El-Andaloussi, N.; Leuchs, B.; Bonifati, S.; Kulkarni, A.; Marttila, T.; Kaufmann, J. K.; Nettelbeck, D. M.; Kleinschmidt, J.; Rommelaere, J.; Marchini, A. *Journal of Virology* **2012**, *86*, 3452–3465 (cit. on pp. 5, 68).

(33) Zamarin, D.; Palese, P. *Future Microbiology* **2012**, *7*, PMID: 22393889, 347–367 (cit. on p. 5).

(34) Müller, L.; Berkeley, R.; Barr, T.; Ilett, E.; Errington-Mais, F. *Cancers* **2020**, *12*, DOI: 10.3390/cancers12113219 (cit. on p. 6).

(35) Nüesch, J. P.; Lacroix, J.; Marchini, A.; Rommelaere, J. *Clinical Cancer Research* **2012**, *18*, 3516–3523 (cit. on pp. 6, 14, 23, 73).

(36) Galluzzi, L.; Kepp, O.; Hett, E.; Kroemer, G.; Marincola, F. M. *Journal of Translational Medicine* **2023**, *21*, 162 (cit. on p. 6).

(37) Kielbik, M.; Szulc-Kielbik, I.; Klink, M. *Cells* **2021**, *10*, DOI: 10.3390/cells10010130 (cit. on pp. 6, 9).

(38) Hasselbalch, H. C.; Sevin, M.; Girodon, F.; Garrido, C.; de Thonel, A. *Mediators of Inflammation* **2015**, *2015*, 970242 (cit. on p. 6).

(39) Fucikova, J.; Kepp, O.; Kasikova, L.; Petroni, G.; Yamazaki, T.; Liu, P.; Zhao, L.; Spisek, R.; Kroemer, G.; Galluzzi, L. *Cell Death & Disease* **2020**, *11*, 1013 (cit. on pp. 6, 63).

(40) Elliott, M. R.; Chekeni, F. B.; Trampont, P. C.; Lazarowski, E. R.; Kadl, A.; Walk, S. F.; Park, D.; Woodson, R. I.; Ostankovich, M.; Sharma, P.; Lysiak, J. J.; Harden, T. K.; Leitinger, N.; Ravichandran, K. S. *Nature* **2009**, *461*, 282–286 (cit. on pp. 6, 37).

(41) Showalter, A.; Limaye, A.; Oyer, J. L.; Igarashi, R.; Kittipatarin, C.; Copik, A. J.; Khaled, A. R. *Cytokine* **2017**, *97*, 123–132 (cit. on pp. 6, 39, 40).

(42) Russell, L.; Peng, K. W.; Russell, S. J.; Diaz, R. M. *BioDrugs* **2019**, *33*, 485–501 (cit. on p. 7).

(43) Kiessling, A.; Wehner, R.; Füssel, S.; Bachmann, M.; Wirth, M. P.; Schmitz, M. *Cancers* **2012**, *4*, 193–217 (cit. on p. 7).

(44) Ma, J.; Ramachandran, M.; Jin, C.; Quijano-Rubio, C.; Martikainen, M.; Yu, D.; Essand, M. *Cell Death & Disease* **2020**, *11*, 48 (cit. on p. 7).

(45) Donnelly, O. G.; Errington-Mais, F.; Steele, L.; Hadac, E.; Jennings, V.; Scott, K.; Peach, H.; Phillips, R. M.; Bond, J.; Pandha, H.; Harrington, K.; Vile, R.; Russell, S.; Selby, P.; Melcher, A. A. *Gene Therapy* **2013**, *20*, 7–15 (cit. on pp. 7, 9, 40, 45).

(46) Angelova, A. L.; Grekova, S. P.; Heller, A.; Kuhlmann, O.; Soyka, E.; Giese, T.; Aprahamian, M.; Bour, G.; Rüffer, S.; Cziepluch, C.; Daeffler, L.; Rommelaere, J.; Werner, J.; Raykov, Z.; Giese, N. A. *Journal of Virology* **2014**, *88*, 5263–5276 (cit. on pp. 7, 15, 16, 18, 20, 33, 35).

(47) Groeneveldt, C.; van Hall, T.; van der Burg, S. H.; Ten Dijke, P.; van Montfoort, N. *Trends in immunology* **2020**, *41*, 406–420 (cit. on p. 8).

(48) Dudek, A.; Martin, S.; Garg, A.; Agostinis, P. *Frontiers in Immunology* **2013**, *4*, DOI: 10.3389/fimmu.2013.00438 (cit. on p. 7).

(49) Kim, M. K.; Kim, J. *RSC Adv.* **2019**, *9*, 11230–11238 (cit. on pp. 7, 9).

(50) Ardavín, C.; Martínez del Hoyo, G.; Martín, P.; Anjuère, F.; Arias, C. F.; Marín, A. R.; Ruiz, S.; Parrillas, V.; Hernández, H. *Trends in Immunology* **2001**, *22*, 691–700 (cit. on p. 9).

(51) Lamberti, M. J.; Nigro, A.; Mentucci, F. M.; Rumie Vittar, N. B.; Casolaro, V.; Dal Col, J. *Pharmaceutics* **2020**, *12*, DOI: 10.3390/pharmaceutics12030256 (cit. on p. 9).

(52) Lee, J.; Ghonime, M. G.; Wang, R.; Cassady, K. A. *Molecular Therapy - Oncolytics* **2019**, *13*, 7–13 (cit. on p. 9).

(53) Gebremeskel, S.; Johnston, B. *Oncotarget* **2015**, *6*, Gebremeskel, Simon Johnston, Brent eng Canadian Institutes of Health Research/Canada Research Support, Non-U.S. Gov't Review 2015/10/22 Oncotarget. 2015 Dec 8;6(39):41600-19. doi: 10.18632/oncotarget.6113., 41600–19 (cit. on p. 9).

(54) Hubo, M.; Trinschek, B.; Kryczanowsky, F.; Tüttenberg, A.; Steinbrink, K.; Jonuleit, H. *Frontiers in Immunology* **2013**, *4*, DOI: 10.3389/fimmu.2013.00082 (cit. on p. 9).

(55) Ilett, E. J.; Barcena, M.; Errington-Mais, F.; Griffin, S.; Harrington, K. J.; Pandha, H. S.; Coffey, M.; Selby, P. J.; Limpens, R. W.; Mommaas, M.; Hoeben, R. C.; Vile, R. G.; Melcher, A. A. *Clin Cancer Res* **2011**, *17*, Ilett, Elizabeth J Barcena, Montserrat Errington-Mais, Fiona Griffin, Stephen Harrington, Kevin J Pandha, Hardev S Coffey, Matthew Selby, Peter J Limpens, Ronald W A L Mommaas, Mieke Hoeben, Rob C Vile, Richard G Melcher, Alan A eng Clin Cancer Res. 2011 May 1;17(9):2767-76. doi: 10.1158/1078-0432.CCR-10-3266. Epub 2011 Mar 9., 2767–76 (cit. on p. 9).

(56) Totsch, S. K.; Schlappi, C.; Kang, K.-D.; Ishizuka, A. S.; Lynn, G. M.; Fox, B.; Beierle, E. A.; Whitley, R. J.; Markert, J. M.; Gillespie, G. Y.; Bernstock, J. D.; Friedman, G. K. *Oncogene* **2019**, *38*, 6159–6171 (cit. on p. 9).

(57) Nishio, N.; Diaconu, I.; Liu, H.; Cerullo, V.; Caruana, I.; Hoyos, V.; Bouchier-Hayes, L.; Savoldo, B.; Dotti, G. *Cancer Research* **2014**, *74*, 5195–5205 (cit. on p. 9).

(58) Prestwich, R. J.; Errington, F.; Steele, L. P.; Ilett, E. J.; Morgan, R. S. M.; Harrington, K. J.; Pandha, H. S.; Selby, P. J.; Vile, R. G.; Melcher, A. A. *The Journal of Immunology* **2009**, *183*, 4312–4321 (cit. on pp. 9, 10, 45).

(59) Del Prete, A.; Salvi, V.; Soriani, A.; Laffranchi, M.; Sozio, F.; Bosisio, D.; Sozzani, S. *Cellular & amp; molecular immunology* **2023**, *20*, 432–447 (cit. on pp. 10, 41, 43, 45, 47).

(60) Hwang, J.-R.; Byeon, Y.; Kim, D.; Park, S.-G. *Experimental & Molecular Medicine* **2020**, *52*, 750–761 (cit. on pp. 10, 45, 47).

(61) Prager, I.; Watzl, C. *Journal of Leukocyte Biology* **2019**, *105*, 1319–1329 (cit. on p. 11).

(62) Panaampon, J.; Sasamoto, K.; Kariya, R.; Okada, S. *Asian Pacific Journal of Cancer Prevention* **2021**, *22*, 1069–1074 (cit. on p. 11).

(63) Campbell, T. M.; McSharry, B. P.; Steain, M.; Ashhurst, T. M.; Slobedman, B.; Abendroth, A. *PLoS Pathog* **2018**, *14*, Campbell, Tessa Mollie McSharry, Brian Patrick Steain, Megan Ashhurst, Thomas Myles Slobedman, Barry Abendroth, Allison eng Research Support, Non-U.S. Gov't 2018/05/01 PLoS Pathog. 2018 Apr 30;14(4):e1006999. doi: 10.1371/journal.ppat.1006999. eCollection 2018 Apr., e1006999 (cit. on p. 11).

(64) Annels, N. E.; Simpson, G. R.; Denyer, M.; Arif, M.; Coffey, M.; Melcher, A.; Harrington, K.; Vile, R.; Pandha, H. *Molecular Therapy - Oncolytics* **2021**, *20*, 434–446 (cit. on p. 11).

(65) Bhat, R.; Rommelaere, J. *BMC Cancer* **2013**, *13*, Bhat, Rauf Rommelaere, Jean eng England 2013/08/02 BMC Cancer. 2013 Jul 31;13:367. doi: 10.1186/1471-2407-13-367., 367 (cit. on pp. 11, 49, 50, 52, 65).

(66) Zádori, Z.; Szelei, J.; Lacoste, M.-C.; Li, Y.; Gariépy, S.; Raymond, P.; Allaire, M.; Nabi, I. R.; Tijssen, P. *Developmental Cell* **2001**, *1*, 291–302 (cit. on p. 12).

(67) Kulkarni, A. et al. *Nature Communications* **2021**, *12*, 3834 (cit. on pp. 12, 25, 60, 72, 73).

(68) Ferreira, T.; Kulkarni, A.; Bretscher, C.; Nazarov, P. V.; Hossain, J. A.; Ystaas, L. A. R.; Miletic, H.; Röth, R.; Niesler, B.; Marchini, A. **2022**, *14*, DOI: 10.3390/v14051018 (cit. on pp. 12, 25, 60, 73).

(69) Ferreira, T.; Kulkarni, A.; Bretscher, C.; Richter, K.; Ehrlich, M.; Marchini, A. **2020**, *12*, DOI: 10.3390/v12101199 (cit. on pp. 14, 23).

(70) Cziepluch, C.; Lampel, S.; Grewenig, A.; Grund, C.; Lichter, P.; Rommelaere, J. *J Virol* **2000**, *74*, Cziepluch, C Lampel, S Grewenig, A Grund, C Lichter, P Rommelaere, J eng 2000/04/25 J Virol. 2000 May;74(10):4807-15. doi: 10.1128/jvi.74.10.4807-4815.2000., 4807–15 (cit. on p. 14).

(71) Caillet-Fauquet, P.; Perros, M.; Brandenburger, A.; Spegelaere, P.; Rommelaere, J. *EMBO J* **1990**, *9*, Caillet-Fauquet, P Perros, M Brandenburger, A Spegelaere, P Rommelaere, J eng Research Support, Non-U.S. Gov't England 1990/09/01 EMBO J. 1990 Sep;9(9):2989-95. doi: 10.1002/j.1460-2075.1990.tb07491.x., 2989–95 (cit. on p. 14).

(72) Ohshima, T.; Iwama, M.; Ueno, Y.; Sugiyama, F.; Nakajima, T.; Fukamizu, A.; Yagami, K. *J Gen Virol* **1998**, *79 (Pt 12)*, Ohshima, T Iwama, M Ueno, Y Sugiyama, F Nakajima, T Fukamizu, A Yagami, K eng Research Support, Non-U.S. Gov't England 1999/01/08 J Gen Virol. 1998 Dec;79 (Pt 12):3067-71. doi: 10.1099/0022-1317-79-12-3067., 3067–71 (cit. on pp. 14, 15, 33, 35).

(73) Di Piazza, M.; Mader, C.; Geletneky, K.; Herrero y Calle, M.; Weber, E.; Schlehofer, J.; Deleu, L.; Rommelaere, J. *Journal of Virology* **2007**, *81*, doi: 10.1128/jvi.02601-06, 4186–4198 (cit. on pp. 14, 15, 61).

(74) Grekova, S.; Aprahamian, M.; Giese, N.; Schmitt, S.; Giese, T.; Falk, C. S.; Daeffler, L.; Cziepluch, C.; Rommelaere, J.; Raykov, Z. *Cancer Biol Ther* **2010**, *10*, Grekova, Svitlana Aprahamian, Marc Giese, Nathalia Schmitt, Steffen Giese, Thomas Falk, Christine S Daeffler, Laurent Cziepluch, Celina Rommelaere, Jean Raykov, Zahari eng Research Support, Non-U.S. Gov't 2010/12/03 Cancer Biol Ther. 2010 Dec 15;10(12):1280-9. doi: 10.4161/cbt.10.12.13455. Epub 2010 Dec 15., 1280–9 (cit. on pp. 14, 20).

(75) Faisst, S.; Guittard, D.; Benner, A.; Cesbron, J. Y.; Schlehofer, J. R.; Rommelaere, J.; Dupressoir, T. *International Journal of Cancer* **1998**, *75*, https://doi.org/10.1002/(SICI)1097-0215(19980209)75:4<584::AID-IJC15>3.0.CO;2-9, 584–589 (cit. on p. 15).

(76) Herrero, Y. C. M.; Cornelis, J. J.; Herold-Mende, C.; Rommelaere, J.; Schlehofer, J. R.; Geletneky, K. *Int J Cancer* **2004**, *109*, Herrero Y Calle, Marta Cornelis, Jan J Herold-Mende, Christel Rommelaere, Jean Schlehofer, Joerg R Geletneky, Karsten eng Research Support, Non-U.S. Gov't 2004/01/22 Int J Cancer. 2004 Mar;109(1):76-84. doi: 10.1002/ijc.11626., 76–84 (cit. on p. 15).

(77) Geletneky, K.; Kiprianova, I.; Ayache, A.; Koch, R.; Herrero, Y. C. M.; Deleu, L.; Sommer, C.; Thomas, N.; Rommelaere, J.; Schlehofer, J. R. *Neuro Oncol* **2010**, *12*, Geletneky, Karsten Kiprianova, Irina Ayache, Ali Koch, Regina Herrero Y Calle, Marta Deleu, Laurent Sommer, Clemens Thomas, Nadja Rommelaere, Jean Schlehofer, Jorg R eng Research Support, Non-U.S. Gov't England 2010/03/20 Neuro Oncol. 2010 Aug;12(8):804-14. doi: 10.1093/neuonc/noq023. Epub 2010 Mar 18., 804–14 (cit. on pp. 15, 68).

(78) Muharram, G.; Le Rhun, E.; Loison, I.; Wizla, P.; Richard, A.; Martin, N.; Roussel, A.; Begue, A.; Devos, P.; Baranzelli, M.-C.; Bonneterre, J.; Caillet-Fauquet, P.; Stehelin, D. *Breast Cancer Research and Treatment* **2010**, *121*, 23–33 (cit. on p. 15).

(79) Li, J.; Bonifati, S.; Hristov, G.; Marttila, T.; Valmary-Degano, S.; Stanzel, S.; Schnölzer, M.; Mougin, C.; Aprahamian, M.; Grekova, S. P.; Raykov, Z.; Rommelaere, J.; Marchini, A. *EMBO Molecular Medicine* **2013**, *5*, https://doi.org/10.1002/emmm.201302796, 1537–1555 (cit. on pp. 15, 18, 20, 27, 60, 61).

(80) Moehler, M.; Zeidler, M.; Schede, J.; Rommelaere, J.; Galle, P. R.; Cornelis, J. J.; Heike, M. *Cancer Gene Ther* **2003**, *10*, Moehler, Markus Zeidler, Maja Schede, Joerg Rommelaere, Jean Galle, Peter R Cornelis, Jan J Heike, Michael eng Research Support, Non-U.S. Gov't England 2003/05/28 Cancer Gene Ther. 2003 Jun;10(6):477-80. doi: 10.1038/sj.cgt.7700591., 477–80 (cit. on pp. 15, 62).

(81) Moehler, M. H.; Zeidler, M.; Wilsberg, V.; Cornelis, J. J.; Woelfel, T.; Rommelaere, J.; Galle, P. R.; Heike, M. *Hum Gene Ther* **2005**, *16*, Moehler, Markus H Zeidler, Maja Wilsberg, Vanessa Cornelis, Jan J Woelfel, Thomas Rommelaere, Jean Galle, Peter R Heike, Michael eng Research Support, Non-U.S. Gov't 2005/08/04 Hum Gene Ther. 2005 Aug;16(8):996-1005. doi: 10.1089/hum.2005.16.996., 996–1005 (cit. on p. 15).

(82) Bhat, R.; Dempe, S.; Dinsart, C.; Rommelaere, J. *Int J Cancer* **2011**, *128*, Bhat, Rauf Dempe, Sebastian Dinsart, Christiane Rommelaere, Jean eng 2010/05/18 Int J Cancer. 2011 Feb 15;128(4):908-19. doi: 10.1002/ijc.25415., 908–19 (cit. on pp. 15, 49).

(83) Moehler, M.; Sieben, M.; Roth, S.; Springsguth, F.; Leuchs, B.; Zeidler, M.; Dinsart, C.; Rommelaere, J.; Galle, P. R. *BMC Cancer* **2011**, *11*, Moehler, Markus Sieben, Maike Roth, Susanne Springsguth, Franziska Leuchs, Barbara Zeidler, Maja Dinsart, Christiane Rommelaere, Jean Galle, Peter R eng Research Support, Non-U.S. Gov't England 2011/10/28 BMC Cancer. 2011 Oct 26;11:464., 464 (cit. on p. 15).

(84) Goepfert, K.; Dinsart, C.; Rommelaere, J.; Foerster, F.; Moehler, M. *Frontiers in Oncology* **2019**, *9* (cit. on pp. 15, 18, 20, 40, 64).

(85) Kotecha, R.; Odia, Y.; Khosla, A. A.; Ahluwalia, M. S. *JCO Oncology Practice* **2023**, *19*, doi: 10.1200/OP.22.00476, 180–189 (cit. on p. 15).

(86) Principe, D. R.; Underwood, P. W.; Korc, M.; Trevino, J. G.; Munshi, H. G.; Rana, A. *Frontiers in Oncology* **2021**, *11*, 688377 (cit. on p. 16).

(87) Geletneky, K.; Huesing, J.; Rommelaere, J.; Schlehofer, J. R.; Leuchs, B.; Dahm, M.; Krebs, O.; von Knebel Doeberitz, M.; Huber, B.; Hajda, J. *BMC Cancer* **2012**, *12*, Geletneky, Karsten Huesing, Johannes Rommelaere, Jean Schlehofer, Joerg R Leuchs, Barbara Dahm, Michael Krebs, Ottheinz von Knebel Doeberitz, Magnus Huber, Bernard Hajda, Jacek eng Clinical Trial, Phase I Clinical Trial, Phase II Research Support, Non-U.S. Gov't England 2012/03/23 BMC Cancer. 2012 Mar 21;12:99. doi: 10.1186/1471-2407-12-99., 99 (cit. on p. 16).

(88) Hajda, J. et al. *Clin Cancer Res* **2021**, *27*, Hajda, Jacek Leuchs, Barbara Angelova, Assia L Frehtman, Veronika Rommelaere, Jean Mertens, Mieke Pilz, Maximilian Kieser, Meinhard Krebs, Ottheinz Dahm, Michael Huber, Bernard Engeland, Christine E Mavratzas, Athanasios Hohmann, Nicolas Schreiber, Jutta Jager, Dirk Halama, Niels Sedlaczek, Oliver Gaida, Matthias M Daniel, Volker Springfeld, Christoph Ungerechts, Guy eng Clinical Trial, Phase II Multicenter Study 2021/08/25 Clin Cancer Res. 2021 Oct 15;27(20):5546-5556. doi: 10.1158/1078-0432.CCR-21-1020. Epub 2021 Aug 23., 5546–5556 (cit. on p. 17).

(89) Fay, E. K.; Graff, J. N. *Cancers (Basel)* **2020**, *12*, Fay, Emily K Graff, Julie N eng Review Switzerland 2020/07/08 Cancers (Basel). 2020 Jul 1;12(7):1752. doi: 10.3390/cancers12071752., DOI: 10.3390/cancers12071752 (cit. on p. 19).

(90) Cokol-Cakmak, M.; Bakan, F.; Cetiner, S.; Cokol, M. *J Vis Exp* **2018**, Cokol-Cakmak, Melike Bakan, Feray Cetiner, Selim Cokol, Murat eng P50 GM107618/GM/NIGMS NIH HHS/ Research Support, N.I.H., Extramural Video-Audio Media 2018/07/10 J Vis Exp. 2018 Jun 21;(136):57713. doi: 10.3791/57713., DOI: 10.3791/57713 (cit. on pp. 20, 27, 60, 71).

(91) Wu, X.; Gong, S.; Roy-Burman, P.; Lee, P.; Culig, Z. *Endocrine-Related Cancer* **2013**, *20*, R155–R170 (cit. on pp. 22, 69).

(92) Cunningham, D.; You, Z. *J Biol Methods* **2015**, *2*, Cunningham, David You, Zongbing eng P20 GM103518/GM/NIGMS NIH HHS/ P20 RR020152/RR/NCRR NIH HHS/ R01 CA174714/CA/NCI NIH HHS/ 2015/07/07 J Biol Methods. 2015;2(1):e17. doi: 10.14440/jbm.2015.63., DOI: 10.14440/jbm.2015.63 (cit. on pp. 22, 27, 65, 69).

(93) Kepp, O.; Galluzzi, L.; Lipinski, M.; Yuan, J.; Kroemer, G. *Nat Rev Drug Discov* **2011**, *10*, Kepp, Oliver Galluzzi, Lorenzo Lipinski, Marta Yuan, Junying Kroemer, Guido eng Research Support, N.I.H., Extramural Research Support, Non-U.S. Gov't Review England 2011/03/02 Nat Rev Drug Discov. 2011 Mar;10(3):221-37. doi: 10.1038/nrd3373., 221–37 (cit. on pp. 22, 31).

(94) El-Andaloussi, N.; Endele, M.; Leuchs, B.; Bonifati, S.; Kleinschmidt, J.; Rommelaere, J.; Marchini, A. *Cancer Gene Therapy* **2011**, *18*, 240–249 (cit. on pp. 23, 69, 70).

(95) Wen, F.; Wan, X.-F. *Trends in Microbiology* **2019**, *27*, 477–479 (cit. on p. 23).

(96) Munshi, A.; Pappas, G.; Honda, T.; McDonnell, T. J.; Younes, A.; Li, Y.; Meyn, R. E. *Oncogene* **2001**, *20*, Munshi, A Pappas, G Honda, T McDonnell, T J Younes, A Li, Y Meyn, R E eng P01 CA06294/CA/NCI NIH HHS/ P30 CA16672/CA/NCI NIH HHS/ R01 CA69003/CA/NCI NIH HHS/ Research Support, U.S. Gov't, P.H.S. England 2001/07/06 Oncogene. 2001 Jun 28;20(29):3757-65. doi: 10.1038/sj.onc.1204504., 3757–65 (cit. on p. 28).

(97) Xu, W.; Ngo, L.; Perez, G.; Dokmanovic, M.; Marks, P. A. *Proc Natl Acad Sci U S A* **2006**, *103*, Xu, Weisheng Ngo, Lang Perez, Gisela Dokmanovic, Milos Marks, Paul A eng P30 CA008748/CA/NCI NIH HHS/ CA-008748/CA/NCI NIH HHS/ Research Support, N.I.H., Extramural Research Support, Non-U.S. Gov't 2006/10/13 Proc Natl Acad Sci U S A. 2006 Oct 17;103(42):15540-5. doi: 10.1073/pnas.0607518103. Epub 2006 Oct 9., 15540–5 (cit. on p. 28).

(98) Murakami, S.; Suzuki, S.; Hanamura, I.; Yoshikawa, K.; Ueda, R.; Takami, A. *Blood* **2018**, *132*, 5154–5154 (cit. on p. 31).

(99) Cerignoli, F.; Abassi, Y. A.; Lamarche, B. J.; Guenther, G.; Santa Ana, D.; Guimet, D.; Zhang, W.; Zhang, J.; Xi, B. *PLOS ONE* **2018**, *13*, 1–21 (cit. on p. 31).

(100) Brentnall, M.; Rodriguez-Menocal, L.; De Guevara, R. L.; Cepero, E.; Boise, L. H. *BMC Cell Biology* **2013**, *14*, 32 (cit. on p. 33).

(101) Ali, A.; Kulik, G. *Cancers (Basel)* **2021**, *13*, Ali, Amaal Kulik, George eng P30CA012197/NH/NIH HHS/ Review Switzerland 2021/03/07 Cancers (Basel). 2021 Feb 24;13(5):937. doi: 10.3390/cancers13050937., DOI: 10.3390/cancers13050937 (cit. on p. 33).

(102) Fitzwalter, B. E.; Towers, C. G.; Sullivan, K. D.; Andrysik, Z.; Hoh, M.; Ludwig, M.; O'Prey, J.; Ryan, K. M.; Espinosa, J. M.; Morgan, M. J.; Thorburn, A. *Developmental Cell* **2018**, *44*, 555–565.e3 (cit. on p. 33).

(103) Santos, L. C.; Vogel, R.; Chipuk, J. E.; Birtwistle, M. R.; Stolovitzky, G.; Meyer, P. *Nature Communications* **2019**, *10*, 1313 (cit. on p. 35).

(104) AU - Rieger, A. M.; AU - Nelson, K. L.; AU - Konowalchuk, J. D.; AU - Barreda, D. R. *JoVE* **2011**, e2597 (cit. on p. 35).

(105) Boya, P.; Kroemer, G. *Oncogene* **2008**, *27*, Boya, P Kroemer, G eng Research Support, Non-U.S. Gov't Review England 2008/10/29 Oncogene. 2008 Oct 27;27(50):6434-51. doi: 10.1038/onc.2008.310., 6434–51 (cit. on pp. 36, 37, 61).

(106) Carneiro, B. A.; El-Deiry, W. S. *Nature Reviews Clinical Oncology* **2020**, *17*, 395–417 (cit. on pp. 36, 61, 62).

(107) Zhao, L.; Liu, P.; Kepp, O.; Kroemer, G. *Methods Enzymol* **2019**, *629*, Zhao, Liwei Liu, Peng Kepp, Oliver Kroemer, Guido eng Research Support, Non-U.S. Govt 2019/11/16 Methods Enzymol. 2019;629:177-193. doi: 10.1016/bs.mie.2019.05.001. Epub 2019 May 27., 177–193 (cit. on p. 37).

(108) Ilett, E. J.; Bárcena, M.; Errington-Mais, F.; Griffin, S.; Harrington, K. J.; Pandha, H. S.; Coffey, M.; Selby, P. J.; Limpens, R. W.; Mommaas, M.; Hoeben, R. C.; Vile, R. G.; Melcher, A. A. *Clinical Cancer Research* **2011**, *17*, 2767–2776 (cit. on p. 40).

(109) Thomas, R.; Al-Khadairi, G.; Roelands, J.; Hendrickx, W.; Dermime, S.; Bedognetti, D.; Decock, J. *Front Immunol* **2018**, *9*, Thomas, Remy Al-Khadairi, Ghaneya Roelands, Jessica Hendrickx, Wouter Dermime, Said Bedognetti, Davide Decock, Julie eng Research Support, Non-U.S. Gov't Review Switzerland 2018/05/18 Front Immunol. 2018 May 1;9:947. doi: 10.3389/fimmu.2018.00947. eCollection 2018., 947 (cit. on pp. 41, 64).

(110) Jäger, E.; Chen, Y.-T.; Drijfhout, J. W.; Karbach, J.; Ringhoffer, M.; Jäger, D.; Arand, M.; Wada, H.; Noguchi, Y.; Stockert, E.; Old, L. J.; Knuth, A. *Journal of Experimental Medicine* **1998**, *187*, 265–270 (cit. on p. 41).

(111) Gnjatic, S.; Nishikawa, H.; Jungbluth, A. A.; Güre, A. O.; Ritter, G.; Jäger, E.; Knuth, A.; Chen, Y.-T.; Old, L. J. In Advances in Cancer Research, Vol. 95; Academic Press: 2006, pp 1–30 (cit. on p. 41).

(112) Bryceson, Y. T.; March, M. E.; Ljunggren, H. G.; Long, E. O. *Immunol Rev* **2006**, *214*, Bryceson, Yenan T March, Michael E Ljunggren, Hans-Gustaf Long, Eric O eng ZIA AI000525-22/Intramural NIH HHS/ Research Support, N.I.H., Intramural Research Support, Non-U.S. Gov't Review England 2006/11/15 Immunol Rev. 2006 Dec;214:73-91. doi: 10.1111/j.1600-065X.2006.00457.x., 73–91 (cit. on pp. 49, 50, 53).

(113) Zingoni, A.; Molfetta, R.; Fionda, C.; Soriani, A.; Paolini, R.; Cippitelli, M.; Cerboni, C.; Santoni, A. *Frontiers in Immunology* **2018**, *9*, DOI: 10.3389/fimmu.2018.00476 (cit. on p. 49).

(114) Cifaldi, L.; Doria, M.; Cotugno, N.; Zicari, S.; Cancrini, C.; Palma, P.; Rossi, P. *International Journal of Molecular Sciences* **2019**, *20*, DOI: 10.3390/ijms20153715 (cit. on p. 49).

(115) Varudkar, N.; Oyer, J. L.; Copik, A.; Parks, G. D. *J Immunother Cancer* **2021**, *9*, Varudkar, Namita Oyer, Jeremiah L Copik, Alicja Parks, Griffith D eng Research Support, Non-U.S. Gov't England 2021/06/27 J Immunother Cancer. 2021 Jun;9(6):e002373. doi: 10.1136/jitc-2021-002373., DOI: 10.1136/jitc-2021-002373 (cit. on pp. 50, 52).

(116) Marchini, A.; Rommelaere, J.; Leuchs, B.; Illarionova, A. Modified parvovirus useful for gene silencing, US Patent 10,227,609, 2019 (cit. on p. 58).

(117) Nieto, K.; Rommelaere, J.; Leuchs, B.; Krammer, P.; Li-Weber, M.; Anna-Paula, D.-O.; Marchini, A.; Li, J. H-1 pv expressing rnai effectors targeting cdk9, US Patent App. 16/464,012, 2020 (cit. on p. 58).

(118) Angelova, A. L.; Geletneky, K.; Nuesch, J. P.; Rommelaere, J. *Front Bioeng Biotechnol* **2015**, *3*, Angelova, Assia L Geletneky, Karsten Nuesch, Jurg P F Rommelaere, Jean eng Review Switzerland 2015/05/09 Front Bioeng Biotechnol. 2015 Apr 22;3:55. doi: 10.3389/fbioe.2015.00055. eCollection 2015., 55 (cit. on p. 60).

(119) Barton, E. S.; Forrest, J. C.; Connolly, J. L.; Chappell, J. D.; Liu, Y.; Schnell, F. J.; Nusrat, A.; Parkos, C. A.; Dermody, T. S. *Cell* **2001**, *104*, 441–451 (cit. on p. 60).

(120) Daniel, S. *Trends Cell Biol* **2009**, *20*, 14–24 (cit. on p. 61).

(121) Rodriguez-Nieto, S.; Zhivotovsky, B. *Current pharmaceutical design* **2006**, *12*, 4411–4425 (cit. on p. 61).

(122) Navone, N. M.; Troncoso, P.; Pisters, L. L.; Goodrow, T. L.; Palmer, J. L.; Nichols, W. W.; Eschenbach, A. C. v.; Conti, C. J. *JNCI: Journal of the National Cancer Institute* **1993**, *85*, 1657–1669 (cit. on p. 61).

(123) Kajiwara, T.; Takeuchi, T.; Ueki, T.; Moriyama, N.; Ueki, K.; Kakizoe, T.; Kawabe, K. *International journal of urology* **1999**, *6*, 520–525 (cit. on p. 61).

(124) Iulianna, T.; Kuldeep, N.; Eric, F. *Cell Death & Disease* **2022**, *13*, 509 (cit. on p. 61).

(125) Hristov, G.; Krämer, M.; Li, J.; El-Andaloussi, N.; Mora, R.; Daeffler, L.; Zentgraf, H.; Rommelaere, J.; Marchini, A. *Journal of virology* **2010**, *84*, 5909–5922 (cit. on p. 61).

(126) Garg, A.; Romano, E.; Rufo, N.; Agostinis, P. *Cell Death & Differentiation* **2016**, *23*, 938–951 (cit. on p. 62).

(127) Green, D. R.; Ferguson, T.; Zitvogel, L.; Kroemer, G. *Nature Reviews Immunology* **2009**, *9*, 353–363 (cit. on p. 62).

(128) Blachère, N. E.; Darnell, R. B.; Albert, M. L. *PLOS Biology* **2005**, *3*, e185 (cit. on p. 62).

(129) Casares, N. et al. *Journal of Experimental Medicine* **2005**, *202*, 1691–1701 (cit. on p. 62).

(130) Basu, S.; Srivastava, P. K. *The Journal of experimental medicine* **1999**, *189*, 797–802 (cit. on p. 62).

(131) Blachere, N. E.; Li, Z.; Chandawarkar, R. Y.; Suto, R.; Jaikaria, N. S.; Basu, S.; Udono, H.; Srivastava, P. K. *The Journal of experimental medicine* **1997**, *186*, 1315–1322 (cit. on p. 62).

(132) Suto, R.; Srivastava, P. K. *Science* **1995**, *269*, 1585–1588 (cit. on p. 62).

(133) Neulinger-Munoz, M.; Schaack, D.; Grekova, S. P.; Bauer, A. S.; Giese, T.; Salg, G. A.; Espinet, E.; Leuchs, B.; Heller, A.; Nuesch, J. P. F.; Schenk, M.; Volkmar, M.; Giese, N. A. *Viruses* **2021**, *13*, Neulinger-Munoz, Matthias Schaack, Dominik Grekova, Svetlana P Bauer, Andrea S Giese, Thomas Salg, Gabriel A Espinet, Elisa Leuchs, Barbara Heller, Anette Nuesch, Jurg P F Schenk, Miriam Volkmar, Michael Giese, Nathalia A eng Research Support, Non-U.S. Gov't Switzerland 2021/06/03 Viruses. 2021 May 28;13(6):1019. doi: 10.3390/v13061019., DOI: 10.3390/v13061019 (cit. on p. 63).

(134) Huang, T.; Sun, X.; Qi, Y.; Yang, X.; Fan, L.; Chen, M.; Yue, Y.; Ge, H.; Li, Y.; Nie, G., et al. *Nano Research* **2023**, 1–9 (cit. on p. 63).

(135) Cirone, M.; Di Renzo, L.; Lotti, L. V.; Conte, V.; Trivedi, P.; Santarelli, R.; Gonnella, R.; Frati, L.; Faggioni, A. *PLoS One* **2012**, *7*, Cirone, Mara Di Renzo, Livia Lotti, Lavinia Vittoria Conte, Valeria Trivedi, Pankaj Santarelli, Roberta Gonnella, Roberta Frati, Luigi Faggioni, Alberto eng Research Support, Non-U.S. Gov't 2012/03/14 PLoS One. 2012;7(3):e31732. doi: 10.1371/journal.pone.0031732. Epub 2012 Mar 7., e31732 (cit. on p. 63).

(136) Antunes, N.; Kundu, B.; Kundu, S. C.; Reis, R. L.; Correlo, V. *Bioengineering (Basel)* **2022**, *9*, Antunes, Nina Kundu, Banani Kundu, Subhas C Reis, Rui L Correlo, Vitor eng FROnTHERA-NORTE-01-0145-FEDER-000023/CCDR-N - Northern Regional Development and Coordination Commission; NORTE2020; FEDER - Fundo Europeu de Desenvolvimento Regional/ n masculine 668983 - FoReCaST/European Union Framework Programme for Research and Innovation Horizon 2020/ PD/BD/143050/2018/Fundacao para a Ciencia e Tecnologia/ PTDC/BTM-ORG/28168/2017/Fundacao para a Ciencia e Tecnologia/ Review Switzerland 2022/04/22 Bioengineering (Basel). 2022 Apr 7;9(4):166. doi: 10.3390/bioengineering9040166., DOI: 10.3390/bioengineering9040166 (cit. on p. 64).

(137) Li, D.-Y.; Gu, C.; Min, J.; Chu, Z.-H.; Ou, Q.-J. *Experimental and therapeutic medicine* **2012**, *4*, 131–134 (cit. on p. 64).

(138) Nair, S.; Archer, G. E.; Tedder, T. F. *Curr Protoc Immunol* **2012**, *Chapter 7*, Nair, Smita Archer, Gerald E Tedder, Thomas F eng U19 AI056363/AI/NIAID NIH HHS/ U54 AI057157/AI/NIAID NIH HHS/ AI56363/AI/NIAID NIH HHS/ Research Support, N.I.H., Extramural Research Support, Non-U.S. Gov't Research Support, U.S. Gov't, Non-P.H.S. 2012/11/07 Curr Protoc Immunol. 2012 Nov;Chapter 7:7.32.1-7.32.23. doi: 10.1002/0471142735.im0732s99., 7 32 1–7 32 23 (cit. on p. 64).

(139) Nouri-Shirazi, M.; Banchereau, J.; Bell, D.; Burkeholder, S.; Kraus, E. T.; Davoust, J.; Palucka, K. A. *J Immunol* **2000**, *165*, Nouri-Shirazi, M Banchereau, J Bell, D Burkeholder, S Kraus, E T Davoust, J Palucka, K A eng CA78846-01A1/CA/NCI NIH HHS/ Research Support, Non-U.S. Gov't Research Support, U.S. Gov't, P.H.S. 2000/10/18 J Immunol. 2000 Oct 1;165(7):3797-803. doi: 10.4049/jimmunol.165.7.3797., 3797–803 (cit. on p. 64).

(140) Heinrich, B.; Klein, J.; Delic, M.; Goepfert, K.; Engel, V.; Geberzahn, L.; Lusky, M.; Erbs, P.; Preville, X.; Moehler, M. *OncoTargets and therapy* **2017**, 2389–2401 (cit. on p. 64).

(141) Liu, X.; Xu, Y.; Xiong, W.; Yin, B.; Huang, Y.; Chu, J.; Xing, C.; Qian, C.; Du, Y.; Duan, T., et al. *Journal for Immunotherapy of Cancer* **2022**, *10* (cit. on p. 64).

(142) Tai, S.; Sun, Y.; Squires, J. M.; Zhang, H.; Oh, W. K.; Liang, C. Z.; Huang, J. *Prostate* **2011**, *71*, Tai, Sheng Sun, Yin Squires, Jill M Zhang, Hong Oh, William K Liang, Chao-Zhao Huang, Jiaoti eng P50 CA092131/CA/NCI NIH HHS/ UL1 RR033176/RR/NCRR NIH HHS/ UL1 TR000124/TR/NCATS NIH HHS/ Comparative Study Research Support, Non-U.S. Gov't Research Support, U.S. Gov't, Non-P.H.S. 2011/03/25 Prostate. 2011 Nov;71(15):1668-79. doi: 10.1002/pros.21383. Epub 2011 Mar 22., 1668–79 (cit. on p. 65).

(143) Saar, M.; Zhao, H.; Nolley, R.; Young, S. R.; Coleman, I.; Nelson, P. S.; Vessella, R. L.; Peehl, D. M. *Cancer Lett* **2014**, *351*, Saar, Matthias Zhao, Hongjuan Nolley, Rosalie Young, Sarah R Coleman, Ilsa Nelson, Peter S Vessella, Robert L Peehl, Donna M eng P01 CA085859/CA/NCI NIH HHS/ P50 CA097186/CA/NCI NIH HHS/ P01CA085859/CA/NCI NIH HHS/ P50CA097186/CA/NCI NIH HHS/ Research Support, N.I.H., Extramural Research Support, Non-U.S. Gov't Ireland 2014/07/08 Cancer Lett. 2014 Sep 1;351(2):272-80. doi: 10.1016/j.canlet.2014.06.014. Epub 2014 Jul 3., 272–80 (cit. on pp. 66, 82).

(144) Young, S. R.; Saar, M.; Santos, J.; Nguyen, H. M.; Vessella, R. L.; Peehl, D. M. *Prostate* **2013**, *73*, Young, Sarah R Saar, Matthias Santos, Jennifer Nguyen, Holly M Vessella, Robert L Peehl, Donna M eng P01 CA085859/CA/NCI NIH HHS/ P50 CA097186/CA/NCI NIH HHS/ P01 CA85859/CA/NCI NIH HHS/ Research Support, N.I.H., Extramural Research Support, Non-U.S. Gov't 2013/06/07 Prostate. 2013 Sep;73(12):1251-62. doi: 10.1002/pros.22610. Epub 2013 Jun 6., 1251–62 (cit. on pp. 66, 82).

(145) Ellis, W. J.; Vessella, R. L.; Buhler, K. R.; Bladou, F.; True, L. D.; Bigler, S. A.; Curtis, D.; Lange, P. H. *Clin Cancer Res* **1996**, *2*, Ellis, W J Vessella, R L Buhler, K R Bladou, F True, L D Bigler, S A Curtis, D Lange, P H eng P050DK47656/DK/NIDDK NIH HHS/ Research Support, Non-U.S. Gov't Research Support, U.S. Gov't, P.H.S. 1996/06/01 Clin Cancer Res. 1996 Jun;2(6):1039-48., 1039–48 (cit. on p. 66).

(146) Idrisova, K.; Simon, H.-U.; Gomzikova, M. *Cancers* **2022**, *15*, 139 (cit. on p. 66).

(147) Petrić, T.; Sabol, M. *International Journal of Molecular Sciences* **2023**, *24*, 5293 (cit. on p. 66).

(148) Eder, T.; Weber, A.; Neuwirt, H.; Grünbacher, G.; Ploner, C.; Klocker, H.; Sampson, N.; Eder, I. E. *International journal of molecular sciences* **2016**, *17*, 1458 (cit. on p. 66).

(149) Smith, D. A.; Beaumont, K.; Maurer, T. S.; Di, L. *Journal of Medicinal Chemistry* **2018**, *62*, 2245–2255 (cit. on p. 68).

(150) De Wolf, C.; Van De Bovenkamp, M.; Hoefnagel, M. *Cytotherapy* **2017**, *19*, 784–797 (cit. on p. 68).

(151) Wolf, C. D.; Van De Bovenkamp, M.; Hoefnagel, M. *Cytotherapy* **2018**, *20*, 1289–1308 (cit. on p. 68).

(152) PG, P. **2019** (cit. on p. 68).

(153) Ramirez-Rosas, M. B.; Park, S. H.; Eber, M.; Kittel, C.; Martin, T.; Munoz-Islas, E.; Jimenez-Andrade, J. M.; Shiozawa, Y.; Parker, R.; Peters, C. *The Journal of Pain* **2021**, *22*, 584 (cit. on p. 68).

(154) Isaacs, J. T.; Isaacs, W. B.; Feitz, W. F.; Scheres, J. *The Prostate* **1986**, *9*, 261–281 (cit. on p. 68).

(155) Halin, S.; Wikström, P.; Rudolfsson, S. H.; Stattin, P.; Doll, J. A.; Crawford, S. E.; Bergh, A. *Cancer research* **2004**, *64*, 5664–5671 (cit. on p. 68).

(156) Fraser, S.; Salvador, V.; Manning, E.; Mizal, J.; Altun, S.; Raza, M.; Berridge, R.; Djamgoz, M. *Journal of cellular physiology* **2003**, *195*, 479–487 (cit. on p. 68).

(157) El-Andaloussi, N.; Leuchs, B.; Bonifati, S.; Rommelaere, J.; Marchini, A. *J Vis Exp* **2012**, DOI: 10.3791/3518 (cit. on pp. 69, 70).

(158) Kestler, J.; Neeb, B.; Struyf, S.; Damme, J. V.; Cotmore, S. F.; D'Abramo, A.; Tattersall, P.; Rommelaere, J.; Dinsart, C.; Cornelis, J. J. *Human Gene Therapy* **1999**, *10*, PMID: 10428207, 1619–1632 (cit. on p. 73).

(159) Bodendorf, U.; Cziepluch, C.; Jauniaux, J.-C.; Rommelaere, J.; Salomé, N. *Journal of Virology* **1999**, *73*, 7769–7779 (cit. on p. 73).

(160) Young, A.; Quandt, Z.; Bluestone, J. A. *Cancer Immunol Res* **2018**, *6*, Young, Arabella Quandt, Zoe Bluestone, Jeffrey A eng P30 DK063720/DK/NIDDK NIH HHS/ Research Support, N.I.H., Extramural Research Support, Non-U.S. Gov't Review 2018/12/05 Cancer Immunol Res. 2018 Dec;6(12):1445-1452. doi: 10.1158/2326-6066.CIR-18-0487., 1445–1452 (cit. on p. 82).